

The application of flow chemistry techniques in medicinal chemistry programs: The development of flow-photocyclization methods for the synthesis of phenanthridinone-type compounds.

by

Yuhua Fang

A Thesis submitted to the Faculty of Graduate Studies of

The University of Manitoba

in partial fulfilment of the requirements of the degree of

MASTER OF SCIENCE

College of Pharmacy, Faculty of Health Sciences

University of Manitoba

Winnipeg

Copyright © 2016 by Yuhua Fang

Acknowledgement

I would like to show my greatest gratitude to all those people who have made this dissertation possible.

I am immensely grateful to my supervisors, Dr. Geoffrey Tranmer for his guidance and encouragement, as well as the essential support and the freedom he gave to me. It was a great privilege and a great fun to work with Dr. Tranmer and I wish the good partnership and relationship will continue.

I owe my greatest gratitude to my parents and my family, who have given me the best support they can provide so that I am able to explore the unknown without any extra-worries. They are the only reason I can be here.

I am grateful to my committee members, Dr. Ted Lakowski and Dr. John Sorenson. Their suggestions are very inspiring and thought-provoking. I am also indebted to my lab members, Jennifer Bao and Dinghua Liang, for their help in the past two years.

I would like to show my deepest appreciation to my friends who have given me help and kept me positive: Jiaqi Yang, Yan Lu, Zirui Xing, Yannick Traore, Marina Mostafizar, Dr. Ivan Stevic, Dr. Pengqi Wang, Ryan Lillico, Miral Fumakia, Tina Ahmad, Yufei Chen, Sidi Yang, Samaa alrushaid, Saran Malhi.

I'm also grateful to Jim Honeyford who has helped me a lot with thesis-writing. And I appreciate the help from Sara Dyck, as well as other staffs from the University of Manitoba.

We thank the University of Manitoba for the University start-up grant as well as the University of Manitoba's College of Pharmacy for their financial support.

Abstract

Flow chemistry can be characterized as a continuous chemical reaction system performed in solution in connecting tubing and flow reactors which is efficient. Photochemistry is the chemical reaction initiated by light, and is the result of the absorption of photon by a reagent or starting material. Poly (ADP-ribose) polymerase is a big family of proteins related to cellular repair and death. Phenanthridinones have been shown to exhibit PARP inhibitory potency as competitive inhibitors. Instead of using conventional costly and low-efficiency coupling reactions, we have managed to develop a method to synthesize phenanthridinone-type compounds by photo-cyclization under flow conditions for the purposes of generating novel PARP inhibitors. In total, we have generated a series of phenanthridinones in yields ranging from 13 % to 99%, 18 examples. Additionally, we have also developed a flow photocyclization method for the synthesis of complex heterocycles, naphthyridinones (5 examples, yields ranging from 24-52%) and thieno-quinolinones (18 examples, yields ranging from 23-90%), molecules that would be much more difficult to construct using conventional batch methods. Overall, we have demonstrated that a flow photocyclization pathway is a robust synthesis route for producing phenanthridinone-type compounds for the purposes of developing novel PARP inhibitors.

Table of Contents

| | |
|---|-----|
| Acknowledgement | I |
| Abstract | II |
| Table of Contents | III |
| List of Tables | IV |
| List of Tables | IV |
| Abbreviation | VI |
| I. Introduction..... | 1 |
| A. General Introduction of Flow Chemistry | 1 |
| B. General Introduction of Photo Chemistry | 7 |
| C. Combination of Flow Chemistry and UV-catalyzed Photo Chemistry..... | 10 |
| D. Applications of Photo-cyclization and –Cycloaddition in Flow Chemistry | 11 |
| E. General Introduction of Poly (ADP-Ribose) Polymerase Inhibitor | 24 |
| F. Synthesis of Phenanthridinone-Type Compounds..... | 30 |
| II. Hypothesis and Objectives..... | 36 |
| III. Experimental Information..... | 37 |
| A. Procedure for Synthesizing Starting Materials..... | 37 |
| 1. Synthesis of 2-chloro- <i>N</i> -phenylbenzamides | 37 |
| 2. Synthesis of 2-chloro- <i>N</i> -phenylnicotinamides | 47 |
| 3. Synthesis of 2-chloro- <i>N</i> -phenylthiophene-3-carboxamides | 51 |
| 4. Synthesis of 3-chloro- <i>N</i> -phenylthiophene-2-carboxamides | 60 |
| B. Procedure for Synthesizing Products | 63 |
| 1. Synthesis of Phenanthridin-6(5H)-ones..... | 63 |
| 2. Synthesis of Benzo[<i>h</i>][1,6]naphthyridin-5(6H)-ones | 73 |
| 3. Synthesis of Thieno[3,2- <i>c</i>]quinolin-4(5H)-ones..... | 77 |
| 4. Synthesis of Thieno[2,3- <i>c</i>]quinolin-4(5H)-ones..... | 86 |
| IV. Results and Discussion | 89 |
| A. Preliminary Reaction and Optimization..... | 89 |
| B. Research Results and Conclusion | 103 |

| | |
|---|-----|
| 1. Synthesis of Phenanthridinones..... | 103 |
| 2. Synthesis of Naphthyridinones..... | 108 |
| 3. Synthesis of Thieno-quinolinones..... | 110 |
| C. Overall Conclusion and Discussion..... | 117 |
| V. References..... | 120 |
| VI. Supplemental Appendix..... | 137 |

List of Tables

| | |
|---|-----|
| Table 1 Attempts to perform the Mallory type reaction directly..... | 92 |
| Table 2 Preliminary Optimization 1..... | 93 |
| Table 3 Optimization 2..... | 96 |
| Table 4 Optimization 3..... | 97 |
| Table 5 Optimization 4..... | 98 |
| Table 6 Optimization 5..... | 100 |
| Table 7 The result of single-step synthesis of phenanthridinones..... | 103 |
| Table 8 The result of single-step synthesis of naphthyridinones..... | 108 |
| Table 9 Results of the synthesis of thieno[3,2- <i>c</i>]quinolin-4(5H)-ones..... | 113 |
| Table 10 Results of the synthesis of thieno[2,3- <i>c</i>]quinolin-4(5H)-ones..... | 116 |

List of Tables

| | |
|---|----|
| Figure 1 The Jablonski Diagram..... | 8 |
| Figure 2 Non-aromatic heterocyclic compounds, e.g. piperidine, pyrrolidine, thiolane..... | 19 |

| | |
|--|----|
| Figure 3 NAD ⁺ , the nature ligand of PARP | 27 |
| Figure 4 Residues with different PARPs and a schematic of D loop | 28 |
| Figure 5 AZ9482, the PARP inhibitor | 29 |
| Figure 6 henanthridin-6(5H)-one | 31 |
| Figure 7 Benzo[<i>h</i>][1,6]naphthyridin-5(6H)-one. | 32 |
| Figure 8 Three types of thieno-quinolinones | 33 |

Abbreviation

| | |
|---------------------|--|
| ADP | Adenosine diphosphate |
| AIBN | Azobisisobutyronitrile |
| C | Carbon |
| CDCl ₃ | Deuterated chloroform |
| Cu | Copper |
| DCM | Dichloromethane |
| DIPEA | <i>N,N</i> -diisopropylethylamine |
| DMF | Dimethylsulfoxide |
| DMSO-D ₆ | Deuterated dimethylsulfoxide |
| DSF | Differential Scanning Fluorimetry |
| EtOH | Ethanol |
| Fe | Iron |
| FEP | Fluorinated ethylene propylene |
| h | Hours |
| H | Hydrogen |
| HATU | 1-[Bis(dimethylamino)methylene]-1H-1,2,3-triazolo[4,5-b]pyridinium 3-oxid hexafluorophosphate |
| HOBt | 1-hydroxybenzotriazole |

| | |
|--------------------------------------|--|
| HPLC | High Performance Liquid Chromatography |
| h ν | Light |
| LC | Liquid Chromatography |
| m | Milli |
| mg | Milligrams |
| ml | Millilitres |
| min | Minutes |
| mol | Millimole |
| MS | Mass spectroscopy |
| NAD ⁺ | Nicotinamide adenine dinucleotide |
| NMR | Nuclear magnetic resonance |
| PARP | Poly(ADP-ribose)polymerase |
| Pd | Palladium |
| PSA | Polar Surface Areas |
| QP-BZA | Quadrapure-benzylamine |
| QP-SA | Quadrapure-sulfonic |
| QP-TU | Quadrapure-thiourea |
| Ru | Ruthenium |
| Ru(bpy) ₃ Cl ₂ | Tris(bipyridine)ruthenium(II) chloride |

| | |
|--|---|
| Ru(bpy) ₃ (PF ₆) ₂ | Tris(2,2'-bipyridine)ruthenium(II) hexafluorophosphate |
| TBTU | O-(benzotriazol-1-yl)- <i>N,N,N',N'</i> -tetramethyluronium tetrafluoroborate |
| TEA | Triethylamine |
| THF | Tetrahydrofuran |
| TNKS | Tankyrase |
| TRF1 | Telomeric repeat-binding factor 1 |
| UV | Ultraviolet |
| WHO | World Health Organization |

I. Introduction

A. General Introduction of Flow Chemistry

Flow chemistry refers to the continuous chemical reactions that are carried out in flowing fluid in connecting tubing and flow reactors ^[1]. A flow chemistry reactor system can be divided into three parts and include an input section, a reacting section and an output section ^[2]. The input section contains reservoirs, injection ports with sample loops, and pumps; the reacting section can include a mixer, a microfluidic chip reactor, a coil reactor and/or a column reactor; the output section includes a back pressure regulator and a reservoir for collection of product. An additional computer-console is usually available among commercial flow chemistry reactor systems for monitoring and controlling of flow reaction parameters ^[2].

In the input section, the reservoir is used to store solvent or a large amount of solution with dissolved reactants; the injection port is used to inject a small amount of reagent solution; the pump ^[2] is used to move solution continuously from a reservoir/ injection sample loop into the reaction section and out of the system from the output. There can be several reservoirs, injection ports with sample loops and pumps in one flow chemistry reactor system to perform single-step or multi-step tasks ^[3]. However, in general, pumps are one-to-one corresponding to reservoirs and/or injection ports.

In the reacting section, the mixer is generally a connector or T-piece to mix two or more solutions together and connects the input section with the reactor ^[4]. In the microfluidic chip reactor, the coil reactor and/or the column reactor is the place where the majority of the reaction is carried out. the coil reactor, or microfluidic chip reactor, is always used to perform liquid phase or liquid-gas phase ^[5] reactions while column reactor favors liquid-solid phase reaction ^[6];

The column reactor can also be used to play a role as scavenger to clean the byproducts or unreacted reagents, which will be discussed below. For a single-step reaction, only one reactor is equipped in the system. However, different kinds of reactors can be combined and equipped in the system together for multi-step tasks^[3]. These reactors include, but are not limited to, heating reactor, cooling reactor, photo reactor, microfluidic chip reactor, etc. Further details about multi-step systems will be introduced below.

The most common type of the reactor is the coil reactor, which is made of stainless steel, metal, or polymer, small-diameter tubing^{[2] [7]}. Based on the reactions that are going to be processed, different coil reactors can be purchased or made. For example, if the reaction requires high temperature conditions, researchers will employ a stainless steel coil reactor which is thermally-stable, while a photochemical reaction will require a polymer coil reactor, which is transparent but unable to tolerate high temperature^[8].

The important reaction condition parameters related to flow chemistry include the flow rate, the temperature and pressure, molar equivalence, lamp power (photochemical reaction), *etc.*^[7]. Among them, the flow rate refers to the flowing speed of the fluid. It reflects the working status of the pump and determines the reacting time, also known as the residence time within a specific reactor.

Other parts of a flow chemistry system include an output section, the back pressure regulator is used to maintain the pressure inside the system, and the reservoir is used to collect the product. A computer console is also often used for control of the whole system. The data from the system reveals the status of reaction progress, such as flow rate, temperature, pressure, lamp power, *etc.* can be read directly from the monitor, by timeline and real-time value. It is also designed to set

up and monitor the whole reaction process in advance for automated working procedures with predetermined reaction conditions. In this case, a computer will take over the system and control the reaction condition and progress. In brief, all the information can be gained from a control panel and all the parameters can be set up at the console as well ^[8].

A typical flow reactor system works in the following manner ^{[4] [8]}. After all the reaction condition parameters are set up and the system starts to work, the pumps will drive the solution from the reservoir, or the solution in the sample loop which is previously manually injected, into the reaction section. If there are two or more solutions involved in the reaction, they will join each other ahead of the reactor in the mixer. The reaction is carried out in the reactor while supernumerary starting material or byproduct will be cleaned by a scavenger (if applicable). The final product (or the crude product) will be collected in the reservoir at the end of the system.

While traditional batch reactions are mainly carried out in fixed-volume flasks, flow chemistry has shown its benefits in performing chemical reactions more efficiently and with easier scale-up for industrial purposes without modifying reaction conditions, as described below.

Most flow chemistry reactors are long and constructed of small-bore tubing. Efficient mixing can be achieved in a few seconds because of the small diameter, which is impossible for fixed volume batch reactions. Based on the collision theory ^{[9] [10]}, it is believed that a well-mixed solution is one of the reasons that a better yield can be achieved under flow conditions over traditional batch condition, and some examples will be mentioned later.

Controllability also contributes to the working efficiency ^[11]. While controlling the reaction sequence of a traditional batch reaction requires adding chemical reagents at a specific timing in order, it is much more convenient to manage the reaction order under flow conditions. Different

reactions are carried out in different reactors. When different reactors are lined up in one system with extra injection ports between (every) two reactors, a multi-step reaction can be carried out in a defined sequence. Multi-step synthesis is useful for natural product synthesis ^{[2] [7]}. Some featured examples include the seven-step synthesis of oxomaritidine and grossamide, which were reported by Ley's lab ^{[12] [13]}. Sharing different reactions in different reactors reduces side-reactions. Lining up all the reactors with tubing to create an enclosed system reduces the following: mechanical loss, contamination of reagents and potential environmental pollution by hazardous intermediate spill ^[7].

Reaction process controllability of flow system is the most superior feature. Compared to the traditional batch reactions, both reaction time and reaction conditions can be better controlled. The reaction time is related to the flow rate ^[7], while the coil reactor which has a fixed volume, the time it takes to pump the fluid through the reactor is steady and can be calculated precisely. That is to say, the time for each reagent to react is the same. The reaction condition always refers to the temperature or light intensity. To the reaction that might produce different products under different temperature, the thin tubing, made from thermally conductive material, with a high surface area to volume ratio ensures rapid heating or cooling. Small bore tubing also ensures that the temperature is the same anywhere inside, avoiding "hot spots", which are common in conventional batch chemical reactions ^{[7] [14]}. Meanwhile, the integration of temperature sensors gives the ability of instant feedback which ensures the temperature is well monitored and controlled. For reactions that are sensitive to light, the system allows a direct control of lamp power and wavelength. Suzuki–Miyaura couplings reported by Fletcher were performed in a glass flow reactor with gold layer/patch underneath or covered around the reactor for better microwave absorption. Temperature was monitored in this research using the combination of two

electrodes attached to the inlet and outlet of tubing, allowing for precise measurement of the reaction temperature and reducing byproducts^[15].

Output control can also allow for the separation or purification of product before final collection, if applicable. In the synthesis of quinolone derivatives reported by Steven Ley and co-workers, “catch and release” protocols are used to separate and purify products. The synthesis of aniline in the first step used Quadrapure-benzylamine (QP-BZA) and Quadrapure-thiourea (QP-TU) to filter out hydrofluoric acid and palladium respectively^[6]. The synthesis of the carboxylic acid in the second step used QP-BZA and K_2CO_3 agent to filter out dimethyl acetylenecarboxylate and water respectively, and then employed Ambersep[®] 900 hydroxide form to catch the product. The third step employed *O*-(benzotriazol-1-yl)-*N,N,N',N'*-tetramethyluronium tetrafluoroborate (TBTU) and 1-hydroxybenzotriazole (HOBt) to release and activate the previous product, and then Quadrapure-sulfonic acid (QP-SA) was used to catch the product and the effluent was directed to waste. The final step employed NH_3 in methanol to release the sequestered product, obtaining a high purity product^[6]. The purification procedure in each step prevents side products, such as hydrofluoric acid, from entering next-step reaction. Comparing to batch reactions, the reagents stay in the reactor system so there will be no mechanical loss or contamination. Meanwhile, taking first step as an example, batch reactions generally took 7 hours to complete the C–N bond formation^[16], while it only took 10 minutes under flow condition.

There are some other benefits of flow chemistry. Full control over each step in a flow chemistry sequence results in cleaner products, with better stereoselectivity in some cases^{[7][17]}, while enabling complex tasks to be completed in-line. Scalability is a significant feature of flow chemistry that may benefit pharma-academia collaborations for drug discovery and production,

with the key feature being the ability to transfer lab results directly into industrial production easily^{[7][18]}.

Due to the connection of the reactor with input and output, and the pump-driving flowing fluid, the reaction can be carried out continuously. That is, the solution of reagent is introduced to the reactor constantly while the solution of product and unreacted starting material is expelled. This working principle of flow chemistry explains how the product accumulates in the collector over time as long as there are enough reagents and starting material solution(s) being induced to the reactor. Compared to traditional batch reactions that are carried out in a flask where the total amount of reagent is fixed, the starting material for flow chemistry reactions can be replenished either by simple injections or by filling up the reservoir. For scaling up, there is no need to change the reactor, theoretically. Thus, rather than developing a new reaction condition for a new and larger reactor, a lab-scale tubing reactor can still be employed, provided that it pumps for a sufficient length of time. The replenishment of starting material is the only requirement for mass production^[19]. Overall, flow chemistry is an efficient method to perform chemical reactions and a flow chemistry reactor will be used in our project.

In 2011 Lévesque and Seeberger reported a total synthesis of anti-malaria drug artemisinin under flow conditions. In the research, dihydroartemisinic acid was transformed into artemisinin with a multi-step flow reactor. Dihydroartemisinic acid, with photosensitizer tetraphenylporphyrin, was introduced into a photo reactor and reacted with singlet oxygen which was converted from triplet oxygen by UV excitation. The resulting product, a tertiary allylic hydroperoxide joined trifluoroacetic acid for a Hock cleavage reaction, followed by oxygen-induced oxidation. The three-step reaction afforded artemisinin as final product. The overall yield was 39% from dihydroartemisinic acid. The authors also demonstrated that approximately

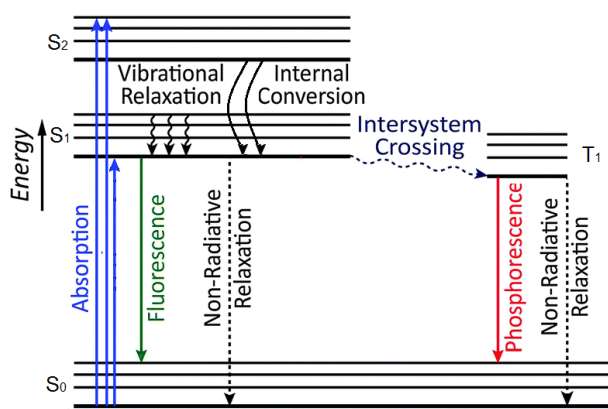
200g of artemisinin could be synthesized per day with the system working continuously. The procedure could be transferred from lab to industry directly as it was estimated that the productivity met the demand for malaria treatment posted by WHO ^[20].

B. General Introduction of Photo Chemistry

Photochemistry or photochemical reaction refers to a branch of chemical reactions that is initiated by the absorption of photons, under the irradiation of ultraviolet (UV), visible or infrared light ^[21]. The mechanism of the excitation can be revealed by the Jablonski Diagram ^[22] ^[23] (**Figure 1**). The photochemical reaction is carried out when one photon is absorbed per molecule in the chemical system, leading to an excited singlet state. Corresponding to the amount of energy which is absorbed, the molecule will be transmitted to different excited electronic states, as well as different vibrational states. As soon as the molecule is excited, there are several ways in which the energy may be dissipated. The first one is vibrational relaxation, which takes place within one excited electronic state level. The energy is converted into kinetic form. The kinetic energy can remain in the same molecule, as well as transferring from one molecule to another. This relaxation is non-radiative and it is very fast. The second one is internal conversion where the electron is transmitted to one vibration level in a lower excited electronic state. The internal conversion is radiative and, compared to the vibrational relaxation, it is very slow. Fluorescence and phosphorescence are two radiative energy-transmitting pathways that lead to the ground state. Fluorescence is a slow photo-emitting pathway from the lowest excited state to the ground state within the same multiplicity. Phosphorescence is also a slow radiative pathway. However, it is different from the fluorescence as the transition starts

from triplet excited state to singlet ground state. The transition between multiplicities, i.e. from singlet excited state to triplet excited state, is termed as intersystem crossing. This kind of transition is even slower than fluorescence [24].

Figure 1. The Jablonski Diagram [25]



Photochemical reactions include, but are not limited to α -cleavage (Norrish Type 1 Photoreaction [26]), Barton reaction [27], Photo-rearrangement (such as Photo-claisen rearrangement [28]), acyl shift (such as Photo-Fries rearrangement [29]), photoisomerizations (such as E/Z photoisomerization [30]), Norrish Type II photoreaction [31] and Norrish–Yang reaction [21] [32], photocycloadditions (such as Paterno–Büchi reaction [33], de Mayo reaction [34]), photocyclization (such as Photo-Bergman cyclization [35]), photochemical nitrogen extrusion [36], photodecarbonylation [37], photodecarboxylation [38], etc.

Compared to thermal methods, the photochemical reaction benefits reactions that produce thermodynamically disfavored products. For any chemical reaction, activation energy and reaction enthalpy are necessary. The activation energy is always described as an energy barrier. For the photochemical reaction, the energy barrier can be easily overcome with the excitation of the reactant. In this way, less activation energy is needed so that a low-temperature reaction condition is possible ^[39].

There are many ways to trigger a photochemical reaction, such as direct irradiation, catalyst-mediated electron transfer and catalyst-mediated energy transfer ^{[40] [41]}. When a reactant is photo-active, it can be excited by light so that a corresponding reaction can take place. In this case, a strong light source is always preferred, that is why UV is always an ideal light source. UV is the most commonly used light for performing photochemical reactions. Rationalized Planck Constant, long-wavelength UV is the most powerful light source ^[42].

However, in some cases, a substrate cannot be activated directly by light when the substrate is poorly photo-sensitive or visible light is used as the source. Photocatalyst can be used as an intermediate between the substrate and light. Upon the absorption of photons, a photocatalyst can be excited to an excitation state to transfer electrons or energy to the reagents and then regenerate itself. Photocatalysts include but not limited to metal complex analogues ^{[43] [44]}, organic dyes (such as Eosin Y ^[45]), and some other kinds of salt (such as triphenylpyrylium tetrafluoroborate ^[46]). Metal complex analogues Tris(bipyridine)ruthenium(II) hexafluorophosphate/chloride are the most attractive catalysts for their excellent optical properties. The photocatalysis process of this catalyst starts from metal to ligand charge transfer (MLCT) upon the absorption of light. An electron which initially locates in a metal-centered π_M orbital transits into a ligand-centered π_L^* orbital. With relaxation, excited-state catalyst decays to singlet lowest-energy level and then

undergoes rapid intersystem crossing to the triplet lowest-energy level. The complex remains a comparably long-term excited state because of spin-forbidden nature so that electron transfer can be achieved ^{[47] [48]}.

C. Combination of Flow Chemistry and UV-catalyzed Photo Chemistry

The conventional way to perform photochemical reactions involves the use of a fixed volume immersion well with light source, such as a low-, medium- and high-pressure mercury lamp, in the center of it ^[49]. The solution containing the reagent fills the reservoir where the reaction is taking place ^[42]. One major disadvantage of light itself is that it cannot penetrate the whole reservoir without any attenuation in an immersion-well and photon intensity diminishes dramatically with the light path travelling in the solvent, according to Beer-Lambert Law ^{[50] [51]} ^{[52] [53]}. In other words, the reaction condition is not all the same due to different photon intensity, and poor light penetration, causing lower yields and reaction rates.

The main benefit of using a flow reactor to perform photochemical reactions is to compensate for this shortcoming by decreasing the light path length in the solvent ^{[7] [54]}. Firstly, it is feasible to make tubing with transparent material and this kind of tubing is also commercially available. Secondly, the tubing used in flow reactors has a very small diameter. Compared to an immersion well, the light path length in the tubing is a minimum, which indicates that light attenuation is also negligible. The photon intensity in any part of the coil reactor is identical. As mentioned above, a flow reactor can control the temperature of the coil reactor easily and efficiently. On the basis of this thermal-control virtue, a flow reactor is able to create uniform conditions for photochemical reactions, especially compared to batch immersion wells.

It is very easy to make a photochemical reactor based on a flow chemistry system ^[54]. Commercially available transparent narrow tubing can be wrapped around the lamp. An HPLC pump can be attached to one end of the tubing with an injection port on it and the other end of the tubing is connected to a collector.

Booker-Milburn *et al* introduced a practical photochemical reactor using commercial available or customized immersion-wells with UV-transparent FEP tubes by simply wrapping around directly onto the outside ^[54]. The author used a normal immersion-well UV reactor, a customized UV immersion-well with narrow-bore FEP and a customized UV immersion-well with wide-bore FEP in the research to perform a series of proven cycloaddition reactions. The research result demonstrated that UV catalyzed photochemical reactions could be carried out in a continuous flow reactor with a considerable yield in a standard laboratory fume hood. In our research, a commercially available flow-photo reactor, Vapourtec[®] R2+/R4 with UV-150, will be used.

D. Applications of Photo-cyclization and –Cycloaddition in Flow Chemistry

Aromatic rings are common building blocks in a great majority of current commercial drugs and natural products. The existence of ring systems significantly affects the pharmacokinetic and pharmacodynamics properties of drugs by changing lipophilicity/aqua-solubility, which is exemplified by Lipinski's "Rule of Five" ^[55]. Ligand-receptor interaction such as H-bond and π -cation stabilization is influenced by aromatic rings as well. Meanwhile, the spatial structure of aromatic rings provides a tough spatial hindrance or a rigid scaffold which enables a drug molecule to embed into the receptor with a designed direction or conformation which may not be preferential originally. In addition, compounds that consist of aromatic rings always possess

good crystallinity which contributes to the stability of a drug. Along with the pharmacological/biochemical properties, these features make aromatic ring necessary for potential drug design ^{[56] [57]}.

To chemistry nowadays, making ring systems or assembling aryl-aryl systems is no longer a difficult task. Classic cycloaddition reactions such as the Dies-Alder reaction makes it easy to produce cyclic compounds from substituted alkenes ^[58]. Metal-catalyst coupling reactions, such as the Suzuki-Miyaura cross-coupling reaction ^[59], are also mature and well learned. The use of metal catalysts such as palladium enables chemists to produce complex ring systems with simple, commercial available building blocks. The Suzuki reaction can also be performed in flow ^[15]. Some other ways to make cyclic products involve the applications of coupling reagents such as HATU ^{[60] [61]}.

Although using metal catalysts or coupling reagents can be a convenient method to get a desired product, it can also be expensive, require many steps and be time-consuming. Photocyclization and photocycloaddition have been known for a while, however they have been criticized for low efficiency. It is possible to perform photocyclization and photocycloaddition under flow condition to increase the yield.

Many cases of photo cycloaddition and photo cyclization in flow studies have been reported in the last ten years. These studies provide important theoretical supports for our research, see below. A typical and famous reaction that makes aromatic ring systems is the Mallory reaction ^{[62] [63]}. It is a stilbene photocyclization under UV irradiation that couples two aromatic rings with a formation of a new C–C bond. An oxidant is necessary in most cases as a hydrogen-receptor.

Some exceptions indicate that the reaction can still work out well in the absence of an oxidant while going through elimination, 1,3-shift or 1,5-shift pathways^{[64][65]}.

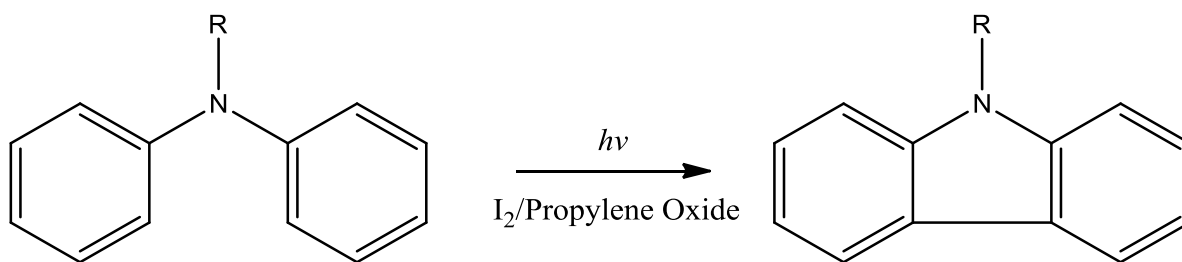
Over the last decade, the Mallory reaction has also achieved a great development under the flow condition, especially by Collins and his lab members. From their research^{[66][67]}, photochemistry combined with flow chemistry can be applied to synthesize simple aromatic compounds to polycyclic aromatic compounds (**Scheme 1**) with a promising future of scaling up for industry use. Synthesis of carbazole, which is the core motif of drug carprofen, which is a non-steroidal anti-inflammatory, is an extraordinary example of performing the Mallory-type reaction in flow. This reaction can be carried out either by UV irradiation or visible light illumination with photo catalyst.

In the case of visible-light-mediated photocyclization, which was reported earlier, a metal complex like a Ru-based or a Cu-based catalyst was used^[66]. During the optimization procedure to synthesize carbazole using a flow reactor, the authors found out that the Cu-Based catalyst had better performance than the Ru-based catalyst. With the optimized procedure and condition, the authors were able to get triarylaminines and diarylaminines under continuous flow condition in 20 hours with the yields ranging from 50%-95%. This visible-light-mediated method was robust enough to make different kinds of carbazoles. In 2014, Collins reported another study towards the synthesis of carbazoles^[67]. Instead of visible light, UV light was employed for the reaction. In the study, they expanded the research to include the synthesis of carprofen and analogues. The continuous flow reactor was made from FEP tubing, which would be irradiated by UV light in a photochamber. With this reactor and optimized reaction condition, which employed I₂/propylene oxide as oxidant, the authors presented a two-step synthesis, starting from a palladium-catalyzed

cross-coupling reaction of *N*-methylaniline and bromoarene, to get carprofen and carprofen derivatives mixed with their regioisomers with a decent yield (70% ~ 80%).

With these two examples, the authors demonstrated that this type of continuous flow reactor combined with UV light was useful for a multi-step reaction to produce a drug like carprofen in a good yield ^[66] ^[67]. Also, it can be utilized in a wide application.

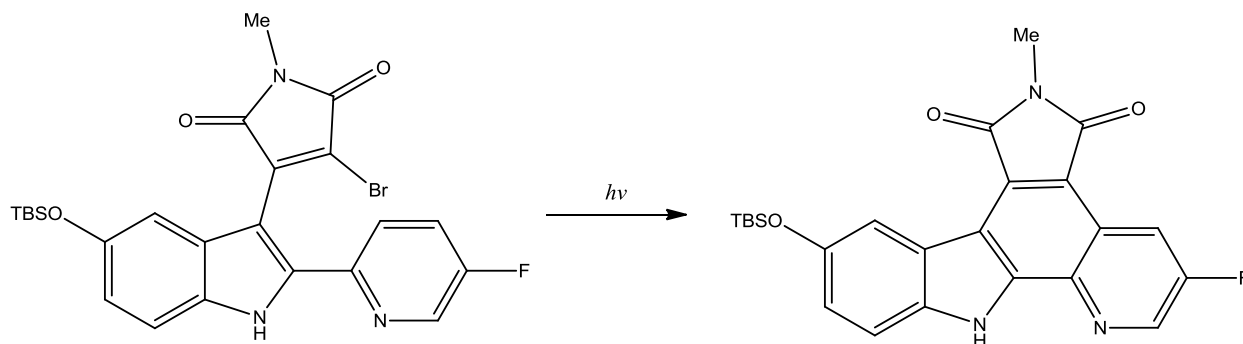
Scheme 1. The general scheme of Collins's reaction. Synthesis of carbazoles.



Pyridocarbazole is a core structure whose analogue indolocarbazole can be found in the natural product staurosporine. Pyridocarbazoles shows strong kinase inhibitory ability when chelated to metal ruthenium, making inhibitors such as a GSK-3 inhibitor ^[68]. Seeberger and his lab reported a non-oxidative type Mallory reaction to make pyridocarbazoles under flow condition. Before that, the crude pyridocarbazole product from the batch reaction is difficult to be purified and the yield was low ^[69]. In this study, the key point was radical-reaction 6π-photoelectrocyclization which closed the ring structure. The radical was created by the leaving of the bromo-substitution on the pyrrole ring. Optimizing reaction time by ¹H-NMR, the authors were able to prepare the target product with 89% yield in 20 min (much shorter than 5 h in batch),

which minimized the byproduct (**Scheme 2**). It is also an example of the superior nature of flow chemistry versus traditional batch reaction.

Scheme 2. The general scheme of Seeberger's reaction. Synthesis of pyridocarbazoles.



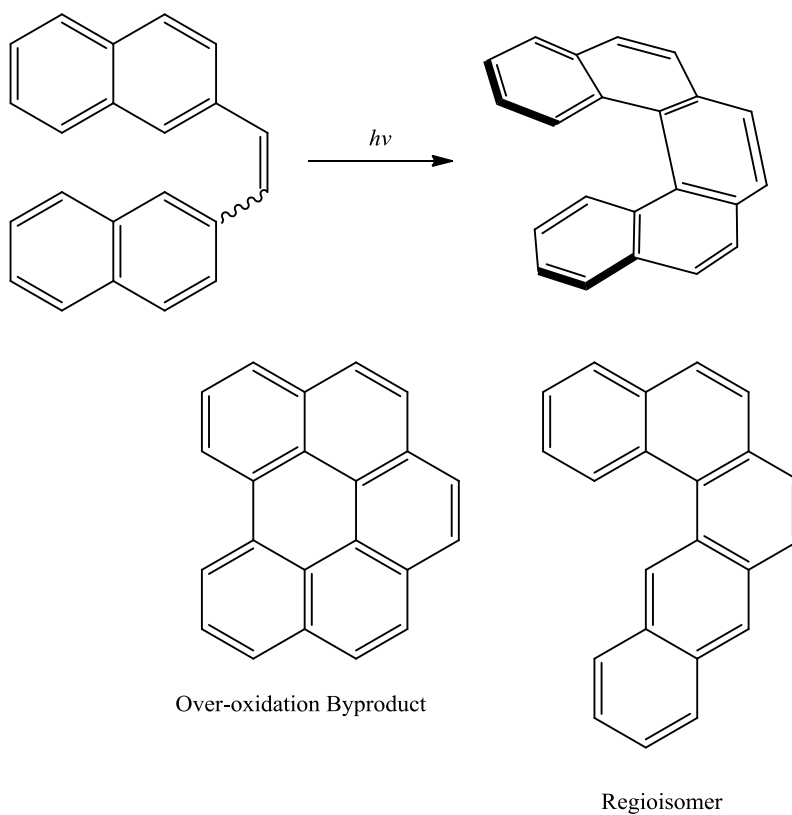
The Mallory type reaction is also applicable for the synthesis of polycyclic aromatic compounds. From the study which was also presented by Collins, Cu-based catalyst was used for the synthesis of [5]helicene which was composed of 5 benzene ring^[70] (**Scheme 3**). In this study, the authors used visible light as the light resource as they found that when employing UV light for the reaction produced a large amount of byproduct while yields of the reaction were 43%-57% when employing visible light and no over-oxidized product or regioisomers was obtained. Considering the choice of metal-based catalyst, the authors investigated the effect of different sensitizer, such as ruthenium complex such as $[\text{Ru}(\text{bpy})_3](\text{PF}_6)_2$, iridium complex such as $[\text{Ir}(\text{dtbbpy})(\text{ppy})_2]\text{PF}_6$, copper complexes such as $[\text{CuDPEPhos}(\text{neo})]\text{BF}_4$ and $\text{Cu}(\text{Xantphos})(\text{dmp})\text{BF}_4$. The conclusion was that ruthenium-based and iridium-base catalyst

delivered the lowest yields and copper complex performed fairly well, while [CuDPEPhos(neo)]BF₄ gave a higher yield. In addition, comparing different oxidant such as I₂, DDQ and t-BuO₂H, I₂ gave a higher yield. The reaction was carried out in batch firstly and then transferred to flow system and scaled up. The comparison between batch and flow reactions revealed that the flow condition gave a much better efficiency, as the batch reaction took 120 hours to give a yield of 42% and flow reaction took 10 hours to give a yield of 40%. The authors also mentioned that visible-light-flow chemistry strategy avoided expensive quartz glassware and dangerous UV lamp.

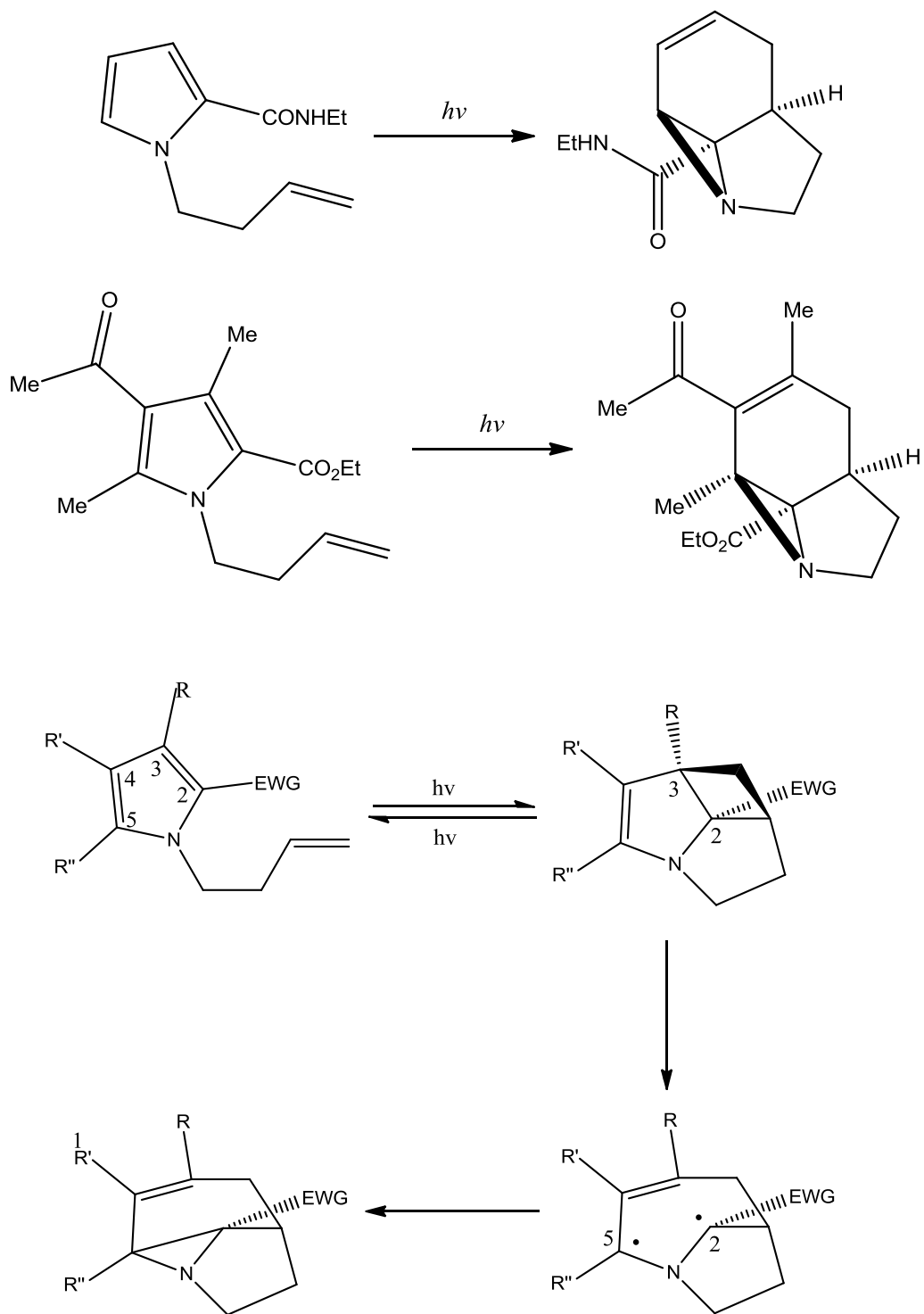
In 2013, Booker-Milburn and coworkers reported a study of photo-rearrangement of pyrroles to make tricyclic aziridines on the basis of their previous research involving 2 types of [2 + 2] cycloaddition of *N*-pentenylpyrrole derivatives to reach triene ^[71] (**Scheme 4**). The authors suggested that the mechanism of the reaction might involve the generation of di-radical intermediate, resulting from the fragmentation of C₃ – C₂ bond in the cyclobutane product of [2 + 2] cycloaddition. Followed by the C₂ – C₅ bond formation of an intermediate, the cyclized product aziridine could be achieved. In addition, the authors suggested that C₄ substitution of pyrrole might play a key role to determine the reaction rate, as non-C₄-substituted pyrroles gave full conversion of cyclobutane in the end of the reaction. With the idea of scaling up, the authors tried to transfer the batch reaction into flow. Instead of low-power lamp used in the previous study, by employing a 36 W 254 nm PL-L lamp coiled by FEP tubing, the authors made a photo-flow reactor with HPLC pumps. The optimized reaction condition ensured the reaction took one hour to produce di-methyl-substituted product with 51% yield and C₃,C₄,C₅-non-substituted pyrrole with 57% yield. The same UV lamp in batch required a customized immersion well with

specific design, flow reactor was thought to be the best choice in this scenario as it was able to synthesize over 100g product per day in a single fume hood.

Scheme 3. The general scheme and byproducts of Collins's reaction. Synthesis [5]Helicene

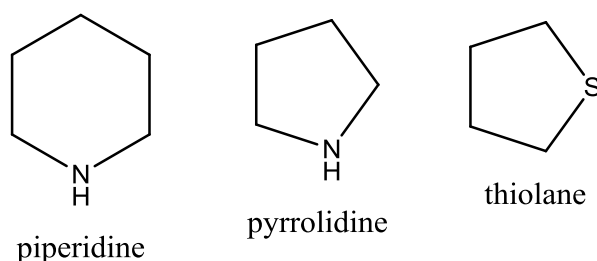


Scheme 4. General scheme of Booker-Milburn's reaction. Synthesis of tricyclic aziridines.



Non-aromatic heterocyclic compounds, e.g. piperidine, pyrrolidine, thiolane, *etc.* (**Figure 2**), are non-conjugated ring systems containing carbon and non-carbon atoms, which can be found in a great number of natural products, e.g. piperidine, nicotine, and drugs, e.g. thioridazine, levetiracetam ^[72] ^[73]. In the past decade, efforts to make heterocyclic compounds, including piperidine, pyrrolidine, under photo-flow condition involved both photocycloaddition and photocyclization.

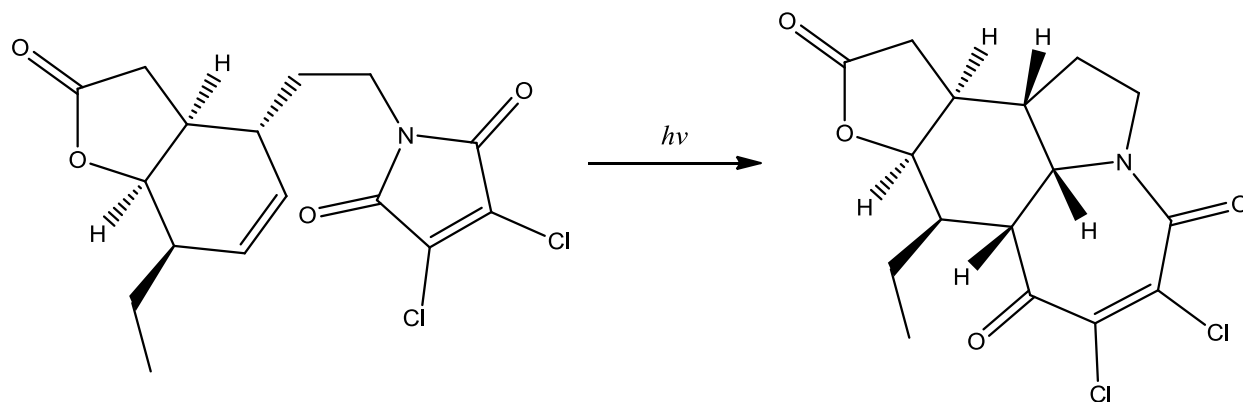
Figure 2. Non-aromatic heterocyclic compounds, e.g. piperidine, pyrrolidine, thiolane.



[5 + 2] Cycloaddition is used to make seven-member ring. According to some previous research like perezone-type [5 + 2] cycloaddition reactions, oxidopyrylium ylide [5 + 2] cycloaddition and vinylcyclopropane cycloaddition reactions, few attempts to make seven-member ring have focused on heterocyclic compounds ^[74]. Booker-Milburn team reported an easy method to make *Stemona* alkaloid (\pm)-neostenine while achieving the core motif pyrrolo[1,2-a]azepine with a [5+2]photocycloaddition performed in flow ^[75] (**Scheme 5**). The authors found that the yield of the reaction in batch was only 40%-60% in 50mg with no starting material recovery. When they scaled up, the yield was even lower. After they transferred the reaction to the flow, the yield reached 63% with 20% starting material recovery, which meant

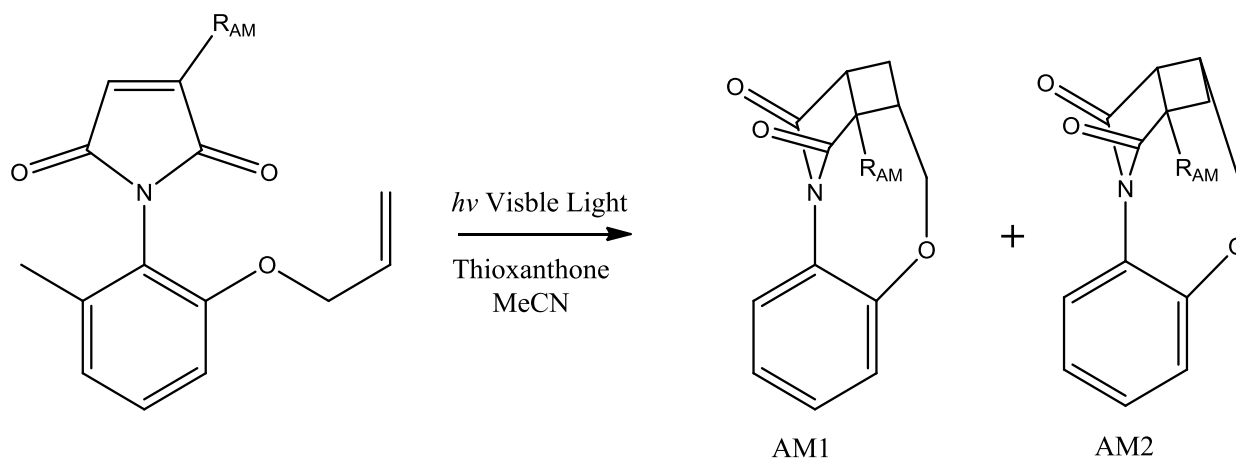
photodegrading was diminished. This result was considered meaningful as it would be a “scale-tolerant” route to prepare key photoadduct pyrrolo[1,2-a]azepine for following synthesizing steps.

Scheme 5. General scheme of Booker-Milburn’s reaction. Synthesis of (±)-neostenine



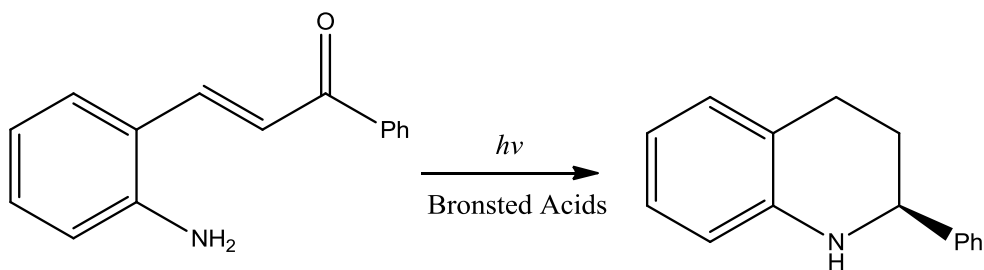
Sivaguru and coworkers have studied stereospecific, visible-light catalyzed photocycloaddition of atropisomeric maleimides with maleimides as substrate and thioxanthone as triplet sensitizer under flow conditions ^[76] (**Scheme 6**). The intramolecular [2+2] photocycloaddition were taken place between a maleimide moiety and an alkene. Due to the maleimide’s *N*-aryl substitution with a highly-restricted N–C(aryl) bond rotation, as well as preferred diradical intermediates, high enantioselectivity could be achieved in this case, especially giving a selectivity of photoproduct AM1 more than 99% over photoproduct AM2 when R_{AM} is phenyl group. Meanwhile, as maleimides could be found in some other molecules such as indolines as building blocks, with a similar reaction condition, a more complex heterocyclic compounds were expected to be synthesized chemoselectively by this approach.

Scheme 6. General scheme of Sivaguru's reaction.



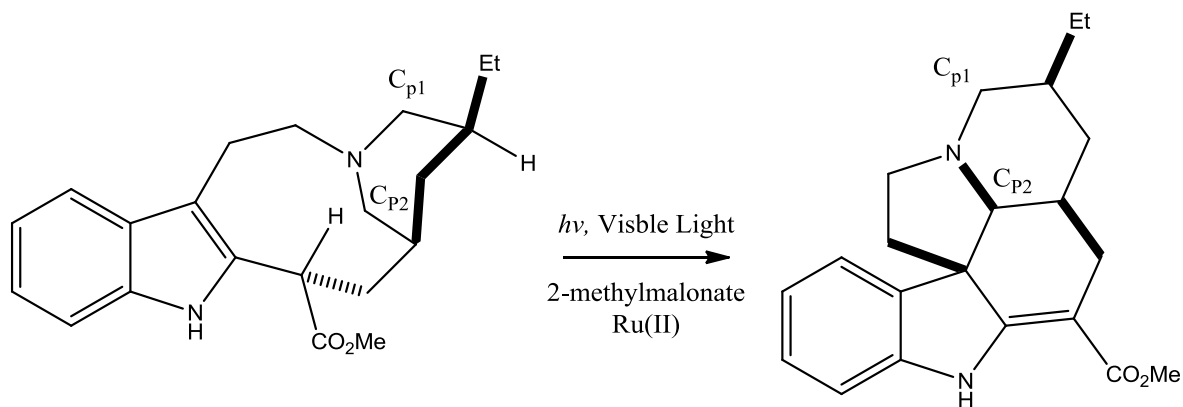
Rueping and his team reported a one-step synthesis of tetrahydroquinolines from commercial-available amino chalcone using glass microreactor accompanied with a high pressure mercury lamp ^[77] (**Scheme 7**). The asymmetric Brønsted-acid-catalyzed photocyclization-reduction reaction showed great enantiomeric selectivity (enantiomeric excess 93%) with a yield of 53% in 60min under flow condition while batch reaction only had 7% yield in the same reacting time, although the enantiomeric excess was 95%. By comparing the results from flow and batch, the authors considered it feasible to scale the reaction up. In addition, the enantioselectivity of this reaction could be observed in both substituted aromatic rings and unsubstituted ones.

Scheme 7. General scheme of Rueping's reaction. Synthesis of tetrahydroquinolines.



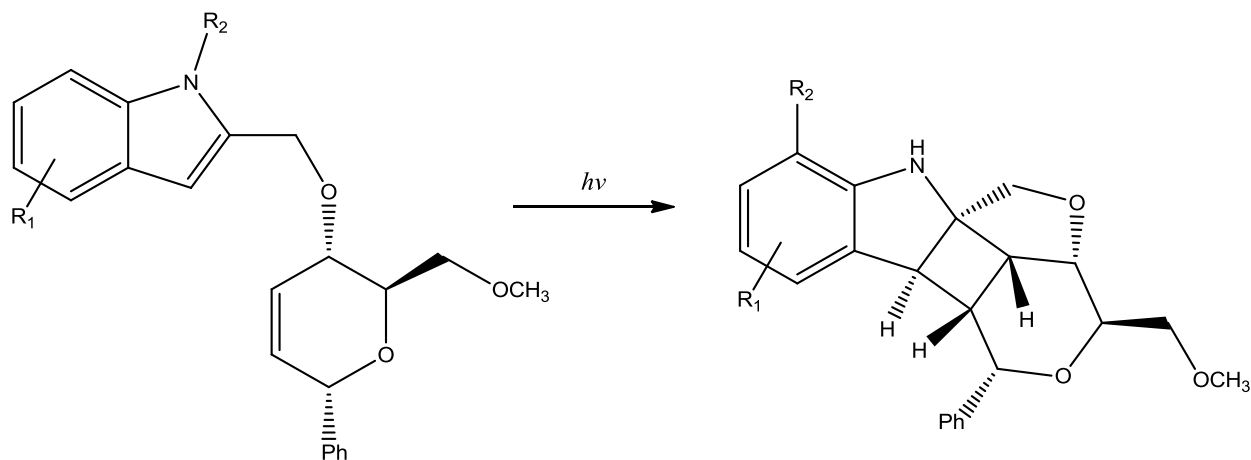
Stephenson and his laboratory members reported a semisynthesis method of natural product (-)-pseudotabersonine, (-)-pseudovincadifformine and (+)-coronaridine with highest yields to date ^[78] (**Scheme 8**). In the synthesis of (-)-pseudovincadifformine, tertiary amine underwent photoredox reaction under flow condition, oxidized by 2-methylmalonate illuminated by visible light to give the final product. Theoretically, the new pyrrolidine ring could be produced by the formation of C-C between C_{p1} or C_{p2}.

Scheme 8. General reaction of Stephenson's reaction. Synthesis of pseudotabersonine derivatives



In 2014, Beeler and co-workers presented a study based on the microfluidic-photo system they designed, which was expected to be used for multidimensional reaction screening ^[79] (**Scheme 9**). The authors indicated that this photo-optical platform show great robustness carrying out different reactions and screening for optimal conditions. The authors studied four different reactions which includes oxa-di- π -methane rearrangement, C–N bond fragmentation, 1, 3-acyl shift and [2 + 2]-cycloaddition. In the [2 + 2]-cycloaddition, the authors found that glycal-derived substrates could undergo either [2 + 2] photocycloaddition or Photo-Fries rearrangement under different wavelength to produce mixture of cyclobutane and indole and only indole product respectively. The controllable platform gave authors opportunity to optimize the reaction further, as previous reaction condition favored photo-Fries rearrangement. A cyclobutane product could be obtained in 24% yield in room temperature following 10 minutes irradiation. A longer wavelength at 290-340 nm actually favored [2 + 2] cycloaddition to afford only cyclobutane.

Scheme 9. General scheme of Beeler’s reaction.



As demonstrated above, it is possible to combine flow with photo chemistry to perform photocyclization reactions. The previous research mentioned above will be the theoretical basis of our project.

E. General Introduction of Poly (ADP-Ribose) Polymerase Inhibitor

Poly (ADP-ribose) polymerase is a large family of enzyme that is involved in DNA repair, cell recovery from DNA damage or programmed cell death in eukaryotic cells ^[80]. The major seven types of PARP that belong to the PARP superfamily include PARP-1, PARP-2, PARP-3, PARP-4, PARP-5a, PARP-5b and PARP-7 ^[80].

PARP -1 is the founding member of PARP family which has also been extensively studied. The function of PARP-1 involves DNA-damage sensor/signaling, DNA-damage-activated chromatin remodeling, transcriptional regulation and cell repair, replication, differentiation or cell death (including apoptosis and necrosis), as well as the maintenance of telomere length and the regulation of cytoskeletal organization. The mechanism of PARP-1 function in response to DNA damage, which activates DNA repair or cell death pathway by intracellular signaling, involves catalyzing and converting NAD^+ (oxidized form of nicotinamide adenine dinucleotide) into nicotinamide and ADP-ribose which is used for the synthesis of long linear or branched polymers poly(ADP-ribose). The polymers are then attached to nuclear proteins such as histone or PARP-1 itself that are mostly located on chromatin covalently. They introduce significant effects with their high negative charges on targeted protein that will affect damage signaling or DNA repair. ^{[81] [82] [84]} That is, the high negative charges on polymers make them mimic nucleic acids, which results in competition with nucleic acids ^[83]. For this feature of

PARP-1, it is considered as a potential target for cancer therapy by increasing efficacy of chemotherapy and radiotherapy.

PARP-2 shares common homology but not fully-overlapped roles with PARP-1. It is believed to associate with PARP-1 in the case of DNA-damage-activated repair. However, the PARP-2's ability to produce ADP-ribose polymer is not as good as PARP-1. PARP-2 may be involved in the nuclear and/or nucleolar^[85] targeting of the protein. Nucleolus is the largest substructure in the nucleus of eukaryotic cells^[86]. In addition, the function of PARP-2 may also function with telomere integrity control^{[81][87]}.

For most conserved binding sites, PARP-1 inhibitors can also act on PARP-2 with no discrimination. PARP-1 and PARP-2 inhibitors which are currently undergoing clinical trials have been shown to have a promising future by enhancing DNA alkylating agents' cytotoxicity (antitumor activity) and topoisomerase I poisons, as well as ionizing radiation by increasing the sensitivity of the target, and showing synthetic lethality with cells lacking homologous recombination repair function which is a common feature in cancer cells^{[84][88][89]}.

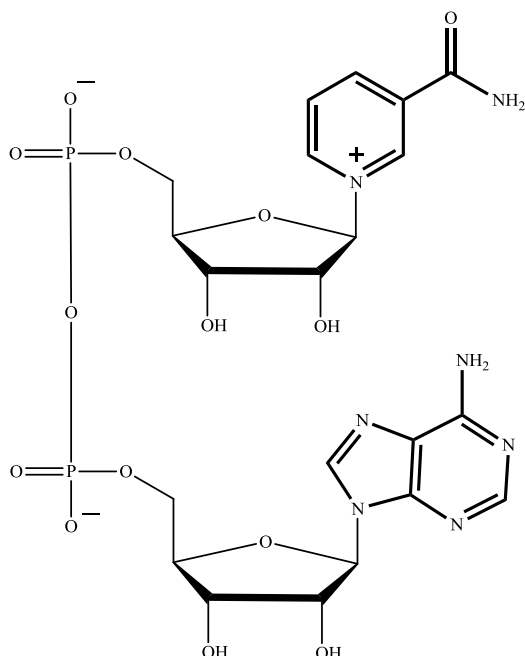
PARP-3 is a mono-ADP-ribosylase that also shares approximately 35% homology between PARP domains with highly conserved nicotinamide binding pocket and important differences in the loop around the active site. PARP-3 mainly interacts with PARP-1 and centrosomes. It helps genome maintenance. It is identified as a key component of centrosome and activating factors of PARP-1 without binding to DNA, which makes PARP-3 different from PARP-1 or PARP-2 functionally. In addition, the research suggests that PARP-3 does not involve in single-strand break, as PARP-3 siRNA-depleted cells have no sensitivity to the topoisomerase I inhibitor camptothecin^{[81][90][91]}.

PARP-4, also known as VPARP (Vault-PARP), is classified as a vault protein. It is associated with cytoplasmic ribonucleoprotein complexes and vault RNA. VPARP is capable of catalyzing a poly(ADP-ribosyl)ation reaction and it may relate with cellular transport ^{[81] [92]}.

PARP-5a and PARP-5b, known as Tankyrase((TRF1-interacting, ankyrin-related ADP-ribose polymerase) 1 and Tankyrase 2, are involved in the regulation of telomerase activity. PARP-5a has been identified to associate with human telomeric protein TRF1 (Telomeric repeat-binding factor 1). PARP-5a is believed to be involved in the centrosome clustering process forming bipolar spindle. Cancer cells in S Phase will produce three or more centrosomes leading to multipolar mitotic spindle and are unable to clustering supernumerary centrosomes into two spindles. It is believed that inhibition of PARP-5a will enable stoppage of cancer cell proliferation after S Phase. Comparing PARP-5a to PARP-5b, they share some common structure and overlapping functions. However, it has been found that PARP-5b may possess some different functions which may induce caspase-independent cell death when overexpressed ^{[81] [82] [93]}.

It is of note that the PARP family shares the same natural substrate/ligand NAD^+ . The structure of nicotinamide adenine dinucleotide (**Figure 3**) contains an adenine base and a nicotinamide, two nucleotides joined through phosphate groups ^{[80] [81]}.

Figure 3. NAD⁺, the nature ligand of PARP



By analyzing the chemical space generated by Differential Scanning Fluorimetry (DSF) ^{[94] [99]}, Elisabet Wahlberg and coworkers tried to categorize PARP inhibitors into 3 regions based on their protein-stabilization ability. These included PARP1-4 selective inhibitors, unselective inhibitors, and TNKS1-2 inhibitors. The authors demonstrated that PARP1-4 inhibitors had the most complicated structure with the highest molecular weight, and they were always hydrophilic with the greatest Polar Surface Areas (PSA); TNKS1-2 selective inhibitors had lower molecular weight while they were more hydrophobic; Non-selective inhibitors had the lowest molecular weight and shared similar hydrophilicity with PARP1-4 inhibitors. The authors assigned the selectivity to their structure and substituents, as they indicated that different PARPs created different hydrophobic/hydrophilic environment inside or outside the nicotinamide binding pocket through less conserved residues and structure. In addition, the rigidity of D-loop lids (between α -

helix 3 and β -sheet 4) (**Figure 4**) which were differed among PARP family also contributed to the selectivity ^[100]. In the narrow sense, this theory seems to be convincible. However, it is possible that polarity, rigidity, *etc.* may affect the selectivity jointly. From this aspect of view, we can find some exceptions. For example, AZ9482 (**Figure 5**) is originally developed as PARP-6 inhibitor ^[101]. However, by the research of David Scott and coworkers, AZ9482 also has potential to block TNKS1/2 activity, as well as PARP1-3, which makes this active compound an unselective inhibitor ^[102]. Shown as **Figure 5**, it has a high molecular weight.

Figure 4. Residues with different PARPs (left) and a schematic of D loop (right)^[100]. Highly conserved residues are framed in the left side. Different colors and numbers are used to point out the corresponding positions on the D-loop in the right side.

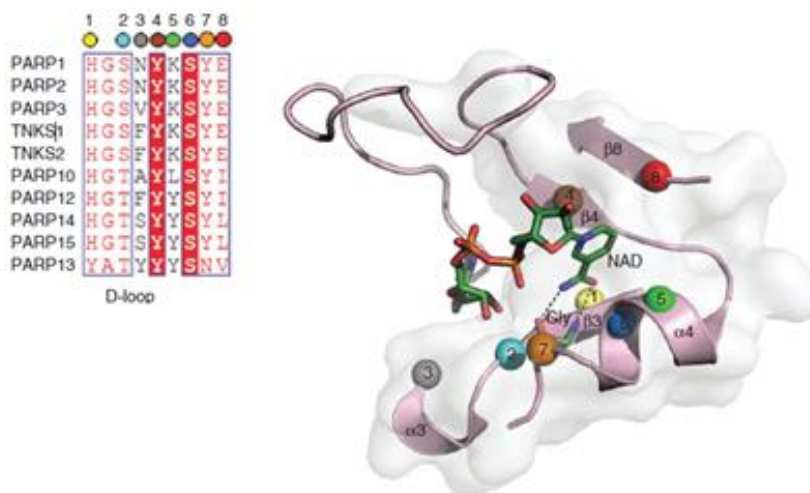
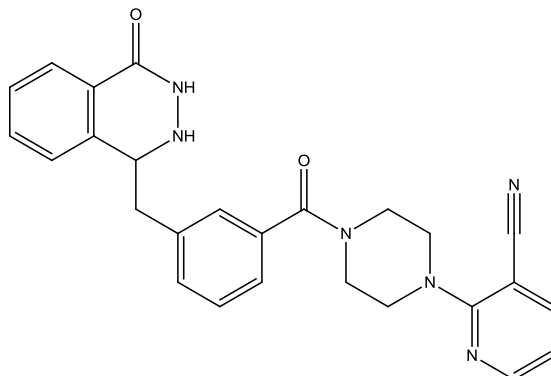


Figure 5. AZ9482, the PARP inhibitor.



Phenanthridinone (**Figure 6**) is a tricyclic compound which contains two benzene rings and an amide bond. The phenanthridinones are known as potent competitive selective/unselective PARP inhibitors. PARP inhibition by the phenanthridinones was able to induce apoptosis of tumor cells such as leukemic cells, which was demonstrated in previous studies ^{[95] [96] [97] [98]}. The competitive inhibition results from the phenanthridinones acting as mimics of the pyridine component of NAD⁺^[100]. With the studies of interactions between some phenanthridinone-type TNKS inhibitors and the TNKS receptor ^{[102] [103] [104] [105] [106]}, it was found that, in addition to mimicking the nicotinamide component of NAD⁺, phenanthridinone motif actually serves as an anchor in the binding pocket. A π -interaction is formed between a residue such as tyrosine and the aromatic ring of carbonyl component. The aromatic ring of amide nitrogen component acts through steric hindrance. The substituent on it extending to the outside of the nicotinamide binding pocket and stacking into the adenosine binding pocket is a key to determine potency and selectivity. The substituent may form additional interaction with some other residues.

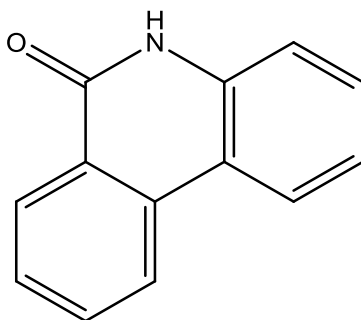
As a conclusion, developing a PARP inhibitor based on the structure of phenanthridinone is promising and novel phenanthridinone-type compounds may have great potency because of PARP inhibitory ability and it could be used as new PARP inhibitor for treatment of different kinds of diseases including cancer.

F. Synthesis of Phenanthridinone-Type Compounds

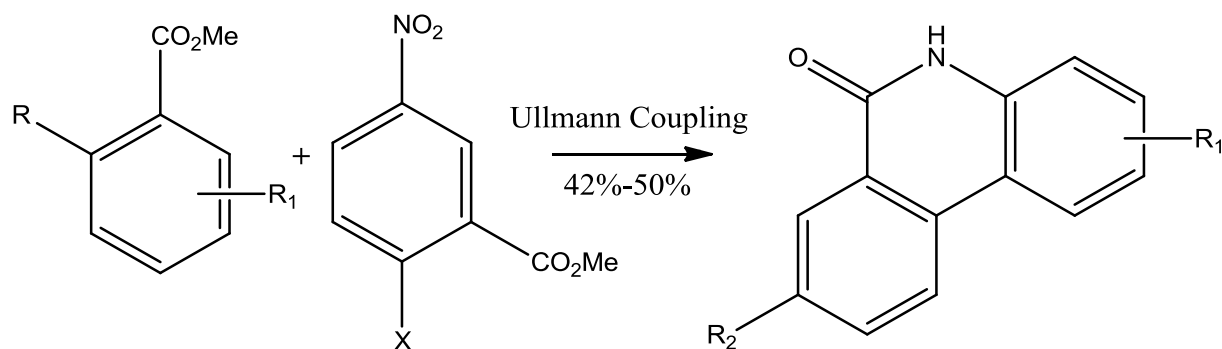
Some synthesis methods have been reviewed regarding the synthesis of phenanthridinone-type compounds. There are multiple ways to reach the desired product. However, the direct coupling reactions are the most popular ones. These direct coupling reactions include the Ullman coupling (**Scheme 10a**), the Suzuki coupling (**Scheme 10b**) and some other annulation reactions ^[107]^[108]^[109]^[110]^[111]. Most of these direct coupling reactions employ palladium catalysis. Although, some direct coupling reactions such as the Suzuki coupling reaction have been used for a while and they are well-known and robust, it is revealed that performing direct coupling reactions can be problematic in some cases. It is always high-cost to perform a reaction using reagents such as palladium catalysts and boronic acids. Meanwhile, a direct coupling reaction always requires a long reaction time, or high pressure/temperature ^[112]^[113]. Some other methods that have been reported include a one-step Schmidt reaction which is fast but potentially explosive ^[107]^[114] and a ring-closure reaction, initiated by AIBN, assisted by KO^tBu which took 14 hours ^[115]. As a result, the synthesis routes that the literatures provide are rather poor and less effective. Publication by Grimshaw revealed a photo-cyclization reaction of 2-chloro-*N*-phenylbenzamides that gave phenanthridinones by assisted hemolytic cleavage of C-Cl bond. The paper described 6 para-

substituent cyclic compounds with yields of 23%-74%. There were no further useful details about the reaction condition provided ^[116].

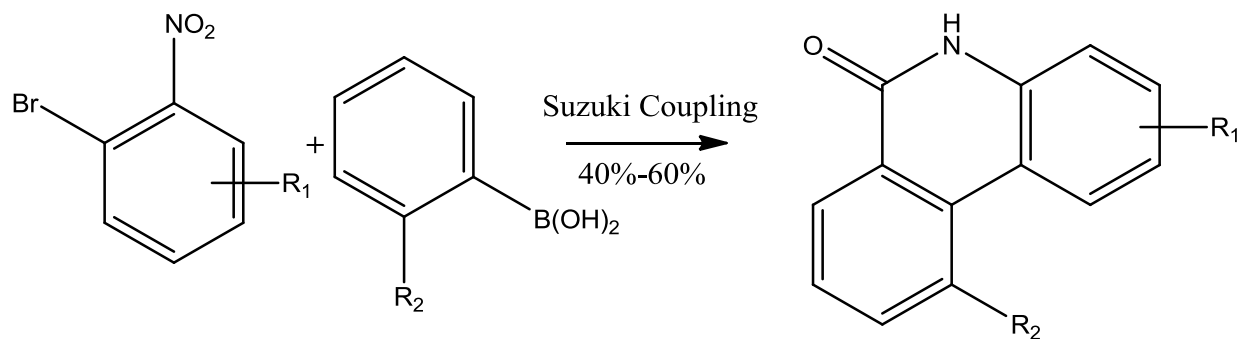
Figure 6. Phenanthridin-6(5H)-one



Scheme 10a. The Ullman coupling

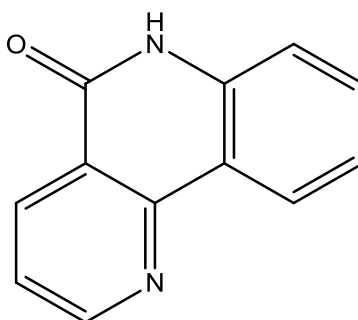


Scheme 10b. The Suzuki coupling



Benzo[*h*][1,6]naphthyridin-5(6H)-one (**Figure 7**) shares a similar component, nicotinamide, with the NAD⁺. It is also a phenanthridinone-type compound. Based on this, it is possible that the naphthyridinones are potent and selective PARP inhibitors [82].

Figure 7. Benzo[*h*][1,6]naphthyridin-5(6H)-one

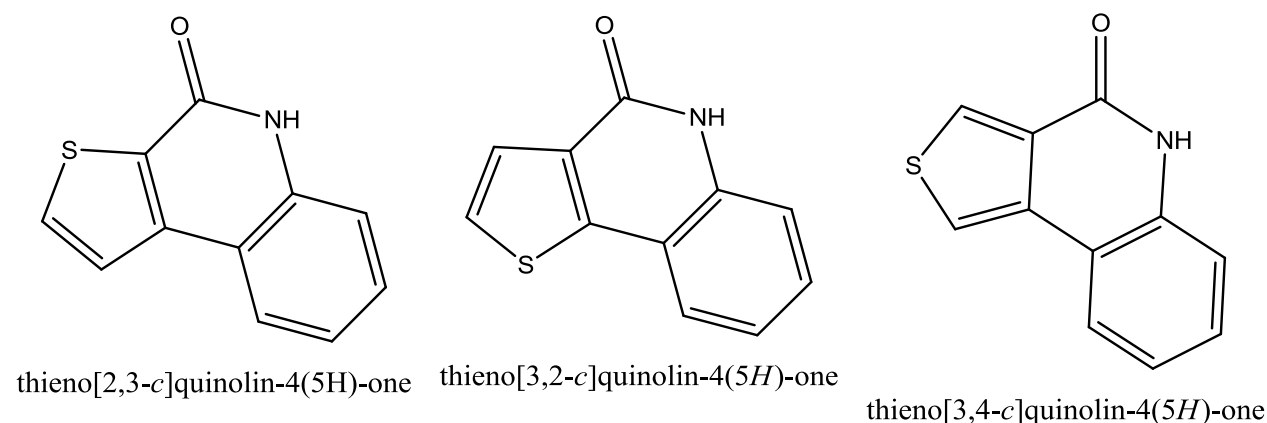


Most synthesis pathways of naphthyridinones can be categorized as direct coupling reactions. A typical reaction that is used is a Suzuki coupling reaction. Introduced by Rault, the authors were able to synthesize the naphthyridinones in two steps using a Suzuki coupling reaction with a yield of around 80% [117]. The reaction starts from 2-fluorophenylboronic acid followed by a formation of a C–C bond. The Suzuki reaction was assisted by microwave to shorten the reaction time from 24-36 hours to 30 min. It was a successful attempt as the Suzuki coupling reaction had proved to be robust for most cases. However the problem remained, as the reaction required boronic acid and nicotinonitrile as starting materials. These reagents can be expensive and toxic, and numerous steps are needed to create the required boronic acids and heteroaryl halides required for the reaction. Lautar also used similar strategy for the synthesis of aza-5[*h*]-phenanthridin-6-ones [118].

For other derivatives of the naphthridinone, Wang introduced an iodine-catalyzed pathway to get dibenzo[*b,h*][1,6]-naphthyridine-11-carboxamides ^[119]. The reaction used 2-aminobenzamides and mucobromic acid. This method took 10 steps to reach the final product with a low yield. Rajendran introduced a synthesis pathway of benzo[*b*] indazolo[6,7-*h*] [1,6] naphthyridines, which started from 3-(6'-amido indazolo quinoline-2[1H]-ones ^[120]. The amide was treated with polyphosphoric acid at 150 °C for 5 hours with yields of 60%-80%. Said introduced a synthesis pathway to produce 5,10-Dimethyl-8H-benzo[*h*]chromeno[2,3-*b*][1,6]naphthyridine-6(5H)-8-dione ^[121]. The reaction was carried out between 2-amino-6-methylchromone-3-carboxaldehyde and 4-hydroxy-1-methylquinolin-2(1H)-one, catalyzed by DBU, with a yield of 57%. All these reactions above are less effective, slow and low-yield.

Thiophene, a classical bioisostere of pyridine and benzene, makes thieno-quinolinone a rationale structure to develop into new PARP inhibitors ^{[122] [123]}. There are three kinds of phenanthridinone-type thieno-quinolinones including thieno[2,3-*c*]quinolin-4(5H)-ones, thieno[3,2-*c*]quinolin-4(5H)-ones, thieno[3,4-*c*]quinolin-4(5H)-ones (**Figure 8**).

Figure 8. Three types of thieno-quinolinones



Synthesis of thieno[2,3-*c*]quinolin-4(5H)-ones from corresponding amides can be dated back to the 1980s, which was first introduced by Mallory^[63]. In the study, the authors used oxygen as the oxidant and benzene with EtOH as the solvent, in the presence of ultraviolet irradiation to produce the desired product. In the last decades, different synthetic pathways to produce several derivatives of thieno[2,3-*c*]quinolin-4(5H)-one have been published^{[124] [125]} and the bioactivity has been well discussed^{[126] [127]}. According to the research mentioned above, the thieno[2,3-*c*]quinolin-4(5H)-one motif has shown great potency and selectivity regarding PARP inhibition.

Compared to thieno[2,3-*c*]quinolin-4(5H)-ones, neither the synthetic methods required to construct, nor the pharmacological activity of thieno[3,2-*c*]quinolin-4(5H)-ones have been studied to any extent. Currently, the literature only describes three ways to synthesize thieno[3,2-*c*]quinolin-4(5H)-ones. The first one employs the Ullmann coupling reaction, which forms a C–C bond first, followed by the closure of the ring^[128]. For the second method, only a single example exists in the literature of the direct conversion of a phenyl-2-halothiophene carboxamide to yield the corresponding thieno[3,2-*c*]quinolin-4(5H)-ones via a radical initiated by AIBN, assisted by KO^tBu under high temperature conditions and this method took 14 h to get a yield of around 75%^[115]. It is highly possible that our flow method can be much more efficient^[114]. The third example starts from aniline and produces 4-oxo-4,5-dihydrothieno[3,2-*c*]quinoline-2-carboxylic acid through the Friedel-Crafts reaction, the Vilsmeier-Haack reaction, and a S_NAr cyclization reaction with a yield of 50%. The last method is very complicated and it takes 20 hours to get the final product^[129]. Overall, the literature describes very few methods for the synthesis of thieno[3,2-*c*]quinolin-4(5H)-ones, and new methods are urgently required to

produce biologically active molecules that possess this core structure, as potential PARP inhibitors.

As with thieno[3,2-*c*]quinolin-4(5H)-ones, the synthesis of thieno[3,4-*c*]quinolin-4(5H)-ones lacks an efficient pathways to access this core structure. Even though thieno[3,4-*c*]quinolin-4(5H)-ones could be valuable to synthesize as potential PARP inhibitors, we found that the starting materials for amidation, thiophene-3-carboxylic acids, are very expensive and we choose to focus on substrate with lower cost starting materials initially, and pursue the production of thieno[3,4-*c*]quinolin-4(5H)-ones via a flow photochemical cyclization at in our future study.

As a conclusion, although conventional coupling techniques are well-known and mature, the traditional ways to synthesize phenanthridinone-type compounds are less effective and costly. Also, these methods are limited and they cannot be used to synthesize some certain types of compounds. It holds great promise to develop a new method to synthesize phenanthridinone-type compounds with a cheap and effective way.

II. Hypothesis and Objectives

As stated previously, current methods, including the use of Suzuki coupling reactions to synthesize phenanthridinone-type compounds are costly and possess low-efficiency, and provides limited access (smaller scope) to potential products. Phenanthridinone-type compounds could find very promising uses as PARP inhibitors, with potential indications to treat different diseases including cancer, a novel pathway to synthesize phenanthridinone-type compounds would surely benefit drug development. Flow chemistry techniques have been shown to offer superior efficiency and ability to scale up in organic chemical synthesis. We propose that flow-photocyclization reactions would be a better way to produce phenanthridinone-type compounds, which would be more cost-effective, scaleable and efficient.

In order to be able to synthesize novel phenanthridinone-type compounds, our aim for this project was to develop a practical flow synthesis method first and then apply it to produce a library of phenanthridinone-type compounds to demonstrate its robustness and efficiency. Meanwhile, we would try to produce some novel phenanthridinone-type compounds for future development as PARP inhibitors.

III. Experimental Information

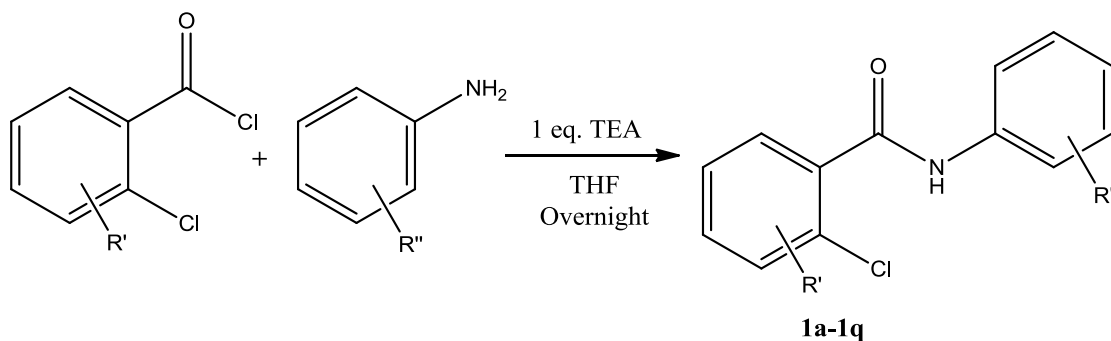
A. Procedure for Synthesizing Starting Materials

1. Synthesis of 2-chloro-*N*-phenylbenzamides

a. General Procedure

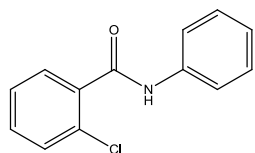
A summary of the synthesis of 2-chloro-*N*-phenylbenzamides is represented in **Scheme 11**. A round-bottom flask with magnetic stir-bar was cleaned and oven-dried. The corresponding acyl chloride (1.1 equiv.) and aniline (1 equiv.) were dissolved in tetrahydrofuran (THF) (5mL per 1mmol reagent) respectively to make two solutions, one of acyl chloride and one of the aniline. The solution of aniline was introduced to the flask and stirred in ice bath at 0°C for 5 minutes. Triethylamine (1 equiv.) was added to the solution of aniline followed by addition of the solution of acyl chloride drop by drop at 0°C. The resulting reaction mixture was stirred at r.t. for overnight after removing the ice bath. The resulting product was filtered twice to remove the solid which was washed by THF. THF was then removed from the solution of crude product by vacuum and the residue was loaded on silica gel, separated and purified by column chromatography (CombiFlash[®] Rf). The purified product was then dried under vacuum.

Scheme 11. General Synthesis Procedure of 2-chloro-*N*-phenylbenzamides



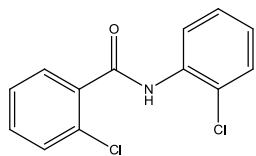
b. Detailed Procedure

2-chloro-*N*-phenylbenzamide (**1a**)



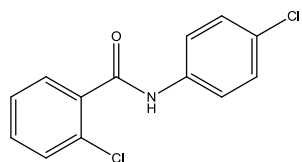
Aniline (93.2 mg, 1 mmol) and 2-chlorobenzoyl chloride (195 mg, 1.11 mmol) were treated according to the general procedure. Purification by CombiFlash[®] Rf afforded the title compound (230 mg, 99%) as a white crystalline solid. $R_f=0.61$ (40% Ethyl acetate/hexane). ^1H NMR (400 MHz, CDCl_3) δ 8.68 (s, 1H), 7.63 (d, $J=7.7$ Hz, 2H), 7.47 (dd, $J=7.6, 1.4$ Hz, 1H), 7.34-7.26 (m, 4H), 7.20 (dt, $J=7.4, 1.6$ Hz, 1H), 7.13 (t, $J=7.2$ Hz, 1H). ^{13}C NMR (100 MHz, CDCl_3) δ 164.52, 137.56, 135.21, 131.72, 130.63, 130.39, 130.35, 129.15, 127.32, 124.89, 120.15.

2-chloro-*N*-(2-chlorophenyl)benzamide (**1b**)



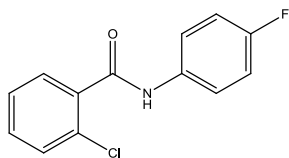
2-chloroaniline (128 mg, 1 mmol) and 2-chlorobenzoyl chloride (194 mg, 1.1 mmol) were treated according to the general procedure. Purification by CombiFlash[®] Rf afforded the title compound (265 mg, 99%) as an off white solid. $R_f=0.77$ (40% Ethyl acetate/hexane). $^1\text{H NMR}$ (400 MHz, CDCl_3) δ 8.60 (d, $J=8.1$ Hz, 1H), 8.52 (s, 1H), 7.84 (dd, $J=7.4, 1.5$ Hz, 1H), 7.55 – 7.40 (m, 4H), 7.37 (t, $J=7.8$ Hz, 1H), 7.13 (td, $J=7.8, 1.5$ Hz, 1H). $^{13}\text{C NMR}$ (101 MHz, CDCl_3) δ 164.35, 134.77, 134.54, 132.02, 130.79, 130.61, 130.61, 129.18, 127.84, 127.37, 125.13, 123.18, 121.82.

2-chloro-*N*-(4-chlorophenyl)benzamide (**1c**)

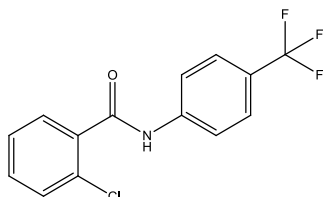


4-chloroaniline (127.6 mg, 1 mmol) and 2-chlorobenzoyl chloride (193 mg, 1.1 mmol) were treated according to the general procedure. Purification by CombiFlash[®] Rf afforded the title compound (231 mg, 99%) as a white crystalline solid. $R_f=0.64$ (40% Ethyl acetate/hexane). $^1\text{H NMR}$ (400MHz, DMSO-d_6): δ 10.66 (s, 1H), 7.76 (d, $J=8.8\text{Hz}$, 2H), 7.61-7.45 (m, 4H), 7.42 (d, $J=8.8\text{Hz}$, 2H) $^{13}\text{C NMR}$ (100 MHz, DMSO-d_6) δ 165.47, 138.33, 137.17, 131.71, 130.36, 130.15, 129.40, 129.19, 127.88, 127.77, 121.55.

2-chloro-*N*-(4-fluorophenyl)benzamide (**1d**)

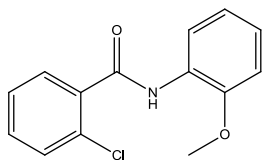


4-Fluoroaniline (111 mg, 1 mmol) and 2-chlorobenzoyl chloride (202mg, 1.2 mmol) were treated according to the general procedure. Purification by CombiFlash[®] Rf afforded the title compound (213mg, 99%) as white crystalline solid. $R_f=0.64$ (40% Ethyl acetate/hexane). ^1H NMR (400 MHz, CDCl_3) δ 7.97 (s, 1H), 7.76 (dd, $J = 7.4, 1.7$ Hz, 1H), 7.66 – 7.58 (m, 2H), 7.50 – 7.36 (m, 3H), 7.13 – 7.05 (m, 2H). ^{13}C NMR (101 MHz, CDCl_3) δ 164.49, 159.72 (d, $J = 243$ Hz), 134.92, 133.52 (d, $J = 2.8$ Hz), 131.83, 130.60, 130.41 (d, $J = 2.5$ Hz), 127.36, 122.07, 121.99, 115.82 (d, $J = 22.6$ Hz). 2-chloro-*N*-(4-(trifluoromethyl)phenyl)benzamide (**1e**)



4-(Trifluoromethyl)aniline (161 mg, 1 mmol) and 2-chlorobenzoyl chloride (201mg, 1.1 mmol) were treated according to the general procedure. Purification by CombiFlash[®] Rf afforded the title compound (272 mg, 91%) as a white crystalline solid. $R_f=0.60$ (40% Ethyl acetate/hexane). ^1H NMR (400 MHz, CDCl_3) δ 8.15 (s, 1H), 7.79 (t, $J = 7.2$ Hz, 3H), 7.65 (d, $J = 8.5$ Hz, 2H), 7.51 – 7.37 (m, 3H). ^{13}C NMR (101 MHz, CDCl_3) δ 164.67, 140.55, 134.57, 132.14, 130.59, 130.52, 127.46, 126.63 (q, $J = 32.3$ Hz), 126.42 (q, $J = 3.8$ Hz), 124.03 (q, $J = 269.8$ Hz), 120.89, 119.73.

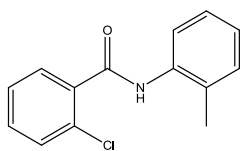
2-chloro-*N*-(2-methoxyphenyl)benzamide (**1f**)



2-Methoxy-benzenamine (123 mg, 1 mmol) and 2-chlorobenzoyl chloride (193 mg, 1.1 mmol) were treated according to the general procedure.

Purification by CombiFlash[®] Rf afforded the title compound (253 mg, 97%) as a white crystalline solid. $R_f=0.68$ (40% Ethyl acetate/hexane). $^1\text{H NMR}$ (400 MHz, DMSO- d_6) δ 9.63 (s, 1H), 7.93 (d, $J = 7.9$ Hz, 1H), 7.59-7.43(m, 4H), 7.17 (t, 1H), 7.09 (d, $J = 7.7$ Hz, 1H), 6.98 (t, $J = 7.5$ Hz, 1H) 3.82 (s, 3H). $^{13}\text{C NMR}$ (101 MHz, DMSO- d_6) δ 165.37, 151.20, 137.13, 131.53, 130.44, 130.13, 129.64, 127.62, 127.17, 125.98, 123.61, 120.70, 111.98, 56.22.

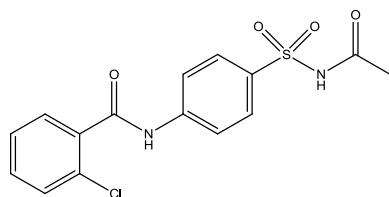
2-chloro-*N*-(2-methylphenyl)benzamide (**1g**)



o-Toluidine (108 mg, 1 mmol) and 2-chlorobenzoyl chloride (202 mg, 1.15 mmol) were treated according to the general procedure. Purification by

CombiFlash[®] Rf afforded the title compound (241 mg, 99%). $R_f=0.61$. $^1\text{H NMR}$ (400 MHz, CDCl_3) δ 8.04 (d, $J = 8.0$ Hz, 1H), 7.86 (dd, $J = 7.3, 2.0$ Hz, 1H), 7.84 (s, 1H, NH), 7.51 – 7.40 (m, 3H), 7.33 – 7.25 (m, 2H), 7.16 (t, $J = 7.1$ Hz, 1H), 2.38 (s, 3H). $^{13}\text{C NMR}$ (101 MHz, DMSO) δ 165.57, 137.55, 136.23, 133.46, 131.40, 130.87, 130.37, 130.10, 129.45, 127.69, 126.47, 126.43, 126.42, 18.47.

N-(4-(*N*-acetylsulfamoyl)phenyl)-2-chlorobenzamide (**1h**)

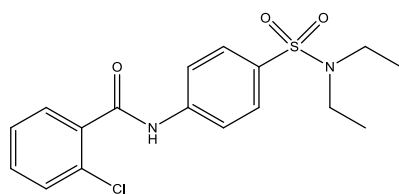


N-((4-aminophenyl)sulfonyl)acetamide and 2-chlorobenzoyl chloride were treated according to the general procedure.

Purification by CombiFlash[®] Rf afforded the title compound.

$R_f=0.61$ (40% Ethyl acetate/hexane). ¹H NMR (400 MHz, DMSO-*d*₆) δ 12.03 (d, $J = 3.7$ Hz, 1H), 10.98 (d, $J = 5.7$ Hz, 1H), 7.97 – 7.86 (m, 4H), 7.66 – 7.44 (m, 4H), 1.93 (t, $J = 5.0$ Hz, 3H). ¹³C NMR (101 MHz, DMSO-*d*₆) δ 169.17, 165.97, 143.78, 136.84, 134.10, 131.94, 130.36, 130.19, 129.45, 129.42, 127.82, 119.60, 23.67.

2-chloro-*N*-(4-(*N,N*-diethylsulfamoyl)phenyl)benzamide (**1i**)

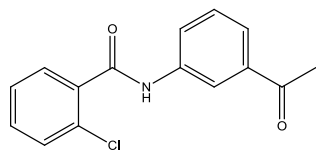


4-amino-*N,N*-diethylbenzenesulfonamide and 2-chlorobenzoyl chloride were treated according to the general procedure.

Purification by CombiFlash[®] Rf afforded the title compound.

$R_f=0.61$ (40% Ethyl acetate/hexane). ¹H NMR (400 MHz, DMSO) δ 10.90 (s, 1H), 7.93 (d, $J = 8.7$ Hz, 1H), 7.79 (d, $J = 8.8$ Hz, 1H), 7.63 (dd, $J = 7.4, 1.6$ Hz, 1H), 7.59 (dd, $J = 7.9, 0.9$ Hz, 1H), 7.54 (td, $J = 7.7, 1.8$ Hz, 1H), 7.48 (td, $J = 7.3, 1.3$ Hz, 1H), 3.16 (q, $J = 7.1$ Hz, 4H), 1.05 (t, $J = 7.1$ Hz, 6H). ¹³C NMR (101 MHz, DMSO) δ 165.88, 142.93, 136.92, 134.76, 131.88, 130.37, 130.19, 129.45, 128.41, 127.79, 119.95, 42.26, 14.57.

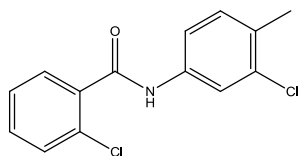
N-(3-acetylphenyl)-2-chlorobenzamide (**1j**)



3'-Aminoacetophenone (135 mg, 1 mmol) and 2-chlorobenzoyl (194 mg, 1.1 mmol) were treated according to the general procedure.

Purification by CombiFlash[®] Rf afforded the title compound (251 mmg, 92%). $R_f=0.44$. $^1\text{H NMR}$ (400 MHz, DMSO- d_6) δ 10.73 (s, 1H), 8.34 (s, 1H), 7.96 (d, $J=8.1$ Hz, 1H), 7.74 (d, $J=7.8$ Hz, 1H), 7.61 (ddd, $J=11.2, 7.6, 1.5$ Hz, 2H), 7.57 – 7.45 (m, 3H), 2.59 (s, 3H). $^{13}\text{C NMR}$ (101 MHz, DMSO- d_6) δ 198.09, 165.65, 139.74, 137.85, 137.15, 131.73, 130.38, 130.17, 129.73, 129.42, 127.77, 124.48, 124.36, 119.22, 27.24.

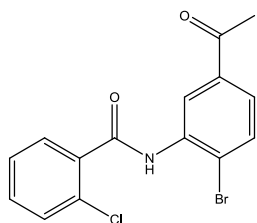
2-chloro-*N*-(3-chloro-4-methylphenyl)benzamide (**1k**)



3-chloro-4-methyl-benzenamine (142 mg, 1 mmol) and 2-chlorobenzoyl chloride (193 mg, 1.1 mmol) were treated according to the general procedure. Purification by CombiFlash[®] Rf afforded the

title compound S13 (280 mg, 99%) as a white crystalline solid. $R_f=0.65$ (40% Ethyl acetate/hexane). $^1\text{H NMR}$ (400MHz, DMSO- d_6): δ 10.62 (s, 1H), 7.91 (s, 1H), 7.61-7.57(m, 2H), 7.55-7.45 (m, 3H), 7.33 (d, $J=8.5$ Hz, 1H), 2.30 (s, 3H). $^{13}\text{C NMR}$ (100 MHz, DMSO- d_6) δ 165.46, 138.48, 137.12, 133.50, 131.72, 130.98, 130.37, 130.16, 129.40, 127.77, 119.91, 118.64, 19.47.

N-(5-acetyl-2-bromophenyl)-2-chlorobenzamide



3'-Amino-4'-bromoacetophenone (214 mg, 1 mmol) and 2-chlorobenzoyl

(193 mg, 1.1 mmol) were treated according to the general procedure.

Purification by CombiFlash[®] Rf afforded the title compound (349 mg,

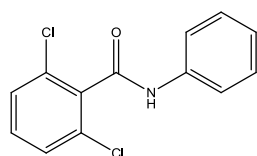
99%). $R_f=0.58$. $^1\text{H NMR}$ (400 MHz, CDCl_3) δ 9.19 (s, 1H), 8.59 (s, 1H),

7.86 (d, $J = 8$ Hz, 1H), 7.72 (d, $J = 8.4$ Hz, 1H), 7.67 (dd, $J = 8.4, 2.0$ Hz, 1H), 7.56 - 7.42 (m,

3H), 2.68 (s, 3H). $^{13}\text{C NMR}$ (100 MHz, CDCl_3) δ 197.23, 137.22, 136.05, 134.34, 132.80,

132.32, 130.79, 130.73, 127.49, 124.71, 122.08, 119.19, 118.75, 114.64, 26.77.

2,6-Dichloro-*N*-phenylbenzamide (**II**)



Aniline (95.8 mg, 1.03 mmol) and 2,6-dichlorobenzoyl chloride (210 mg, 1

mmol) were treated according to the general procedure. Purification by

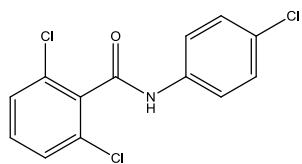
S11 CombiFlash[®] Rf afforded the title compound (255 mg, 96%). $R_f=0.57$

(40% Ethyl acetate/hexane). $^1\text{H NMR}$ (400 MHz, CDCl_3) δ 7.65 (d, $J = 7.6$ Hz, 2H), 7.53 (s, 1H),

7.44 - 7.36 (m, 4H), 7.32 (dd, $J = 9.3, 6.5$ Hz, 1H), 7.22 (dd, $J = 9.1, 5.8$ Hz, 1H). $^{13}\text{C NMR}$ (101

MHz, CDCl_3) δ 162.47, 137.17, 135.89, 132.44, 130.98, 129.19, 128.19, 125.22, 120.35.

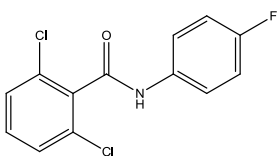
2,6-Dichloro-*N*-(4-chlorophenyl)benzamide (**1m**)



4-chloroaniline (127.8 mg 1mmol), and 2,6-dichlorobenzoyl chloride (209 mg, 1 mmol) were treated according to the general procedure.

Purification by CombiFlash[®] Rf afforded the title compound (254 mg 85%) as a white crystalline solid. $R_f = 0.58$ (40% Ethyl acetate/hexane). $^1\text{H NMR}$ (400 MHz, DMSO- d_6) δ 10.91 (s, 1H), 7.76 – 7.70 (m, 2H), 7.63 – 7.57 (m, 2H), 7.55 – 7.49 (m, 1H), 7.47 – 7.41 (m, 2H). $^{13}\text{C NMR}$ (101 MHz, DMSO- d_6) δ 162.60, 137.92, 136.56, 132.02, 131.62, 129.36, 128.76, 128.23, 121.52.

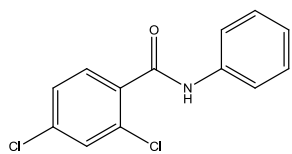
2,6-Dichloro-*N*-(4-fluorophenyl)benzamide (**1n**)



4-Fluoroaniline (115mg, 1mmol) and 2,6-dichlorobenzoyl chloride (216mg, 1mmol) were treated according to the general procedure.

Purification by CombiFlash[®] Rf afforded the title compound (282 mg, 96%) as a white crystalline solid. $^1\text{H NMR}$ (400 MHz, MeOD) δ 7.72 – 7.66 (m, 2H), 7.47 (m, 3H), 7.17 – 7.10 (m, 2H). $^{13}\text{C NMR}$ (100 MHz, MeOD) δ 163.71, 159.69 (d, $J = 241$ Hz), 136.10, 134.20 (d, $J = 2.8$ Hz), 131.90, 130.96, 127.92, 121.91 (d, $J = 7.9$ Hz), 115.09 (d, $J = 22.5$ Hz).

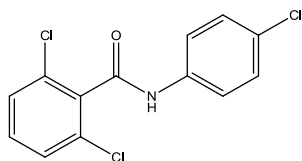
2,4-Dichloro-*N*-(4-chlorophenyl)benzamide (**1o**)



4-chloroaniline (127.7 mg 1 mmol) and 2,4-dichlorobenzoyl chloride (213 mg, 1 mmol) were treated according to the general procedure.

Purification by CombiFlash[®] Rf afforded the title compound (290 mg, 97%) as a white crystalline solid. $R_f = 0.71$ (40% Ethyl acetate/hexane). $^1\text{H NMR}$ (400 MHz, CDCl_3) δ 7.98 (s, 1H), 7.72 (d, $J = 8.3$ Hz, 1H), 7.65 (d, $J = 7.9$ Hz, 2H), 7.49 (d, $J = 1.4$ Hz, 1H), 7.45 – 7.35 (m, 3H), 7.21 (t, $J = 7.4$ Hz, 1H). $^{13}\text{C NMR}$ (101 MHz, CDCl_3) δ 163.49, 137.33, 137.26, 133.52, 131.47, 130.21, 129.20, 129.20, 129.20, 127.76, 125.10, 120.21, 120.21.

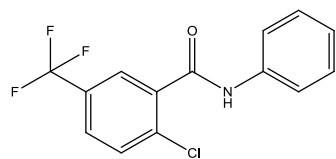
2,4-Dichloro-*N*-(4-chlorophenyl)benzamide (**1p**)



4-chloroaniline (127.7 mg 1 mmol) and 2,4-dichlorobenzoyl chloride (213 mg, 1 mmol) were treated according to the general procedure.

Purification by CombiFlash[®] Rf afforded the title compound (290 mg, 97%) as a white crystalline solid. $R_f = 0.72$ (40% Ethyl acetate/hexane). $^1\text{H NMR}$ (400 MHz, DMSO-d_6) δ 10.70 (s, 1H), 7.79 (d, $J = 1.5$ Hz, 1H), 7.74 (d, $J = 8.7$ Hz, 2H), 7.66 (d, $J = 8.2$ Hz, 1H), 7.57 (dd, $J = 8.2, 1.4$ Hz, 1H), 7.43 (d, $J = 8.7$ Hz, 2H). $^{13}\text{C NMR}$ (100 MHz, DMSO-d_6) δ 164.55, 138.14, 135.96, 135.47, 131.69, 130.83, 129.71, 129.24, 128.04, 127.98, 121.58.

2-chloro-*N*-phenyl-5-(trifluoromethyl)benzamide (**1q**)



Aniline (96.4 mg 1.04 mmol) and 2-chloro-5-(trifluoromethyl)benzoyl chloride (243 mg 1 mmol) were treated according to the general procedure. Purification by CombiFlash[®] Rf afforded the title compound (290 mg, 97%) as brown crystalline solid. $R_f = 0.72$ (40% Ethyl acetate/hexane). $^1\text{H NMR}$ (400 MHz, CDCl_3) δ 8.04 (d, $J = 1.5$ Hz, 1H), 7.94 (s, 1H), 7.71 – 7.59 (m, 4H), 7.42 (t, $J = 7.9$ Hz, 2H), 7.23 (t, $J = 7.4$ Hz, 1H). $^{13}\text{C NMR}$ (101 MHz, CDCl_3) δ 163.06, 137.11, 135.94, 134.44, 131.10, 130.00 (q, $J = 34$ Hz), 129.25, 128.27 (q, $J = 3.6$ Hz), 127.50 (q, $J = 3.8$ Hz), 125.32, 123.22 (q, $J = 271$ Hz), 120.28.

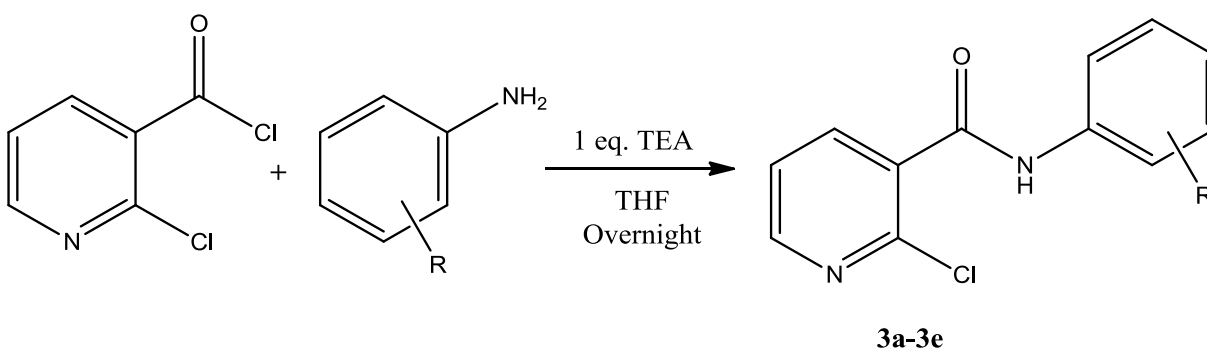
2. Synthesis of 2-chloro-*N*-phenylnicotinamides

a. General Procedure

A summary of the reaction is represented in **Scheme 12**. A round-bottom flask with magnetic stir-bar was cleaned and oven-dried. The corresponding acyl chloride (1.1 equiv.) and aniline (1 equiv.) were dissolved in tetrahydrofuran (THF) (5mL per 1mmol reagent) respectively to make two solutions, one of acyl chloride and one of the aniline. The solution of aniline was introduced to the flask and stirred in ice bath at 0°C for 5 minutes. Triethylamine (1 equiv.) was added to the solution of aniline followed by addition of the solution of acyl chloride drop by drop at 0°C. The resulting reaction mixture was stirred at r.t. for overnight after removing the ice bath. The resulting product was filtered twice to remove the solid which was washed by THF. THF was then removed from the solution of crude product by vacuum and the residue was loaded on silica

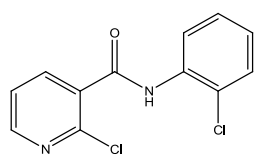
gel, separated and purified by column chromatography (CombiFlash[®] Rf). The purified product was then dried under vacuum.

Scheme 12. General Synthesis Procedure of 2-chloro-*N*-phenylnicotinamides



b. Detailed Procedure

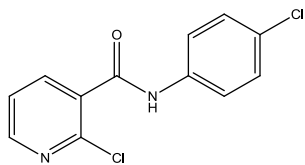
2-chloro-*N*-(2-chlorophenyl)nicotinamide (**1a**)



2-chloroaniline (128 mg, 1 mmol) and 2-chloronicotinoyl chloride (183 mg, 1 mmol) were treated according to the general procedure. Purification by CombiFlash[®] Rf afforded the title compound (230 mg, 86%) as a white

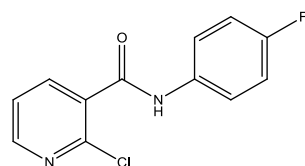
crystalline solid. $R_f=0.44$ (50% Ethyl acetate/hexane). ^1H NMR (400 MHz, CDCl_3) δ 8.83 (s, 1H, NH), 8.57 (m, 2H), 8.29 (dd, $J=7.7, 1.7$ Hz, 1H), 7.46 (m, 2H), 7.38 (t, $J=7.6$ Hz, 1H), 7.16 (td, $J=7.9, 1.4$ Hz, 1H). ^{13}C NMR (101 MHz, CDCl_3) δ 162.47, 151.61, 147.06, 140.43, 134.21, 130.96, 129.31, 127.87, 125.57, 123.47, 123.00, 121.97.

2-chloro-*N*-(4-chlorophenyl)nicotinamide (**1b**)



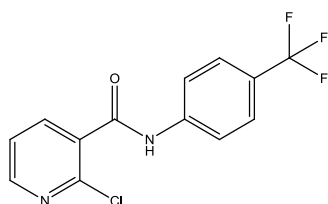
4-chloroaniline (128 mg, 1 mmol) and 2-chloronicotinoyl chloride (185 mg, 1 mmol) were treated according to the general procedure. Purification by CombiFlash[®] Rf afforded the title compound (245 mg, 92%) as a white crystalline solid. $R_f=0.25$ (50% Ethyl acetate/hexane). ^1H NMR (400 MHz, CDCl_3) δ 8.53 (dd, $J = 4.7, 1.9$ Hz, 1H), 8.27 (s, 1H, NH), 8.21 (dd, $J = 7.7, 1.9$ Hz, 1H), 7.62 (d, $J = 8.8$ Hz, 2H), 7.42 (dd, $J = 7.7, 4.8$ Hz, 1H), 7.40 – 7.36 (d, $J = 8.8$ Hz, 2H). ^{13}C NMR (101 MHz, CDCl_3) δ 162.54, 151.49, 146.91, 140.13, 135.70, 131.08, 130.41, 129.28, 123.01, 121.56.

2-chloro-*N*-(4-fluorophenyl)nicotinamide (**1c**)



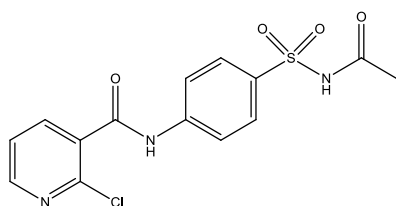
4-fluoroaniline (111 mg, 1 mmol) and 2-chloronicotinoyl chloride (185 mg, 1 mmol) were treated according to the general procedure. Purification by CombiFlash[®] Rf afforded the title compound (200 mg, 80%) as a white crystalline solid. $R_f=0.22$ (50% Ethyl acetate/hexane). ^1H NMR (400 MHz, DMSO-d_6) δ 10.69 (s, 1H), 8.55 (dd, $J = 4.8, 1.9$ Hz, 1H), 8.09 (dd, $J = 7.5, 1.9$ Hz, 1H), 7.78 – 7.68 (m, 2H), 7.57 (dt, $J = 15.9, 7.9$ Hz, 1H), 7.27 – 7.17 (m, 2H). ^{13}C NMR (101 MHz, DMSO-d_6) δ 163.92, 160.13, 157.74, 151.03, 146.94, 138.67, 135.55, 135.52, 133.52, 123.65, 121.91, 121.84, 116.08, 115.86.

2-chloro-*N*-(4-(trifluoromethyl)phenyl)nicotinamide (**1d**)



2-(trifluoromethyl)aniline (161 mg, 1 mmol) and 2-chloronicotinoyl chloride (184 mg, 1 mmol) were treated according to the general procedure. Purification by CombiFlash[®] Rf afforded the title compound (228 mg, 75%) as a white crystalline solid. $R_f=0.28$ (50% Ethyl acetate/hexane). ^1H NMR (400 MHz, DMSO- d_6) δ 11.00 (s, 1H, NH), 8.57 (dd, $J=4.8, 1.9$ Hz, 1H), 8.13 (dd, $J=7.5, 1.9$ Hz, 1H), 7.92 (d, $J=8.5$ Hz, 2H), 7.76 (d, $J=8.6$ Hz, 2H), 7.60 (dd, $J=7.5, 4.8$ Hz, 1H). ^{13}C NMR (101 MHz, DMSO- d_6) δ 164.53, 151.26, 146.87, 142.65, 138.76, 133.21, 126.70 (q, $J=3.7$ Hz), 124.62 (d, $J=31.9$ Hz), 123.758 (q, $J=269.9$ Hz) 123.69, 120.04

N-(4-(*N*-acetylsulfamoyl)phenyl)-2-chloronicotinamide (**1f**)



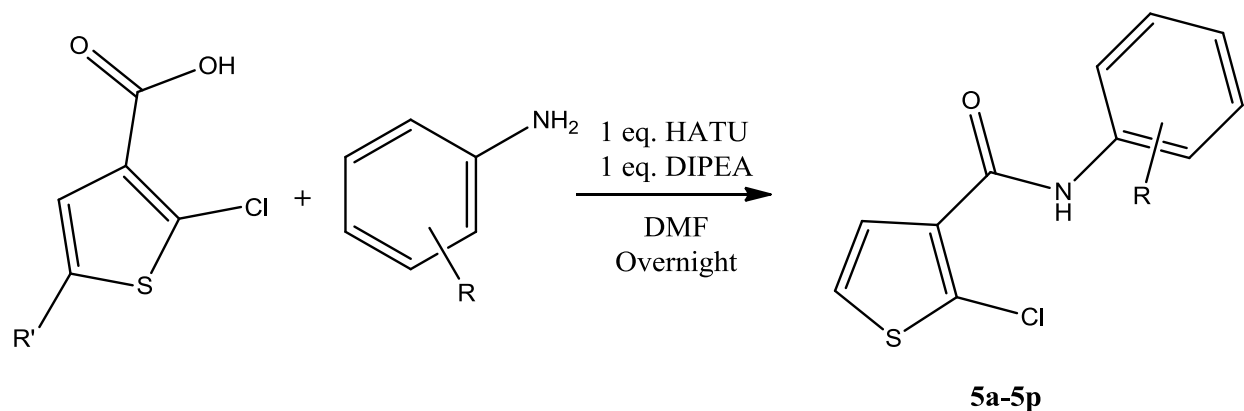
N-((2-aminobenzyl)sulfonyl)acetamide (229 mg, 1 mmol) and 2-chloronicotinoyl chloride (185 mg, 1 mmol) were treated according to the general procedure. Purification by CombiFlash[®] Rf afforded the title compound (187 mg, 51%) as a white crystalline solid. $R_f=0.66$ (20% DCM/methanol). ^1H NMR (400 MHz, DMSO- d_6) δ 12.01 (s, 1H, NH), 11.09 (s, 1H, NH), 8.61 – 8.53 (m, 1H), 8.12 (dd, $J=7.5, 1.8$ Hz, 1H), 7.97 – 7.87 (m, 4H), 7.59 (dd, $J=7.5, 4.9$ Hz, 1H), 1.93 (s, 3H). ^{13}C NMR (101 MHz, DMSO- d_6) δ 169.20, 164.62, 151.29, 146.84, 143.51, 138.76, 134.47, 133.12, 129.48, 123.70, 119.68, 23.65.

3. Synthesis of 2-chloro-*N*-phenylthiophene-3-carboxamides

a. General Procedure

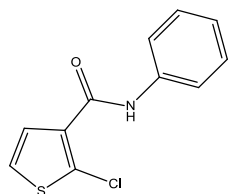
A summary of the synthesis of 2-chloro-*N*-phenylthiophene-3-carboxamides is represented in **Scheme 13**. A round-bottom flask with magnetic stir-bar was cleaned and oven-dried. The carboxylic acid (1 equiv.) was dissolved in Dimethylformamide (DMF) (0.5 mL per 0.1mmol reagent) with 1-[Bis(dimethylamino)methylene]-1*H*-1,2,3-triazolo[4,5-*b*]pyridinium 3-oxid hexafluorophosphate (HATU) (1 equiv.). *N,N*-diisopropylethylamine (DIPEA) was added afterward and the resulting solution was stirred for 2 minutes at room temperature. Corresponding aniline (1 equiv.) was added to the solution in the end. The mixture was stirred for 24 hours at room temperature. The resulting reaction mixture was stirred at room temperature for overnight. The solvent DMF was removed by vacuum after silica gel is added into the crude product in the round bottom flask. The dry crude product loaded on silica gel was separated and purified by column chromatography (CombiFlash[®] Rf). The solvent was then removed under vacuum and purified product was then dried in the oven.

Scheme 13. General Synthesis Procedure of 2-chloro-*N*-phenylthiophene-3-carboxamides



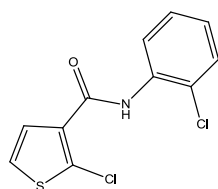
b. Detailed Procedure

2-chloro-*N*-phenylthiophene-3-carboxamide (**5a**)



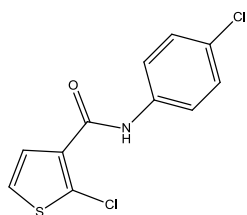
Starting material 2-chlorothiophene-3-carboxylic acid (32.5 mg, 0.2 mmol), HATU (76.1 mg, 0.2 mmol) and aniline (18.7 mg, 0.2 mmol) was treated according to the general procedure. Purification by CombiFlash® Rf afforded the title compound (36.9 mg, 78%) as a white crystalline solid. $R_f = 0.76$ (Hexane: Ethyl acetate = 1: 1). ¹H NMR (400 MHz, CDCl₃) δ 8.24 (s, 1H), 7.66 (d, $J = 7.7$ Hz, 2H), 7.50 (d, $J = 5.9$ Hz, 1H), 7.43 – 7.37 (m, 2H), 7.19 (m, 1H), 7.17 (d, 8 Hz, 1H). ¹³C NMR (101 MHz, CDCl₃) δ 159.50, 137.47, 133.51, 129.27, 129.22, 129.16, 124.82, 123.19, 120.24.

2-chloro-*N*-(2-chlorophenyl)thiophene-3-carboxamide (**5b**)



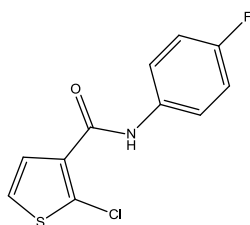
Starting material 2-chlorothiophene-3-carboxylic acid (32.4 mg, 0.2 mmol), HATU (76.1 mg, 0.2 mmol) and 2-chloroaniline (25.6 mg, 0.2 mmol) was treated according to the general procedure. Purification by CombiFlash® Rf afforded the title compound (27.5 mg, 51%) as a white crystalline solid. $R_f = 0.57$ (Hexane: Ethyl acetate = 1: 1). ^1H NMR (400 MHz, CDCl_3) δ 8.91 (s, 1H), 8.58 (dd, $J = 8.3, 1.4$ Hz, 1H), 7.53 (d, $J = 5.9$ Hz, 1H), 7.44 (dd, $J = 8.0, 1.5$ Hz, 1H), 7.37 – 7.32 (m, 1H), 7.18 (d, $J = 5.9$ Hz, 1H), 7.11 (td, $J = 7.7, 1.5$ Hz, 1H). ^{13}C NMR (101 MHz, CDCl_3) δ 159.38, 134.66, 133.19, 130.12, 129.38, 129.17, 127.80, 124.91, 123.17, 123.04, 121.80.

2-chloro-*N*-(4-chlorophenyl)thiophene-3-carboxamide (**5c**)



Starting material 2-chlorothiophene-3-carboxylic acid (32.5 mg, 0.2 mmol), HATU (76.1 mg, 0.2 mmol) and 4-chloroaniline (25.5 mg, 0.2 mmol) was treated according to the general procedure. Purification by CombiFlash® Rf afforded the title compound (27.3 mg, 50%) as a white crystalline solid. $R_f = 0.79$ (Hexane: Ethyl acetate = 1: 1). ^1H NMR (400 MHz, CDCl_3) δ 8.27 (s, 1H), 7.64 – 7.58 (m, 2H), 7.48 (d, $J = 5.9$ Hz, 1H), 7.38 – 7.32 (m, 2H), 7.17 (d, $J = 5.9$ Hz, 1H). ^{13}C NMR (101 MHz, CDCl_3) δ 159.48, 136.04, 133.16, 129.80, 129.46, 129.16, 123.32, 121.46.

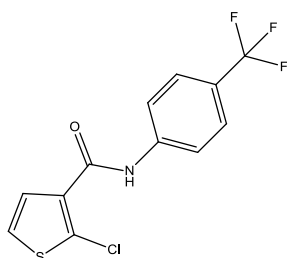
2-chloro-*N*-(4-fluorophenyl)thiophene-3-carboxamide (**5d**)



Starting material 2-chlorothiophene-3-carboxylic acid (48.8 mg, 0.3 mmol), HATU (114.0 mg, 0.3 mmol) and 4-fluoroaniline (33.5 mg, 0.3 mmol) was treated according to the general procedure. Purification by CombiFlash® R_f afforded the title compound (56.1 mg, 73%) as a white crystalline solid.

R_f = 0.76 (Hexane: Ethyl acetate = 1: 1). ¹H NMR (400 MHz, CDCl₃) δ 8.25 (s, 1H), 7.66 – 7.56 (m, 2H), 7.48 (d, *J* = 5.9 Hz, 1H), 7.17 (d, *J* = 5.9 Hz, 1H), 7.12 – 7.05 (m, 2H). ¹³C NMR (101 MHz, CDCl₃) δ 159.68 (d, *J* = 243 Hz), 159.54, 133.44 (d, *J* = 3 Hz), 133.26, 129.36, 129.17, 123.26, 122.12 (d, *J* = 8 Hz), 115.82 (d, *J* = 23 Hz)

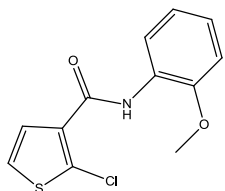
2-chloro-*N*-(4-(trifluoromethyl)phenyl)thiophene-3-carboxamide (**5e**)



Starting material 2-chlorothiophene-3-carboxylic acid (32.4 mg, 0.2 mmol), HATU (76.0 mg, 0.2 mmol) and 4-(trifluoromethyl)aniline (32.1 mg, 0.2 mmol) was treated according to the general procedure. Purification by CombiFlash® R_f afforded the title compound (50.7 mg,

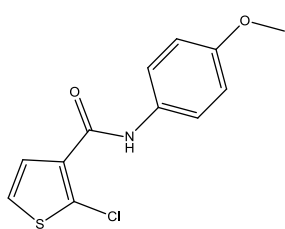
55%) as a white crystalline solid. R_f = 0.80 (Hexane: Ethyl acetate = 1: 1). ¹H NMR (400 MHz, CDCl₃) δ 8.41 (s, 1H), 7.79 (d, *J* = 8.5 Hz, 2H), 7.65 (d, *J* = 8.6 Hz, 2H), 7.50 (d, *J* = 5.9 Hz, 1H), 7.19 (d, *J* = 5.9 Hz, 1H). ¹³C NMR (101 MHz, CDCl₃) δ 159.61, 140.52, 132.95, 129.78, 129.18, 126.53 (d, *J* = 3.3 Hz), 126.41 (d, *J* = 3.8 Hz), 124.03 (d, *J* = 269.6 Hz), 123.47, 119.80.

2-chloro-*N*-(2-methoxyphenyl)thiophene-3-carboxamide (**5f**)



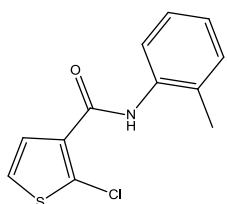
Starting material 2-chlorothiophene-3-carboxylic acid (48.9 mg, 0.3 mmol), HATU (114.2 mg, 0.3 mmol) and 2-methoxyaniline (37.5 mg, 0.3 mmol) was treated according to the general procedure. Purification by CombiFlash® Rf afforded the title compound (63 mg, 78%) as a white crystalline solid. $R_f = 0.82$ (Hexane: Ethyl acetate = 1: 1). ^1H NMR (400 MHz, CDCl_3) δ 9.03 (s, 1H), 8.53 (d, $J = 7.9$ Hz, 1H), 7.51 (d, $J = 5.9$ Hz, 1H), 7.15 (d, $J = 5.9$ Hz, 1H), 7.14 – 7.09 (m, 1H), 7.03 (t, $J = 7.5$ Hz, 1H), 6.95 (d, $J = 8.0$ Hz, 1H), 3.95 (s, 3H). ^{13}C NMR (101 MHz, CDCl_3) δ 159.27, 148.22, 133.88, 129.47, 129.30, 127.61, 124.08, 122.91, 121.22, 120.05, 110.07, 55.94.

2-chloro-*N*-(4-methoxyphenyl)thiophene-3-carboxamide (**5g**)



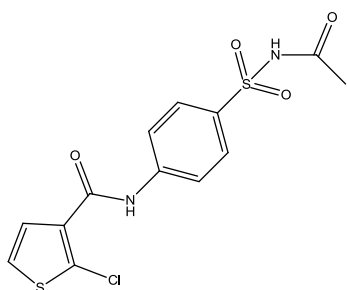
Starting material 2-chlorothiophene-3-carboxylic acid (48.9 mg, 0.3 mmol), HATU (114.2 mg, 0.3 mmol) and 4-methoxyaniline (37.1 mg, 0.3 mmol) was treated according to the general procedure. Purification by CombiFlash® Rf afforded the title compound (70.9 mg, 88%) as a white crystalline solid. $R_f = 0.73$ (Hexane: Ethyl acetate = 1: 1). ^1H NMR (400 MHz, CDCl_3) δ 8.16 (s, 1H), 7.59 – 7.52 (m, 2H), 7.47 (d, $J = 5.9$ Hz, 1H), 7.15 (d, $J = 5.8$ Hz, 1H), 6.96 – 6.89 (m, 2H), 3.83 (s, 3H). ^{13}C NMR (101 MHz, CDCl_3) δ 159.46, 156.79, 133.55, 130.52, 129.22, 129.05, 123.10, 122.10, 114.27, 55.53.

2-chloro-*N*-(*o*-tolyl)thiophene-3-carboxamide (**5h**)



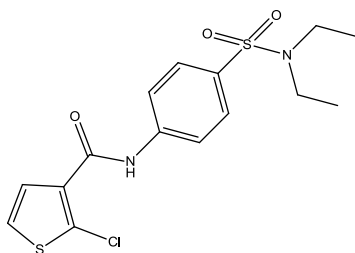
Starting material 2-chlorothiophene-3-carboxylic acid (48.8 mg, 0.3 mmol), HATU (114.0 mg, 0.3 mmol) and *o*-toluidine (32.3 mg, 0.3 mmol) was treated according to the general procedure. Purification by CombiFlash® Rf afforded the title compound (74 mg, 98%) as a white crystalline solid. $R_f = 0.80$ (Hexane: Ethyl acetate = 1: 1). $^1\text{H NMR}$ (400 MHz, CDCl_3) δ 8.18 (s, 1H), 8.09 (d, $J = 8.0$ Hz, 1H), 7.54 (d, $J = 5.8$ Hz, 1H), 7.32 – 7.24 (m, 2H), 7.18 (d, $J = 5.9$ Hz, 1H), 7.14 (t, $J = 7.5$ Hz, 1H), 2.39 (s, 3H). $^{13}\text{C NMR}$ (101 MHz, CDCl_3) δ 159.45, 135.64, 133.71, 130.57, 129.70, 128.89, 128.66, 126.91, 125.28, 123.12, 122.77, 18.24.

2-chloro-*N*-(*o*-tolyl)cyclopenta-1,4-dienecarboxamide (**5i**)



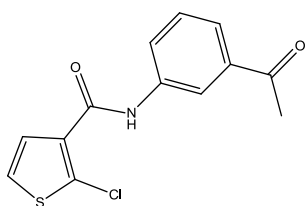
Starting material 2-chlorothiophene-3-carboxylic acid (49.0 mg, 0.3 mmol), HATU (114.2 mg, 0.3 mmol) and *N*-((4-aminophenyl)sulfonyl)acetamide (66.4 mg, 0.3 mmol) was treated according to the general procedure. Purification by CombiFlash® Rf afforded the title compound (73.2 mg, 68%) as a white crystalline solid. $R_f = 0.72$ (Dichloromethane: Methanol = 5: 1). $^1\text{H NMR}$ (400 MHz, DMSO-d_6) δ 12.03 (s, 1H), 10.69 (s, 1H), 7.95 – 7.88 (m, 4H), 7.60 (dd, $J = 5.8, 2.7$ Hz, 1H), 7.41 (dd, $J = 5.8, 2.7$ Hz, 1H), 1.92 (d, $J = 2.5$ Hz, 3H). $^{13}\text{C NMR}$ (101 MHz, DMSO-d_6) δ 169.17, 161.39, 143.74, 134.17, 134.06, 131.21, 129.30, 127.90, 125.45, 119.88, 23.67.

2-chloro-*N*-(4-(*N,N*-diethylsulfamoyl)phenyl)thiophene-3-carboxamide (**5j**)



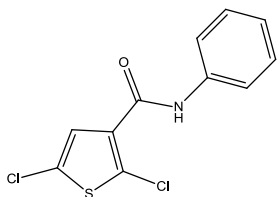
Starting material 2-chlorothiophene-3-carboxylic acid (32.4 mg, 0.2 mmol), HATU (76.2 mg, 0.2 mmol) and 4-amino-*N*-(penta-*N*-3-yl)benzenesulfonamide (46.0 mg, 0.3 mmol) was treated according to the general procedure. Purification by CombiFlash® Rf afforded the title compound (38.2 mg, 82 %) as a white crystalline solid. R_f = 0.64 (Hexane: Ethyl acetate = 1: 1). ^1H NMR (400 MHz, CDCl_3) δ 8.47 (s, 1H), 7.84 – 7.77 (m, 4H), 7.49 (d, J = 5.9 Hz, 1H), 7.20 (d, J = 5.9 Hz, 1H), 3.26 (q, J = 7.1 Hz, 4H), 1.15 (t, J = 7.2 Hz, 6H). ^{13}C NMR (101 MHz, CDCl_3) δ 159.65, 141.04, 135.87, 132.82, 130.03, 129.09, 128.34, 123.54, 119.87, 42.04, 14.16.

N-(3-acetylphenyl)-2-chlorothiophene-3-carboxamide (**5k**)



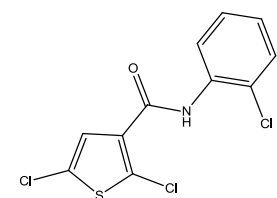
Starting material 2-chlorothiophene-3-carboxylic acid (49.3 mg, 0.3 mmol), HATU (114.4 mg, 0.3 mmol) and 1-(3-aminophenyl)ethanone (42.1 mg, 0.3 mmol) was treated according to the general procedure. Purification by CombiFlash® Rf afforded the title compound (68.5 mg, 82%) as a white crystalline solid. R_f = 0.72 (Hexane: Ethyl acetate = 1: 1). ^1H NMR (400 MHz, CDCl_3) δ 8.43 (s, 1H), 8.15 (t, J = 1.8 Hz, 1H), 8.05 – 7.98 (m, 1H), 7.77 (ddd, J = 7.8, 1.5, 1.1 Hz, 1H), 7.53 – 7.48 (m, 2H), 7.18 (d, J = 5.9 Hz, 1H), 2.65 (s, 3H). ^{13}C NMR (101 MHz, CDCl_3) δ 197.80, 159.76, 138.01, 137.90, 133.05, 129.78, 129.49, 129.10, 124.83, 124.65, 123.37, 119.68, 26.75.

2,5-dichloro-*N*-phenylthiophene-3-carboxamide (**5l**)



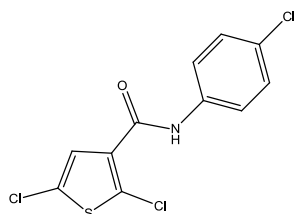
Starting material 2,5-dichlorothiophene-3-carboxylic acid (60.1 mg, 0.3 mmol), HATU (114.4 mg, 0.3 mmol) and aniline (28.5 mg, 0.3 mmol) was treated according to the general procedure. Purification by CombiFlash® Rf afforded the title compound (65 mg, 80%) as a white crystalline solid. $R_f=0.92$ (Hexane: Ethyl acetate =1: 1). ^1H NMR (400 MHz, CDCl_3) δ 8.16 (s, 1H), 7.62 (d, $J=7.8$ Hz, 2H), 7.43 – 7.36 (m, 2H), 7.31 (s, 1H), 7.23 – 7.17 (m, 1H). ^{13}C NMR (101 MHz, CDCl_3) δ 158.47, 137.15, 133.55, 129.19, 127.89, 127.28, 126.15, 125.06, 120.32.

2,5-dichloro-*N*-(2-chlorophenyl)thiophene-3-carboxamide (**5m**)



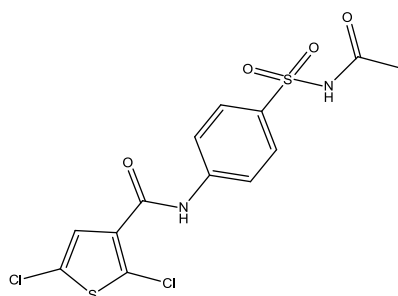
Starting material 2,5-dichlorothiophene-3-carboxylic acid (60.9 mg, 0.3 mmol), HATU (114.1 mg, 0.3 mmol) and 2-chloroaniline (39.0 mg, 0.3 mmol) was treated according to the general procedure. Purification by CombiFlash® Rf afforded the title compound (61.6 mg, 67%) as a white crystalline solid. $R_f=0.94$ (Hexane: Ethyl acetate =1: 1). ^1H NMR (400 MHz, CDCl_3) δ 8.81 (s, 1H), 8.54 (dd, $J=8.4$ Hz, 0.8 Hz, 1H), 7.44 (dd, $J=8.0, 1.1$ Hz, 1H), 7.36 (s, 1 Hz), 7.34 (t, $J=6.8$ Hz, 1H), 7.12 (td, $J=7.8, 1.3$ Hz, 1H). ^{13}C NMR (101 MHz, CDCl_3) δ 158.29, 134.39, 133.23, 129.20, 128.06, 127.84, 127.22, 126.91, 125.15, 123.06, 121.83.

2,5-dichloro-*N*-(4-chlorophenyl)thiophene-3-carboxamide (**5n**)



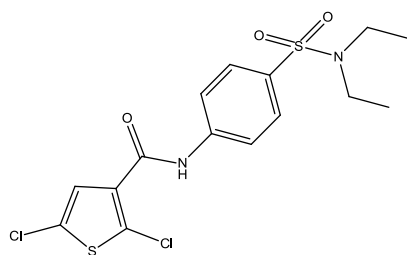
Starting material 2,5-dichlorothiophene-3-carboxylic acid (59.5 mg, 0.3 mmol), HATU (114.0 mg, 0.3 mmol) and 4-chloroaniline (38.7 mg, 0.3 mmol) was treated according to the general procedure. Purification by CombiFlash® Rf afforded the title compound (87.2 mg, 95%) as a white crystalline solid. R_f = 0.94 (Hexane: Ethyl acetate = 1: 1). ^1H NMR (400 MHz, CDCl_3) δ 8.16 (s, 1H), 7.58 (d, J = 8.7 Hz, 2H), 7.35 (d, J = 8.7 Hz, 2H), 7.30 (s, 1H). ^{13}C NMR (101 MHz, CDCl_3) δ 158.43, 135.71, 133.20, 130.09, 129.22, 127.82, 127.45, 126.34, 121.53. ^{13}C NMR (101 MHz, CDCl_3) δ 159.45, 135.64, 133.71, 130.57, 129.70, 128.89, 128.66, 126.91, 125.28, 123.12, 122.77, 18.24.

N-(4-(*N*-acetylsulfamoyl)phenyl)-2,5-dichlorothiophene-3-carboxamide (**5o**)



Starting material 2,5-dichlorothiophene-3-carboxylic acid (59.6 mg, 0.3 mmol), HATU (114.2 mg, 0.3 mmol) and *N*-((4-aminophenyl)sulfonyl)acetamide (66.5 mg, 0.3 mmol) was treated according to the general procedure. Purification by CombiFlash® Rf afforded the title compound (60.0mg, 50%) as a white crystalline solid. R_f = 0.71 (Dichloromethane: Methanol = 5: 1). ^1H NMR (400 MHz, DMSO-d_6) δ 12.05 (s, 1H), 10.73 (s, 1H), 7.91 (s, 4H), 7.55 (s, 1H), 1.92 (s, 3H). ^{13}C NMR (101 MHz, DMSO-d_6) δ 169.18, 160.08, 143.47, 134.28, 134.17, 129.35, 128.81, 127.59, 125.95, 119.91, 23.67.

2,5-dichloro-*N*-(4-(*N,N*-diethylsulfamoyl)phenyl)thiophene-3-carboxamide (**5p**)



Starting material 2,5-dichlorothiophene-3-carboxylic acid (60.7 mg, 0.3 mmol), HATU (114.2 mg, 0.3 mmol) and 4-amino-*N*-(penta-*N*-3-yl)benzenesulfonamide (68.9 mg, 0.3 mmol) was treated according to the general procedure.

Purification by CombiFlash® Rf afforded the title compound (106.2 mg, 87%) as a white crystalline solid. $R_f = 0.94$ (Hexane: Ethyl acetate = 1: 1). $^1\text{H NMR}$ (400 MHz, CDCl_3) δ 8.37 (s, 1H), 7.79 (dd, $J = 22.1, 8.8$ Hz, 4H), 7.30 (d, $J = 11.5$ Hz, 1H), 3.26 (q, $J = 7.1$ Hz, 4H), 1.16 (t, $J = 7.1$ Hz, 6H). $^{13}\text{C NMR}$ (101 MHz, CDCl_3) δ 158.60, 140.75, 136.21, 132.90, 128.34, 127.68, 126.98, 119.97, 42.04, 14.14.

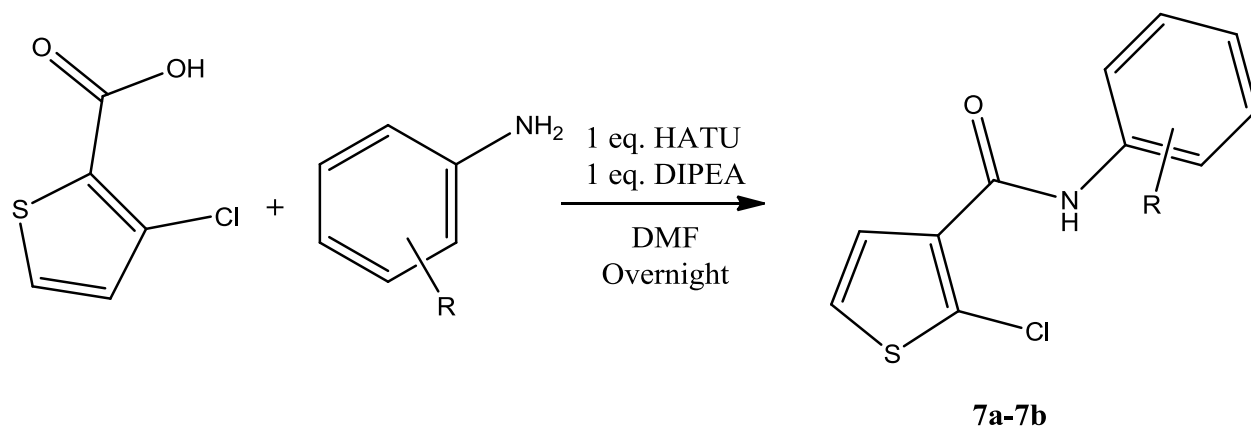
4. Synthesis of 3-chloro-*N*-phenylthiophene-2-carboxamides

a. General Procedure

A summary of the synthesis of 3-chloro-*N*-phenylthiophene-2-carboxamides is presented in the **Scheme 14**. A round-bottom flask with magnetic stir-bar was cleaned and oven-dried. The carboxylic acid (1 equiv.) was dissolved in dimethylformamide (DMF) (0.5 mL per 0.1 mmol reagent) with 1-[Bis(dimethylamino)methylene]-1H-1,2,3-triazolo[4,5-*b*]pyridinium 3-oxid hexafluorophosphate (HATU) (1 equiv.). *N,N*-diisopropylethylamine (DIPEA) was added afterward and the resulting solution was stirred for 2 minutes at room temperature. Corresponding aniline (1 equiv.) was added to the solution in the end. The mixture was stirred for 24 hours at room temperature. The resulting reaction mixture was stirred at room temperature for overnight. The solvent DMF was removed by vacuum after silica gel is added into the crude

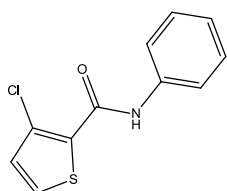
product in the round bottom flask. The dry crude product loaded on silica gel was separated and purified by column chromatography (CombiFlash[®] Rf). The solvent was then removed under vacuum and purified product was then dried in the oven.

Scheme 14. General Synthesis Procedure of 3-chloro-*N*-phenylthiophene-2-carboxamides



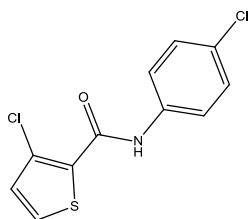
b. Detailed Procedure

3-chloro-*N*-phenylthiophene-2-carboxamide (**7a**)



Starting material 3-chlorothiophene-2-carboxylic acid (49.6 mg, 0.3 mmol), HATU (114.0 mg, 0.3 mmol) and aniline (28.5 mg, 0.3 mmol) was treated according to the general procedure. Purification by CombiFlash® Rf afforded the title compound (60.6 mg, 85%) as a white crystalline solid. R_f = 0.82 (Hexane: Ethyl acetate = 1: 1). ^1H NMR (400 MHz, CDCl_3) δ 8.78 (s, 1H), 7.66 (d, J = 8.1 Hz, 2H), 7.56 (d, J = 5.3 Hz, 1H), 7.40 (t, J = 7.8 Hz, 2H), 7.19 (t, J = 7.4 Hz, 1H), 7.06 (d, J = 5.3 Hz, 1H). ^{13}C NMR (101 MHz, CDCl_3) δ 158.22, 137.28, 133.52, 130.09, 129.55, 129.18, 124.91, 122.86, 120.33.

3-chloro-*N*-(4-chlorophenyl)thiophene-2-carboxamide (**7b**)



Starting material 3-chlorothiophene-2-carboxylic acid (49.8 mg, 0.3 mmol), HATU (114.1 mg, 0.3 mmol) and 4-chloroaniline (38.9 mg, 0.3 mmol) was treated according to the general procedure. Purification by CombiFlash® Rf afforded the title compound (75.1 mg, 92%) as a white crystalline solid. R_f = 0.82 (Hexane: Ethyl acetate = 1: 1). ^1H NMR (400 MHz, CDCl_3) δ 8.78 (s, 1H), 7.62 (d, J = 8.7 Hz, 2H), 7.57 (d, J = 5.3 Hz, 1H), 7.36 (d, J = 8.7 Hz, 2H), 7.06 (d, J = 5.3 Hz, 1H). ^{13}C NMR (101 MHz, CDCl_3) δ 158.21, 135.86, 133.15, 130.38, 129.90, 129.59, 129.20, 123.02, 121.52.

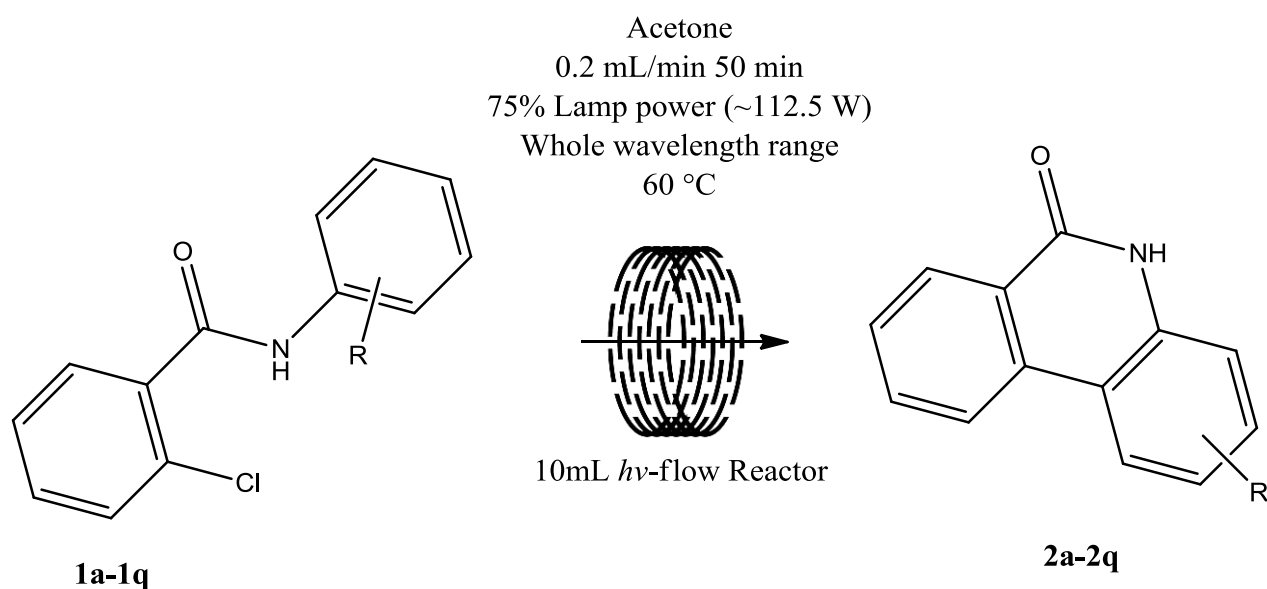
B. Procedure for Synthesizing Products

1. Synthesis of Phenanthridin-6(5H)-ones

a. General Procedure

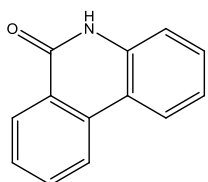
A summary of the synthesis of phenanthridin-6(5H)-ones is presented in **Scheme 15**. A solution of corresponding 2-chloro-*N*-phenylbenzamide as starting material (0.1 mmol, 0.005 mmol/mL) in acetone (20 mL) was driven continuously through the Vapourtec[®] UV-150 photochemical flow reactor using a Vapourtec[®] R2+/R4 flow chemistry system at a rate of 0.200 mL/min (reacting time 50min). The UV-150 reactor uses a medium-pressure high-intensity pure Hg lamp (lamp power 75%, approximately 112.5 watts), a 10mL FEP reactor coil, and a filter (type 1, quartz, whole-wavelength range). The temperature was set and maintained at 60°C using the Vapourtec[®] R4 reactor module, and the UV reactor coil flow stream was passed through an 8 bar back pressure regulator, with the Vapourtec[®] R2+ pressure limit set at 12 bar. The reaction stream of crude product was collected into a round-bottom flask which was covered by aluminum foil. Solvent acetone was removed by a rotary vacuum and the residue was loaded on silica gel and purified by column chromatography (CombiFlash[®] Rf) using 10% to 50% ethyl acetate in hexanes. The purified product was dried under vacuum and weighed. The product was analyzed by 400 MHz Bruker NMR spectrometer at 400 and 100 MHz, respectively. and LC-MS (Shimadzu, LC-MS 2020).

Scheme 15. General Synthesis Procedure of Phenanthridin-6(5H)-ones



b. Detailed Procedure

Phenanthridin-6(5H)-one (**2a**)

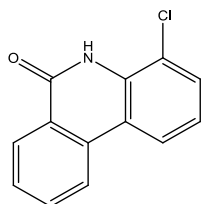


2-chloro-*N*-phenylbenzamide was treated according to the general procedure as starting material. Purification by CombiFlash[®] Rf afforded the

title compound (19.4 mg, 99%) as a pale yellow crystalline solid. $R_f = 0.22$ (40%

Ethyl acetate/hexane). ¹H NMR (400 MHz, DMSO-*d*₆) δ 11.71 (s, 1H), 8.51 (d, $J = 8.1$ Hz, 1H), 8.39 (d, $J = 7.9$ Hz, 1H), 8.33 (dd, $J = 7.9, 1.2$ Hz, 1H), 7.91 – 7.82 (m, 1H), 7.65 (t, $J = 7.3$ Hz, 1H), 7.53 – 7.46 (m, 1H), 7.39 – 7.35 (m, 1H), 7.30 – 7.23 (m, 1H). ¹³C NMR (100 MHz, DMSO-*d*₆) δ 161.27, 137.03, 134.72, 133.27, 130.03, 128.39, 127.93, 126.15, 123.72, 123.09, 122.73, 118.02, 116.57. C₁₃H₉NO (ESI+, M+1) = 196.10

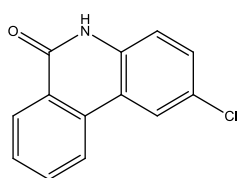
4-chlorophenanthridin-6(5H)-one (**2b**)



2-chloro-*N*-(2-chlorophenyl)benzamide was treated according to the general procedure as starting material. Major product was separated and purified by CombiFlash[®] Rf, affording the title compound (17 mg, 74%) as off-white solid.

$R_f=0.11$ (40% Ethyl acetate/hexane). ¹H NMR (400 MHz, DMSO-*d*₆) δ 10.82 (s, 1H), 8.56 (d, $J=8.2$ Hz, 1H), 8.44 (d, $J=8.0$ Hz, 1H), 8.36 (dd, $J=8.0, 1.1$ Hz, 1H), 7.94 – 7.88 (m, 1H), 7.74 – 7.68 (m, 1H), 7.66 (dd, $J=7.8, 1.1$ Hz, 1H), 7.30 (t, $J=8.0$ Hz, 1H). ¹³C NMR (100 MHz, DMSO-*d*₆) δ 161.27, 134.11, 133.84, 133.31, 130.26, 129.25, 128.10, 126.01, 123.62, 123.33, 122.99, 120.06, 119.75. C₁₃H₈NOCl (ESI+, M+1) =230.10.

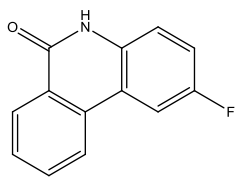
2-chlorophenanthridin-6(5H)-one (**2c**)



2-chloro-*N*-(4-chlorophenyl)benzamide was treated according to the general procedure as starting material. Major product was separated and purified by CombiFlash[®] Rf affording the title compound (21.3 mg, 93%) as a yellow

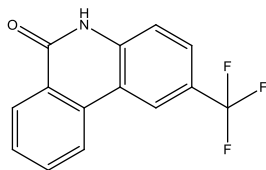
crystalline solid. $R_f=0.31$ (40% Ethyl acetate/ Hexane) ¹H NMR (400 MHz, DMSO-*d*₆) δ 11.82 (s, 1H), 8.57 (d, $J=8.1$ Hz, 1H), 8.48 (d, $J=2.2$ Hz, 1H), 8.32 (dd, $J=7.9, 1.2$ Hz, 1H), 7.90 – 7.83 (m, 1H), 7.69 (t, $J=7.5$ Hz, 1H), 7.54 (dd, $J=8.7, 2.2$ Hz, 1H), 7.37 (d, $J=8.7$ Hz, 1H). ¹³C NMR (100 MHz, DMSO-*d*₆) δ 161.08, 135.80, 133.65, 133.43, 129.89, 129.11, 127.92, 127.03, 126.27, 123.59, 123.33, 119.61, 118.35. C₁₃H₈NOCl (ESI+, M+1) =230.10.

2-Fluorophenanthridin-6(5H)-one (**2d**)



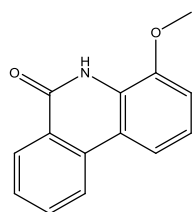
2-chloro-*N*-(4-fluorophenyl)benzamide was treated according to the general procedure as starting material. Major product was separated and purified by CombiFlash[®] Rf affording the title compound (17 mg, 80%) as off-white solid. R_f = 0.26 (40% Ethyl acetate/ Hexane) ¹H NMR (400 MHz, DMSO- d_6) δ 11.76 (s, 1H, NH), 8.52 (d, J = 8.1 Hz, 1H), 8.33 (d, J = 7.9 Hz, 1H), 8.28 (d, J = 10.3 Hz, 1H), 7.86 (t, J = 7.6 Hz, 1H), 7.68 (t, J = 7.5 Hz, 1H), 7.38 (m, 2H). ¹³C NMR (100 MHz, DMSO- d_6) δ 160.99, 158.31 (d, J = 233 Hz), 134.05 (d, J = 3 Hz), 133.62, 133.31, 129.05, 127.94, 126.29, 123.68, 119.31 (d, J = 8.4 Hz), 118.23 (d, J = 8.5 Hz), 117.66 (d, J = 24.2 Hz), 109.65 (d, J = 24.0 Hz). $C_{13}H_8NOF$ (ESI+, $M+1$) = 214.10.

2-(Trifluoromethyl)phenanthridin-6(5H)-one (2e)



2-chloro-*N*-(4-(trifluoromethyl)phenyl)benzamide was treated according to the general procedure as starting material. Major compound was separated and purified by CombiFlash[®] Rf affording the title compound (23mg, 86%) R_f = 0.39 (40% Ethyl acetate/ Hexane) ¹H NMR (400 MHz, DMSO- d_6) δ 12.03 (s, 1H, NH), 8.74 (s, 1H), 8.69 (d, J = 8.1 Hz, 1H), 8.34 (dd, J = 7.9, 1.0 Hz, 1H), 7.93 – 7.86 (m, 1H), 7.82 (dd, J = 8.6, 1.4 Hz, 1H), 7.72 (t, J = 7.5 Hz, 1H), 7.53 (d, J = 8.5 Hz, 1H). ¹³C NMR (100 MHz, DMSO- d_6) δ 161.47, 139.77, 133.80, 133.64, 129.35, 127.96, 126.44 (q, J = 3.6 Hz), 126.34, 125.00 (q, J = 270 Hz), 123.75, 123.25 (q, J = 32.5 Hz), 121.39 (q, J = 3.8 Hz), 118.17, 117.42. $C_{14}H_8NOF_3$ (ESI+, $M+1$) = 264.15.

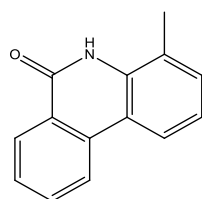
2-Methoxyphenanthridin-6(5H)-one (**2f**)



2-chloro-*N*-(2-methoxyphenyl)benzamide was treated according to the general procedure as starting material. Major product was separated and purified by CombiFlash[®] Rf affording the title compound (18.1 mg, 80%) as off-white solid.

$R_f = 0.25$ (40% Ethyl acetate/hexane). ¹H NMR (400 MHz, DMSO-*d*₆) δ 10.61 (s, 1H, NH), 8.49 (d, $J = 8.2$ Hz, 1H), 8.35 (dd, $J = 7.9, 1.1$ Hz, 1H), 7.98 (d, $J = 8.0$ Hz, 1H), 7.89 – 7.83 (m, 1H), 7.65 (dd, $J = 11.1, 3.9$ Hz, 1H), 7.24 (t, $J = 8.0$ Hz, 1H), 7.17 (d, $J = 7.3$ Hz, 1H), 3.94 (s, 3H). ¹³C NMR (100 MHz, DMSO-*d*₆) δ 160.81, 146.72, 134.73, 133.38, 128.53, 128.05, 126.61, 126.30, 123.51, 122.67, 118.52, 115.39, 110.95, 56.54. C₁₄H₁₁NO₂ (ESI+, M+1) = 226.10

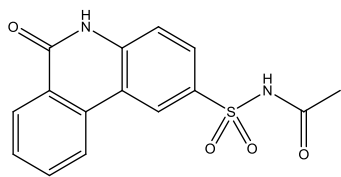
4-Methylphenanthridin-6(5H)-one (**2g**)



2-chloro-*N*-(2-methylphenyl)benzamide was treated according to the general procedure as starting material. Major product was separated and purified by CombiFlash[®] Rf affording the title compound (4.4 mg, 21%) as a pale yellow

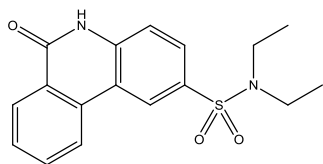
crystalline solid $R_f = 0.37$ (40% Ethyl acetate/ Hexane) ¹H NMR (400 MHz, DMSO-*d*₆) δ 10.72 (s, 1H, NH), 8.52 (d, $J = 8.2$ Hz, 1H), 8.35 (dd, $J = 7.9, 1.2$ Hz, 1H), 8.27 (d, $J = 8.0$ Hz, 1H), 7.89 – 7.81 (m, 1H), 7.65 (dd, $J = 11.1, 3.9$ Hz, 1H), 7.36 (d, $J = 7.2$ Hz, 1H), 7.19 (t, $J = 7.7$ Hz, 1H), 2.48 (s, 3H). ¹³C NMR (100 MHz, DMSO-*d*₆) δ 161.66, 135.24, 135.00, 133.42, 131.48, 128.33, 127.93, 125.82, 124.65, 123.29, 122.46, 121.62, 118.02, 18.14. C₁₄H₁₁NO (ESI+, M+1) = 210.15.

N-((6-oxo-5,6-dihydrophenanthridin-2-yl)sulfonyl)acetamide (**2h**)



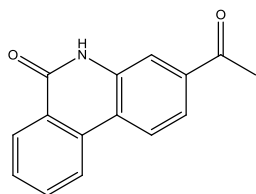
N-(4-(*N*-acetylsulfamoyl)phenyl)-2-chlorobenzamide was treated according to the general procedure as starting material. Purification by CombiFlash[®] Rf afforded the title compound (28.8 mg, 91%) as a white crystalline solid. $R_f = 0.60$ (11% Methanol/ Dichloromethane). ^1H NMR (400 MHz, DMSO- d_6) δ 12.13 (s, 2H, NH), 8.80 (s, 1H), 8.46 (d, $J = 8.1$ Hz, 1H), 8.34 (d, $J = 7.9$ Hz, 1H), 8.01 – 7.91 (m, 2H), 7.73 (t, $J = 7.5$ Hz, 1H), 7.53 (d, $J = 8.6$ Hz, 1H), 1.93 (s, 3H). ^{13}C NMR (101 MHz, DMSO- d_6) δ 169.41, 161.41, 140.61, 133.94, 133.44, 133.14, 129.52, 128.72, 128.12, 126.27, 123.90, 123.09, 117.58, 117.26, 23.77. $\text{C}_{15}\text{H}_{12}\text{N}_2\text{O}_4\text{S}$ (ESI+, $M+1$) = 317.10

N,N-diethyl-6-oxo-5,6-dihydrophenanthridine-2-sulfonamide (**2i**)



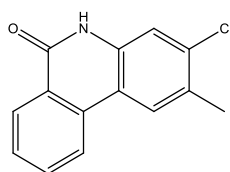
2-chloro-*N*-(4-(*N,N*-diethylsulfamoyl)phenyl)benzamide was treated according to the general procedure as starting material. Purification by CombiFlash[®] Rf afforded the title compound (9.9 mg, 30%) ^1H NMR (400 MHz, DMSO- d_6) δ 12.04 (s, 1H), 8.67 (d, $J = 1.5$ Hz, 1H), 8.63 (d, $J = 8.2$ Hz, 1H), 8.35 (d, $J = 7.9$ Hz, 1H), 7.92 (d, $J = 7.8$ Hz, 1H), 7.89 (dd, $J = 8.3, 2.0$ Hz, 1H), 7.73 (t, $J = 7.6$ Hz, 1H), 7.52 (d, $J = 8.6$ Hz, 1H), 3.22 (q, $J = 7.1$ Hz, 4H), 1.07 (t, $J = 7.1$ Hz, 6H). ^{13}C NMR (101 MHz, DMSO- d_6) δ 161.37, 139.85, 133.86, 133.77, 133.66, 129.41, 128.16, 128.02, 126.32, 123.59, 122.64, 118.06, 117.51, 42.36, 14.65. $\text{C}_{17}\text{H}_{18}\text{N}_2\text{O}_3\text{S}$. $\text{C}_{15}\text{H}_{12}\text{N}_2\text{O}_4\text{S}$ (ESI+, $M+1$) = 331.40

3-Acetylphenanthridin-6(5H)-one (**2j**)



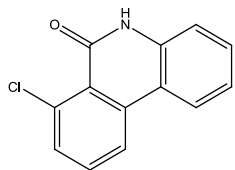
2-chloro-*N*-(3-chloro-4-methylphenyl)benzamide was treated according to the general procedure as starting material. Major product was separated and purified by CombiFlash[®] Rf, affording the title compound (17.9 mg, 76%) as pale yellow crystalline solid. $R_f=0.48$ (40% Ethyl acetate/ Hexane) ¹H NMR (400 MHz, DMSO-*d*₆) δ 11.86 (s, 1H), 8.59 (d, $J=8.1$ Hz, 1H), 8.54 (d, $J=8.4$ Hz, 1H), 8.35 (dd, $J=7.9$, 1.1 Hz, 1H), 7.94 – 7.88 (m, 2H), 7.82 (dd, $J=8.4$, 1.7 Hz, 1H), 7.73 (t, $J=7.2$ Hz, 1H), 2.64 (s, 3H). ¹³C NMR (100 MHz, DMSO-*d*₆) δ 197.70, 161.23, 137.50, 137.00, 133.78, 133.53, 129.59, 128.05, 126.83, 124.24, 123.97, 122.26, 121.81, 116.23, 27.30. $C_{15}H_{11}NO_2$ (ESI+, M+1) =238.15.

3-chloro-2-methylphenanthridin-6(5H)-one (**2k**)



2-chloro-*N*-(3-chloro-4-methylphenyl)benzamide was treated according to the general procedure as starting material. Purification by CombiFlash[®] Rf afforded the title compound (3.2 mg, 13%) as a white crystalline solid. $R_f=0.45$ (40% Ethyl acetate/ Hexane). ¹H NMR (400 MHz, DMSO-*d*₆) δ 11.69 (s, 1H), 8.49 (d, $J=8.1$ Hz, 1H), 8.40 (s, 1H), 8.30 (dd, $J=8.0$, 1.1 Hz, 1H), 7.89 – 7.83 (m, 1H), 7.69 – 7.61 (m, 1H), 7.38 (s, 1H), 2.42 (s, 3H). ¹³C NMR (100 MHz, DMSO-*d*₆) δ 161.14, 136.09, 134.67, 134.00, 133.38, 129.49, 128.63, 127.98, 126.07, 125.99, 123.25, 117.12, 116.07, 19.68. $C_{14}H_{10}NOCl$ (ESI+, M+1) =244.10.

7-chlorophenanthridin-6(5H)-one (**2l**)

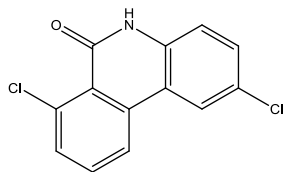


2,6-Dichloro-*N*-phenylbenzamide was treated according to the general procedure as starting material. Major Product was purified by CombiFlash[®]

R_f, re-dissolved in 1 mL methanol and dried, affording the title compound

(15.1 mg, 67%) as yellowish white solid. R_f = 0.32 (40% Ethyl acetate/ Hexane) ¹H NMR (400 MHz, DMSO-*d*₆) δ 11.67 (s, 1H), 8.51 (dd, *J* = 8.4, 1.0 Hz, 1H), 8.35 (t, *J* = 6.2 Hz, 1H), 7.76 (t, *J* = 8.0 Hz, 1H), 7.65 (dd, *J* = 7.8, 1.0 Hz, 1H), 7.53 – 7.47 (m, 1H), 7.33 (dd, *J* = 8.2, 1.0 Hz, 1H), 7.24 (ddd, *J* = 8.3, 7.2, 1.2 Hz, 1H). ¹³C NMR (100 MHz, DMSO-*d*₆) δ 159.54, 138.02, 137.19, 134.98, 133.28, 131.69, 130.72, 124.30, 122.71, 122.58, 122.36, 117.31, 116.07. C₁₃H₈NOCl (ESI+, M+1) = 230.15.

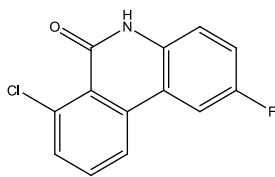
2,7-dichlorophenanthridin-6(5H)-one (**2m**)



2,6-Dichloro-*N*-(4-chlorophenyl)benzamide was treated according to the general procedure as starting material. Major Product was separated and purified by CombiFlash[®] R_f, re-dissolved in 1 mL methanol and dried,

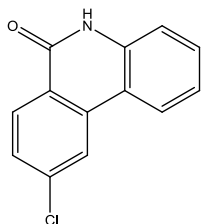
affording the title compound (17 mg, 74%) as a white solid. R_f = 0.39 (40% Ethyl acetate/ Hexane). ¹H NMR (400 MHz, DMSO-*d*₆) δ 11.77 (s, 1H), 8.56 (dd, *J* = 8.3, 0.9 Hz, 1H), 8.45 (d, *J* = 2.2 Hz, 1H), 7.76 (t, *J* = 8.0 Hz, 1H), 7.71 – 7.66 (m, 1H), 7.57 – 7.51 (m, 1H), 7.32 (d, *J* = 8.7 Hz, 1H). ¹³C NMR (100 MHz, DMSO-*d*₆) δ 159.35, 136.92, 135.97, 135.01, 133.42, 132.37, 130.58, 126.97, 123.85, 123.08, 122.51, 118.87, 117.86. C₁₃H₇NOCl₂ (ESI+, M+1) = 264.10.

7-chloro-2-fluorophenanthridin-6(5H)-one (**2n**)



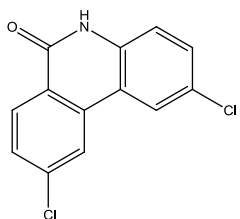
2,6-dichloro-*N*-(4-fluorophenyl)benzamide was treated according to the general procedure as starting material. Major product was separated and purified by CombiFlash[®] Rf, re-dissolved in 1 mL methanol and dried, affording the title compound (15.5 mg, 67%) as white solid. $R_f = 0.42$ (40% Ethyl acetate/Hexane). ¹H NMR (400 MHz, DMSO-*d*₆) δ 11.70 (s, 1H), 8.55 – 8.48 (m, 1H), 8.25 (dd, $J = 10.7, 2.5$ Hz, 1H), 7.77 (t, $J = 8.0$ Hz, 1H), 7.69 (dd, $J = 7.8, 1.0$ Hz, 1H), 7.44 – 7.30 (m, 2H). ¹³C NMR (100 MHz, DMSO-*d*₆) δ 159.27, 158.18 (d, $J = 236$ Hz), 137.28 (d, $J = 3$ Hz), 135.03, 133.83, 133.31, 132.32, 123.19, 122.53, 118.53 (d, $J = 8.7$ Hz), 118.45 (d, $J = 24.2$ Hz), 117.77 (d, $J = 8.4$ Hz), 110.18 (d, $J = 24.0$ Hz). C₁₃H₇NOCIF (ESI⁺, M+1) = 248.15.

9-chlorophenanthridin-6(5H)-one (**2o**)



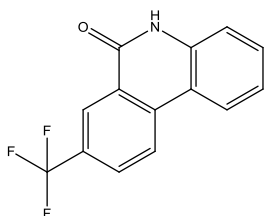
2,4-Dichloro-*N*-phenylbenzamide was treated according to the general procedure as starting material. Major Product was purified by CombiFlash[®] Rf, re-dissolved in 1 mL methanol and dried, affording the title compound (19 mg) as yellowish white solid. $R_f = 0.33$ (40% Ethyl acetate/Hexane). ¹H NMR (400 MHz, DMSO-*d*₆) δ 11.80 (s, 1H), 8.62 (d, $J = 1.7$ Hz, 1H), 8.45 (d, $J = 8.0$ Hz, 1H), 8.30 (d, $J = 8.5$ Hz, 1H), 7.68 (dd, $J = 8.5, 1.8$ Hz, 1H), 7.53 (t, $J = 7.3$ Hz, 1H), 7.37 (d, $J = 7.9$ Hz, 1H), 7.27 (t, $J = 7.3$ Hz, 1H). ¹³C NMR (100 MHz, DMSO-*d*₆) δ 160.64, 138.74, 137.49, 136.56, 130.81, 130.18, 128.56, 124.83, 124.29, 122.89, 122.86, 117.07, 116.65. C₁₃H₈NOCl (ESI⁺, M+1) = 230.05.

2,9-dichlorophenanthridin-6(5H)-one (**2p**)



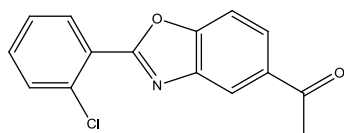
2,4-Dichloro-*N*-(4-chlorophenyl)benzamide was treated according to the general procedure as starting material. Major Product was separated and purified by CombiFlash[®] Rf, affording the title compound (19 mg, 83%) $R_f = 0.35$ (40% Ethyl acetate/ Hexane). ¹H NMR (400 MHz, DMSO-*d*₆) δ 11.89 (s, 1H), 8.70 (d, $J = 1.9$ Hz, 1H), 8.56 (d, $J = 2.2$ Hz, 1H), 8.29 (dd, $J = 8.4, 4.5$ Hz, 1H), 7.70 (dd, $J = 8.5, 1.9$ Hz, 1H), 7.56 (dd, $J = 8.7, 2.2$ Hz, 1H), 7.35 (d, $J = 8.7$ Hz, 1H). ¹³C NMR (100 MHz, DM DMSO-*d*₆SO) δ 160.46, 138.94, 136.25, 135.47, 130.62, 130.09, 129.22, 127.24, 124.95, 123.88, 123.41, 118.61, 118.39. C₁₃H₇NOCl₂ (ESI+, M+1) =264.05.

8-(Trifluoromethyl)phenanthridin-6(5H)-one (**2q**)



2-chloro-*N*-phenyl-5-(trifluoromethyl)benzamide was treated according to the general procedure as starting material. Major product was purified by CombiFlash[®] Rf, re-dissolved in 1 mL methanol and dried, affording the title compound (6.7mg, 26%) as yellow crystalline solid. $R_f = 0.38$ (40% Ethyl acetate/ Hexane). ¹H NMR (400 MHz, DMSO-*d*₆) δ 12.00 (s, 1H), 8.76 (d, $J = 8.6$ Hz, 1H), 8.56 (s, 1H), 8.49 (d, $J = 7.9$ Hz, 1H), 8.17 (dd, $J = 8.5, 2.0$ Hz, 1H), 7.63 – 7.54 (m, 1H), 7.44 – 7.38 (m, 1H), 7.36 – 7.29 (m, 1H). ¹³C NMR (100 MHz, DMSO-*d*₆) δ 160.45, 138.09, 137.75, 131.46, 129.20 (q, $J = 3.3$ Hz), 128.57, 128.41 (q, $J = 32.6$ Hz), 126.31, 125.80, 124.88 (q, $J = 4.1$ Hz), 124.40 (q, $J = 279$ Hz), 123.18, 117.01, 116.88. C₁₄H₈NOF₃ (ESI+, M+1) =264.10.

1-(2-(2-chlorophenyl)benzo[d]oxazol-5-yl)ethanone:



N-(5-acetyl-2-bromophenyl)-2-chlorobenzamide treated according to the general procedure as starting material. Major Product was purified by CombiFlash[®] Rf affording the title compound (17 mg) as a yellowish white crystalline solid. (17 mg, 63%) as a yellowish white crystalline solid. R_f = 0.47 (40% Ethyl acetate/ Hexane) ¹H NMR (400 MHz, DMSO-*d*₆) δ 8.50 (d, J = 1.5 Hz, 1H), 8.18 (dd, J = 7.7, 1.7 Hz, 1H), 8.09 (dd, J = 8.6, 1.7 Hz, 1H), 7.94 (d, J = 8.6 Hz, 1H), 7.74 (dd, J = 8.0, 1.1 Hz, 1H), 7.67 (td, J = 7.7, 1.7 Hz, 1H), 7.60 (td, J = 7.5, 1.2 Hz, 1H). ¹³C NMR (100 MHz, DMSO-*d*₆) δ 197.57, 161.99, 153.31, 141.72, 134.75, 133.74, 132.78, 132.50, 131.85, 128.30, 126.72, 125.44, 121.54, 111.69, 27.47. C₁₅H₁₀NO₂Cl (ESI+, $M+1$) = 272.10.

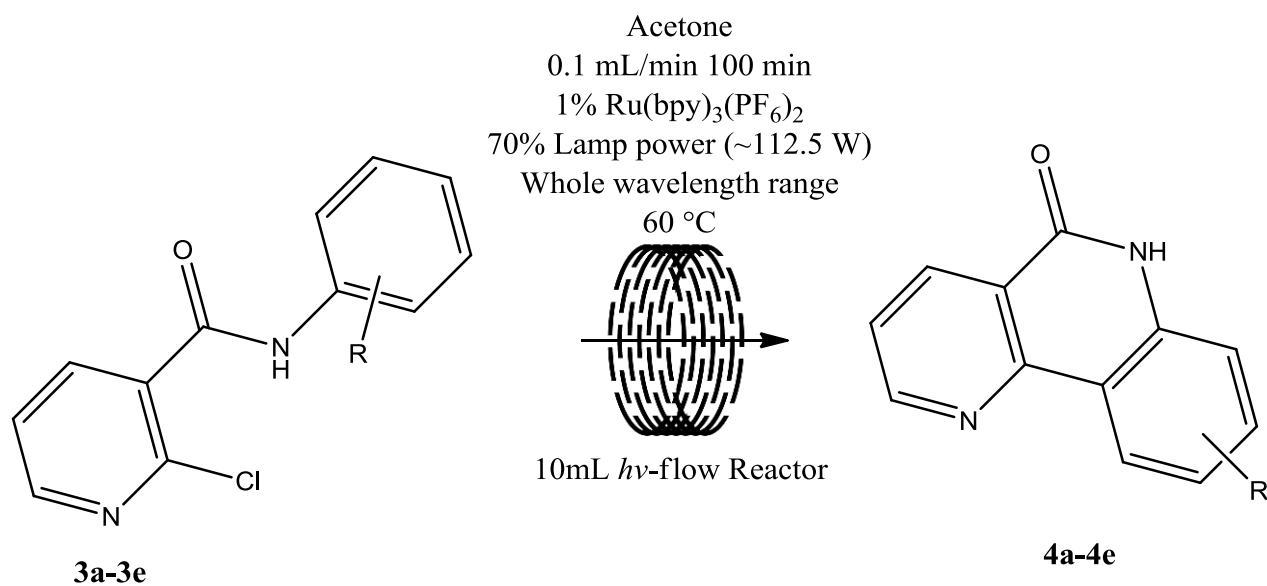
2. Synthesis of Benzo[*h*][1,6]naphthyridin-5(6H)-ones

a. General Procedure

A summary of the reaction along with the reaction condition is represented in **Scheme 16**. A solution of corresponding 2-chloro-*N*-phenylnicotinamides as starting material (0.1 mmol, 0.005 mmol/mL) in acetone (20 mL) was driven continuously through the Vapourtec[®] UV- 150 photochemical flow reactor using a Vapourtec[®] R2+/R4 flow chemistry system at a rate of 0.100 mL/min (reacting time 100min). The UV-150 reactor uses a medium-pressure high-intensity pure Hg lamp (lamp power 80%, approximately 112.5 watts), a 10mL FEP reactor coil, and a filter (type 1, quartz, whole-wavelength range). The temperature was set and maintained at 60°C using the Vapourtec[®] R4 reactor module, and the UV reactor coil flow stream was passed through an 8 bar back pressure regulator, with the Vapourtec[®] R2+ pressure limit set at 12 bar. The reaction

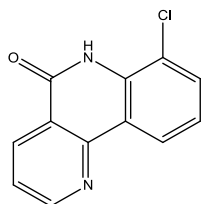
stream of crude product was collected into a round-bottom flask which was covered by aluminum foil. Solvent acetone was removed by a rotary vacuum and the residue was loaded on silica gel and purified by column chromatography (CombiFlash[®] Rf) using 10% to 50% ethyl acetate in hexanes. The purified product was dried under vacuum and weighed.

Scheme 16. General Synthesis Procedure of Benzo[*h*][1,6]naphthyridin-5(6H)-ones



b. Detailed Procedure

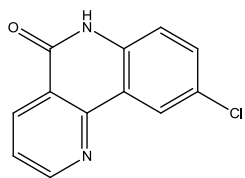
7-chlorobenzo[*h*][1,6]naphthyridin-5(6H)-one (**4a**)



2-chloro-*N*-(2-chlorophenyl)nicotinamide was treated according to the general procedure as starting material. Purification by CombiFlash[®] Rf afforded the title compound (10.9 mg, 47%) as a pale yellow crystalline solid. $R_f = 0.44$ (50%

Ethyl acetate/hexane). ¹H NMR (400 MHz, CDCl₃) δ 9.08 (s, 1H, NH), 9.07 (dd, $J = 4.6, 1.8$ Hz, 1H), 8.77 (dd, $J = 8.0, 1.9$ Hz, 1H), 8.73 (dd, $J = 8.1, 1.2$ Hz, 1H), 7.65 (dd, $J = 7.9, 1.3$ Hz, 1H), 7.60 (dd, $J = 8.0, 4.6$ Hz, 1H), 7.32 (t, $J = 8.0$ Hz, 1H). ¹³C NMR (101 MHz, CDCl₃) δ 161.07, 154.36, 150.88, 136.52, 133.42, 130.95, 123.91, 123.52, 123.32, 121.47, 121.33, 119.57. C₁₂H₇ClN₂O. (ESI+, M+1) = 231.25

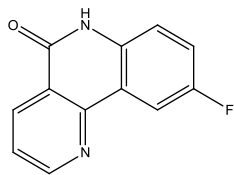
9-chlorobenzo[*h*][1,6]naphthyridin-5(6H)-one (**4b**)



2-chloro-*N*-(4-chlorophenyl)nicotinamide was treated according to the general procedure as starting material. Purification by CombiFlash[®] Rf afforded the title compound (5.5 mg, 24%) as a pale yellow crystalline solid.

$R_f = 0.28$ (50% Ethyl acetate/hexane). ¹H NMR (400 MHz, DMSO-*d*₆) δ 12.03 (s, 1H, NH), 9.08 (dd, $J = 4.6, 1.8$ Hz, 1H), 8.62 (dd, $J = 8.0, 1.8$ Hz, 1H), 8.54 (d, $J = 2.5$ Hz, 1H), 7.73 (q, $J = 8.0$ Hz, 4.8 Hz, 1H), 7.65 (dd, $J = 8.7, 2.5$ Hz, 1H), 7.41 (d, $J = 8.7$ Hz, 1H). ¹³C NMR (101 MHz, DMSO-*d*₆) δ 161.16, 154.74, 149.84, 137.15, 136.35, 131.52, 127.11, 124.55, 123.57, 122.03, 120.70, 118.46. C₁₂H₇ClN₂O. (ESI+, M+1) = 231.05

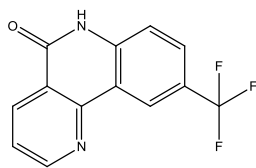
9-fluorobenzo[*h*][1,6]naphthyridin-5(6H)-one (**4c**)



2-chloro-*N*-(4-fluorophenyl)nicotinamide was treated according to the general procedure as starting material. Purification by CombiFlash[®] Rf afforded the title compound (5.5 mg, 26%) as a pale yellow crystalline solid.

R_f = 0.22 (50% Ethyl acetate/hexane). ¹H NMR (400 MHz, DMSO-*d*₆) δ 11.94 (s, 1H, NH), 9.08 (m, J = 8.0, 1.7 Hz, 1H), 8.63 (dd, J = 8.0, 1.7 Hz, 1H), 8.28 (dd, J = 9.6, 2.8 Hz, 1H), 7.73 (dd, J = 8.0, 4.6 Hz, 1H), 7.50 (td, J = 8.6, 2.9 Hz, 1H), 7.43 (dd, J = 8.9, 4.9 Hz, 1H). ¹³C NMR (101 MHz, DMSO-*d*₆) δ 161.03, 158.22 (d, J = 237 Hz), 154.62, 136.36, 135.04, 124.47, 123.65, 122.05, 121.87 (d, J = 8.1 Hz), 119.47 (d, J = 24 Hz), 118.44 (d, J = 8.2 Hz), 109.61 (d, J = 24 Hz), C₁₂H₇FN₂O. (ESI+, M+1) = 215.05

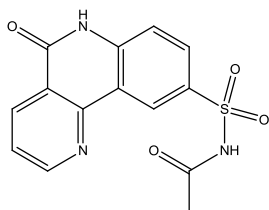
9-(trifluoromethyl)benzo[*h*][1,6]naphthyridin-5(6H)-one (**4d**)



2-chloro-*N*-(4-(trifluoromethyl)phenyl)nicotinamide was treated according to the general procedure as starting material. Purification by CombiFlash[®] Rf afforded the title compound (13.2 mg, 50%) as a pale yellow crystalline solid.

R_f = 0.23 (50% Ethyl acetate/hexane). ¹H NMR (400 MHz, DMSO-*d*₆) δ 12.20 (s, 1H, NH), 9.10 (dd, J = 4.6 Hz, 1.6 Hz, 1H), 8.86 (d, J = 1.5 Hz, 1H), 8.63 (dd, J = 8.0, 1.8 Hz, 1H), 7.92 (dd, J = 8.6, 1.7 Hz, 1H), 7.75 (dd, J = 8.0, 4.6 Hz, 1H), 7.56 (d, J = 8.6 Hz, 1H). ¹³C NMR (101 MHz, DMSO-*d*₆) δ 161.50, 154.86, 150.02, 141.06, 136.39, 127.96 (q, J = 3.4 Hz), 124.85 (q, J = 269.6 Hz), 124.73, 123.26 (q, J = 32.2 Hz), 122.16, 121.63 (q, J = 4.2 Hz), 119.27, 117.53 C₁₅H₇FN₂O. (ESI+, M+1) = 318.05

N-((5-oxo-5,6-dihydrobenzo[*h*][1,6]naphthyridin-9-yl)sulfonyl)acetamide (**4e**)



N-(4-(*N*-acetylsulfamoyl)phenyl)-2-chloronicotinamide was treated according to the general procedure as starting material. Purification by CombiFlash[®] Rf afforded the title compound (16.6 mg, 52%) as a pale yellow crystalline solid. $R_f = 0.23$ (20% DCM/methanol). ¹H NMR (400 MHz, DMSO-*d*₆) δ 12.27 (s, 1H, NH), 12.10 (s, 1H), 9.18 (d, $J = 2.1$ Hz, 1H), 9.13 (dd, $J = 4.5, 1.6$ Hz, 1H), 8.64 (dd, $J = 8.0, 1.6$ Hz, 1H), 8.07 (dd, $J = 8.6, 2.2$ Hz, 1H), 7.76 (dd, $J = 8.0, 4.6$ Hz, 1H), 7.56 (d, $J = 8.7$ Hz, 1H), 1.93 (s, 3H). ¹³C NMR (101 MHz, DMSO-*d*₆) δ 169.24, 161.60, 154.95, 150.01, 141.84, 136.40, 133.34, 130.28, 125.26, 124.80, 122.16, 119.02, 117.11, 23.70. C₁₄H₁₁N₃O₄S. (ESI+, $M+1$) = 331.15

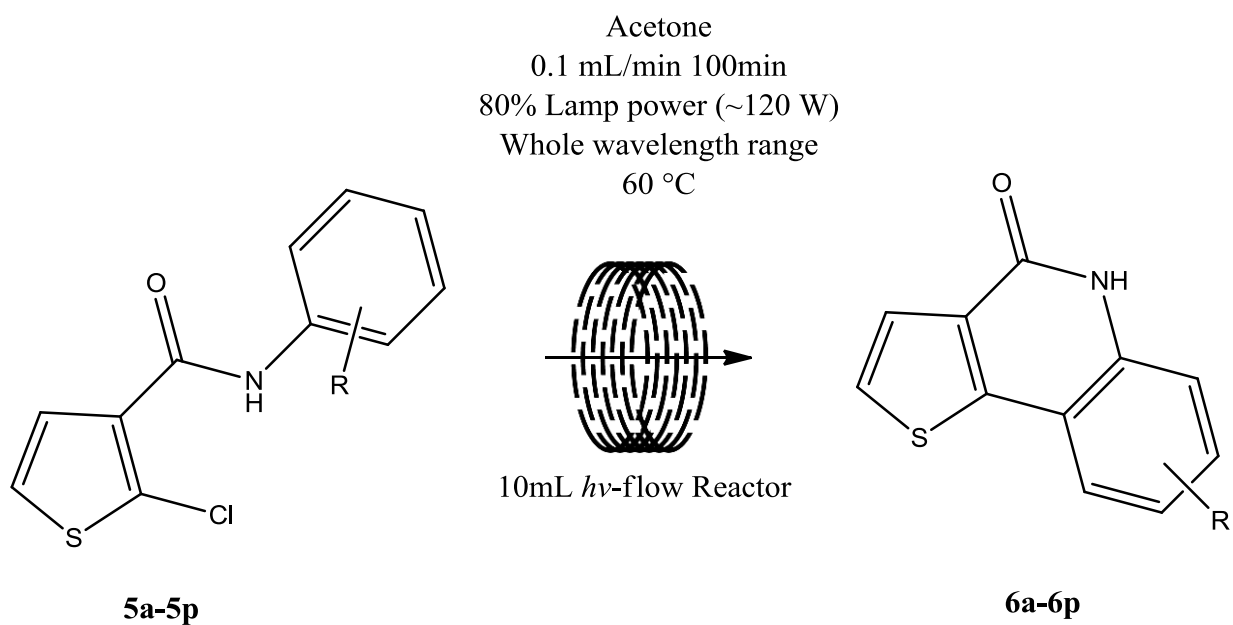
3. Synthesis of Thieno[3,2-*c*]quinolin-4(5H)-ones

a. General Procedure

A summary of the synthesis of thieno[3,2-*c*]quinolin-4(5H)-ones is presented in **Scheme 17**. A solution of starting material (corresponding 2-chloro-*N*-phenylthiophene-3-carboxamide derivative or 3-chloro-*N*-phenylthiophene-2-carboxamide derivative) (0.1 mmol, 0.005 mmol/mL) in acetone (20mL) was passed continuously through the Vapourtec[®] UV- 150 photochemical flow reactor using a Vapourtec[®] R2+/R4 flow chemistry system at a rate of 0.100 mL/min (reacting time 100min). The UV-150 reactor uses a medium-pressure pure Hg lamp (lamp power 80%, approximately 112.5 watts), a 10mL FEP reactor coil, and a filter (type 1, quartz, whole-wavelength range). The temperature was set and maintained at 60°C using the Vapourtec[®] R4 reactor module, and the UV reactor coil flow stream was passed through an 8 bar

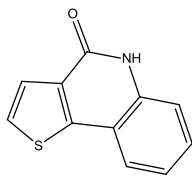
back pressure regulator, with the Vapourtec[®] R2+ pressure limit set at 12 bar. The reaction stream of crude product was collected into a round-bottom flask which was covered by aluminum foil. Solvent acetone was removed by a rotary vacuum and the residue was loaded on silica gel and purified by column chromatography (CombiFlash[®] Rf) using 10% ethyl acetate in hexanes to 50% ethyl acetate in hexanes. The purified product was dried under vacuum and weighed.

Scheme 17. General Synthesis Procedure of Thieno[3,2-*c*]quinolin-4(5H)-ones



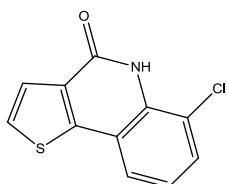
a. Detailed Procedure

Thieno[3,2-*c*]quinolin-4(5H)-one (**6a**)



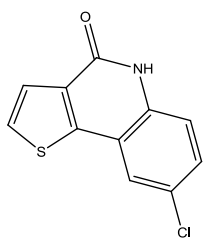
2-chloro-*N*-phenylthiophene-3-carboxamide was treated according to the general procedure as starting material. Major product was separated and purified by Combiflash[®] Rf, affording the title compound (12.7 mg, 64%) as beige white solid. $R_f=0.27$ (Hexane: Ethyl acetate =1: 1). ^1H NMR (400 MHz, DMSO- d_6) δ 11.77 (s, 1H, NH), 7.84 (d, $J = 7.5$ Hz, 1H), 7.79 (d, $J = 5.2$ Hz, 1H), 7.59 (d, $J = 5.2$ Hz, 1H), 7.49 (ddd, $J = 8.3, 7.1, 1.3$ Hz, 1H), 7.42 (dd, $J = 8.3, 0.8$ Hz, 1H), 7.27 – 7.21 (m, 1H). ^{13}C NMR (101 MHz, DMSO- d_6) δ 158.60, 146.02, 136.64, 131.56, 129.81, 127.13, 125.71, 123.82, 122.89, 116.72, 116.61. $\text{C}_{11}\text{H}_7\text{NOS}$. (ESI+, $\text{M}+1$) =202.05.

6-chlorothieno[3,2-*c*]quinolin-4(5H)-one (**6b**)



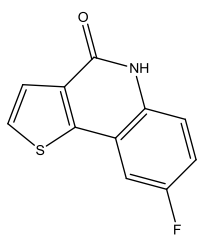
2-chloro-*N*-(2-chlorophenyl)thiophene-3-carboxamide was treated according to the general procedure as starting material. Major product was separated and purified by Combiflash[®] Rf, affording the title compound (12.7 mg, 54%) as beige white solid. $R_f=0.49$ (Hexane: Ethyl acetate =1: 1). ^1H NMR (400 MHz, DMSO- d_6) δ 10.93 (s, 1H, NH), 7.85 (dd, $J = 8.4, 6.8$ Hz, 2H), 7.63 (d, $J = 6$ Hz, 2H), 7.25 (t, $J = 7.9$ Hz, 1H). ^{13}C NMR (101 MHz, DMSO- d_6) δ 158.39, 145.76, 133.04, 132.02, 129.94, 128.50, 125.82, 123.60, 123.07, 119.80, 118.39. $\text{C}_{11}\text{H}_6\text{ClNOS}$. (ESI+, $\text{M}+1$) =236.00.

8-chlorothieno[3,2-*c*]quinolin-4(5H)-one (**6c**)



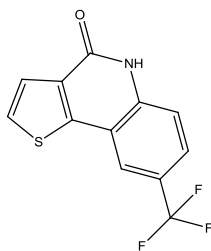
2-chloro-*N*-(4-chlorophenyl)thiophene-3-carboxamide carboxamide was treated according to the general procedure as starting material. Major product was separated and purified by Combiflash[®] Rf, affording the title compound (16.7 mg, 72%) as beige white solid. $R_f=0.31$ (Hexane: Ethyl acetate =1: 1). ¹H NMR (400 MHz, DMSO-*d*₆) δ 11.88 (s, 1H, NH), 7.92 (d, $J = 1.9$ Hz, 1H), 7.85 (d, $J = 5.2$ Hz, 1H), 7.60 (d, $J = 5.2$ Hz, 1H), 7.53 (dd, $J = 8.8, 2.2$ Hz, 1H), 7.42 (d, $J = 8.8$ Hz, 1H). ¹³C NMR (101 MHz, DMSO-*d*₆) δ 158.38, 144.62, 135.40, 132.27, 129.61, 128.30, 126.77, 125.72, 122.93, 118.45, 117.99. C₁₁H₆ClNOS. (ESI+, M+1) =235.95.

8-fluorothieno[3,2-*c*]quinolin-4(5H)-one (**6d**)



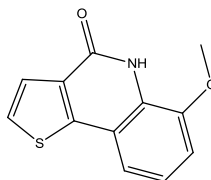
2-chloro-*N*-(4-fluorophenyl)thiophene-3-carboxamide was treated according to the general procedure as starting material. Major product was separated and purified by Combiflash[®] Rf, affording the title compound (14.2 mg, 65%) as beige white solid. $R_f=0.21$ (Hexane: Ethyl acetate =1: 1). ¹H NMR (400 MHz, DMSO-*d*₆) δ 11.82 (s, 1H, NH), 7.85 (d, $J = 5.2$ Hz, 1H), 7.74 (dd, $J = 9.2, 2.6$ Hz, 1H), 7.60 (d, $J = 5.2$ Hz, 1H), 7.44 (dd, $J = 9.0, 5.0$ Hz, 1H), 7.39 (td, $J = 8.8, 2.7$ Hz, 1H). ¹³C NMR (101 MHz, DMSO-*d*₆) δ 158.32, 157.76 (d, $J = 237.5$ Hz), 145.03 (d, $J = 3$ Hz), 133.33, 132.27, 128.19, 125.76, 118.48 (d, $J = 9$ Hz), 117.58 (d, $J = 24$ Hz), 117.48 (d, $J = 9$ Hz), 109.28 (d, $J = 23$ Hz). C₁₁H₆FNOS. (ESI+, M+1) =220.00.

8-(trifluoromethyl)thieno[3,2-*c*]quinolin-4(5H)-one (**6e**)



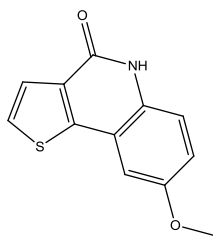
2-chloro-*N*-(4-(trifluoromethyl)phenyl)thiophene-3-carboxamide was treated according to the general procedure as starting material. Major product was separated and purified by Combiflash[®] Rf, affording the title compound (20.7 mg, 77%) as beige white solid. $R_f=0.46$ (Hexane: Ethyl acetate =1: 1). ^1H NMR (400 MHz, DMSO- d_6) δ 12.09 (s, 1H, NH), 8.13 (d, $J=0.5$ Hz, 1H), 7.88 (d, $J=5.2$ Hz, 1H), 7.79 (dd, $J=8.7, 1.6$ Hz, 1H), 7.62 (d, $J=5.2$ Hz, 1H), 7.57 (d, $J=8.6$ Hz, 1H). ^{13}C NMR (101 MHz, DMSO- d_6) δ 158.59, 145.11, 139.19, 132.41, 128.55, 125.96 (q, $J=3.6$ Hz), 125.69, 124.64 (q, $J=269.8$ Hz), 123.1 (q, $J=32$ Hz), 121.05 (q, $J=4$ Hz) 117.54, 116.56. $\text{C}_{12}\text{H}_6\text{F}_3\text{NOS}$. (ESI+, $\text{M}+1$) =270.00.

6-methoxythieno[3,2-*c*]quinolin-4(5H)-one (**6f**)



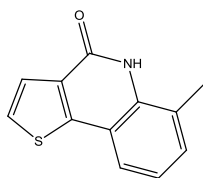
2-chloro-*N*-(2-methoxyphenyl)thiophene-3-carboxamide was treated according to the general procedure as starting material. Major product was separated and purified by Combiflash[®] Rf, affording the title compound (11.6 mg, 50%) as beige white solid. $R_f=0.31$ (Hexane: Ethyl acetate =1: 1). ^1H NMR (400 MHz, DMSO- d_6) δ 10.76 (s, 1H, NH), 7.80 (d, $J=5.2$ Hz, 1H), 7.61 (d, $J=5.2$ Hz, 1H), 7.41 (d, $J=7.8$ Hz, 1H), 7.21 (t, $J=7.9$ Hz, 1H), 7.14 (d, $J=7.9$ Hz, 1H), 3.93 (s, 3H). ^{13}C NMR (101 MHz, DMSO- d_6) δ 158.12, 146.89, 146.03, 131.89, 127.36, 126.45, 125.85, 123.12, 117.07, 115.55, 110.59, 56.56. $\text{C}_{12}\text{H}_9\text{NO}_2\text{S}$. (ESI+, $\text{M}+1$) =232.00.

8-methoxythieno[3,2-*c*]quinolin-4(5H)-one (**6g**)



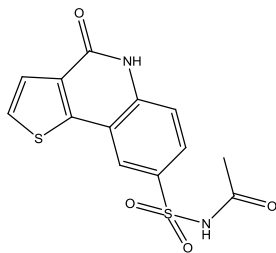
2-chloro-*N*-(4-methoxyphenyl)thiophene-3-carboxamide was treated according to the general procedure as starting material. Major product was separated and purified by Combiflash[®] Rf, affording the title compound (5.3 mg, 23%) as beige white solid. R_f =0.16 (Hexane: Ethyl acetate =1: 1). ¹H NMR (400 MHz, DMSO-*d*₆) δ 11.66 (s, 1H, NH), 7.80 (d, J =5.2 Hz, 1H), 7.58 (d, J =5.2 Hz, 1H), 7.36 (d, J =9.0 Hz, 1H), 7.26 (d, J =2.6 Hz, 1H), 7.14 (dd, J =9.0, 2.6 Hz, 1H), 3.85 (s, 3H). ¹³C NMR (101 MHz, DMSO-*d*₆) δ 158.20, 155.06, 145.57, 131.87, 130.92, 127.22, 125.81, 118.68, 118.05, 117.26, 105.70, 56.09. C₁₂H₉NO₂S. (ESI+, M+1) =232.05.

6-methylthieno[3,2-*c*]quinolin-4(5H)-one (**6h**)



2-chloro-*N*-(*o*-tolyl)thiophene-3-carboxamide was treated according to the general procedure as starting material. Major product was separated and purified by Combiflash[®] Rf, affording the title compound (8.4 mg, 39%) as beige white solid. R_f =0.41 (Hexane: Ethyl acetate =1: 1). ¹H NMR (400 MHz, DMSO-*d*₆) δ 10.83 (s, 1H, NH), 7.78 (d, J =5.2 Hz, 1H), 7.69 (d, J =7.8 Hz, 1H), 7.61 (d, J =5.3 Hz, 1H), 7.34 (d, J =7.3 Hz, 1H), 7.16 (t, J =7.6 Hz, 1H) 2.49 (s, 1H). ¹³C NMR (101 MHz, DMSO-*d*₆) δ 158.90, 146.76, 134.97, 131.29, 131.19, 127.17, 125.73, 125.03, 122.71, 121.84, 116.72, 18.26. C₁₂H₉NOS. (ESI+, M+1) =216.05.

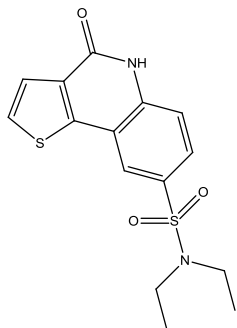
N-((4-oxo-4,5-dihydrothieno[3,2-*c*]quinolin-8-yl)sulfonyl)acetamide (**6i**)



2-chloro-*N*-(*o*-tolyl)cyclopenta-1,4-dienecarboxamide was treated according to the general procedure as starting material. Major product was separated and purified by Combiflash[®] Rf, affording the title compound (13.2 mg, 41%) as beige white solid. $R_f = 0.51$.

(Dichloromethane: Methanol =5: 1). ¹H NMR (400 MHz, DMSO-*d*₆) δ 12.20 (s, 1H, NH), 12.14 (s, 1H), 8.28 (d, $J = 1.6$ Hz, 1H), 7.96 (dd, $J = 8.7, 1.8$ Hz, 1H), 7.92 (d, $J = 5.2$ Hz, 1H), 7.65 (d, $J = 5.2$ Hz, 1H), 7.59 (d, $J = 8.7$ Hz, 1H), 1.93 (s, 3H). ¹³C NMR (101 MHz, DMSO-*d*₆) δ 169.38, 158.61, 144.99, 140.02, 132.97, 132.45, 128.65, 128.21, 125.88, 123.91, 117.33, 116.16, 23.74. C₁₃H₁₀N₂O₄S₂. (ESI⁺, M+1) =323.00.

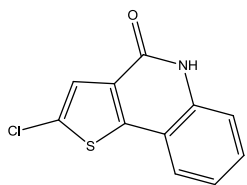
N,N-diethyl-4-oxo-4,5-dihydrothieno[3,2-*c*]quinoline-8-sulfonamide (**6j**)



2-chloro-*N*-(4-(*N,N*-diethylsulfamoyl)phenyl)thiophene-3-carboxamide was treated according to the general procedure as starting material. Major product was separated and purified by Combiflash[®] Rf, affording the title compound (9.7 mg, 29%) as white solid. $R_f = 0.19$ (Hexane: Ethyl acetate =1:1). ¹H NMR (400 MHz, DMSO-*d*₆) δ 12.15 (s, 1H, NH), 8.11 (s, 1H),

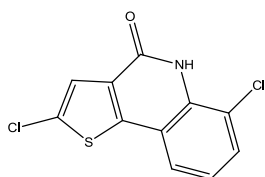
7.91 (d, $J = 5.2$ Hz, 1H), 7.88 (dd, $J = 8.7, 1.7$ Hz, 1H), 7.64 (d, $J = 5.2$ Hz, 1H), 7.58 (d, $J = 8.7$ Hz, 1H), 3.20 (q, $J = 7.0$ Hz, 4H), 1.06 (t, $J = 7.1$ Hz, 6H). ¹³C NMR (101 MHz, DMSO-*d*₆) δ 158.57, 145.09, 139.27, 133.78, 132.46, 128.60, 127.64, 125.82, 122.48, 117.70, 116.47, 42.32, 14.61. C₁₅H₁₆N₂O₃S₂. (ESI⁺, M+1) =337.10.

2-chlorothieno[3,2-*c*]quinolin-4(5H)-one (**6l**)



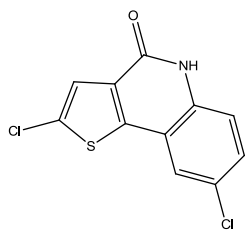
2,5-dichloro-*N*-phenylthiophene-3-carboxamide was treated according to the general procedure as starting material. Major product was separated and purified by Combiflash[®] Rf, affording the title compound (9.7 mg, 41%) as beige white solid. $R_f=0.43$ (Hexane: Ethyl acetate =1: 1). ^1H NMR (400 MHz, DMSO- d_6) δ 11.87 (s, 1H), 7.77 (d, $J=7.6$ Hz, 1H), 7.58 (s, 1H), 7.54 – 7.49 (m, 1H), 7.42 (d, $J=8.2$ Hz, 1H), 7.25 (t, $J=7.5$ Hz, 1H). ^{13}C NMR (101 MHz, DMSO- d_6) δ 157.40, 144.99, 136.80, 130.85, 130.35, 129.63, 125.03, 123.76, 123.12, 116.78, 115.77. $\text{C}_{11}\text{H}_6\text{ClNOS}$. (ESI+, $M+1$) =235.95.

2,6-dichlorothieno[3,2-*c*]quinolin-4(5H)-one (**6m**)



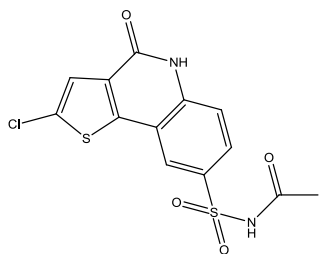
2,5-dichloro-*N*-phenylthiophene-3-carboxamide was treated according to the general procedure as starting material. Major product was separated and purified by Combiflash[®] Rf, affording the title compound (8.1 mg, 30%) as beige white solid. $R_f=0.54$ (Hexane: Ethyl acetate =1: 1). ^1H NMR (400 MHz, DMSO- d_6) δ 11.07 (s, 1H, NH), 7.80 (d, $J=7.9$ Hz, 1H), 7.68 (d, $J=7.8$ Hz, 1H), 7.66 (s, 1H), 7.27 (t, $J=7.9$ Hz, 1H). ^{13}C NMR (101 MHz, DMSO- d_6) δ 157.26, 144.66, 133.23, 131.43, 130.87, 130.48, 125.22, 123.81, 123.06, 119.96, 117.46. $\text{C}_{11}\text{H}_5\text{Cl}_2\text{NOS}$. (ESI+, $M+1$) =269.95.

2,8-dichlorothieno[3,2-*c*]quinolin-4(5H)-one (**6n**)



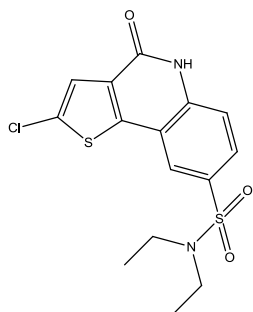
2,5-dichloro-*N*-phenylthiophene-3-carboxamide was treated according to the general procedure as starting material. Major product was separated and purified by Combiflash[®] Rf, affording the title compound (12.1 mg, 45%) as beige white solid. R_f = 0.43 (Hexane: Ethyl acetate = 1: 1). ¹H NMR (400 MHz, DMSO-*d*₆) δ 12.02 (s, 1H, NH), 7.94 (d, J = 2.3 Hz, 1H), 7.61 (s, 1H), 7.56 (dd, J = 8.8, 2.3 Hz, 1H), 7.41 (d, J = 8.8 Hz, 1H). ¹³C NMR (101 MHz, DMSO-*d*₆) δ 157.19, 143.55, 135.57, 131.63, 130.77, 130.16, 127.03, 125.08, 122.98, 118.61, 117.01. C₁₁H₅Cl₂NOS. (ESI+, M+1) = 270.00

N-((2-chloro-4-oxo-4,5-dihydrothieno[3,2-*c*]quinolin-8-yl)sulfonyl)acetamide (**6o**)



N-(4-(*N*-acetylsulfamoyl)phenyl)-2,5-dichlorothiophene-3-carboxamide was treated according to the general procedure as starting material. Major product was separated and purified by Combiflash[®] Rf, affording the title compound (15.3 mg, 43%) as beige white solid. R_f = 0.57 (Dichloromethane: Methanol = 5: 1). ¹H NMR (400 MHz, DMSO-*d*₆) δ 12.28 (s, 1H, NH), 8.17 (d, J = 1.8 Hz, 1H), 7.98 (dd, J = 8.7, 1.9 Hz, 2H), 7.65 (s, 1H), 7.56 (d, J = 8.8 Hz, 1H), 1.93 (s, 3H). ¹³C NMR (101 MHz, DMSO-*d*₆) δ 169.40, 157.39, 143.85, 140.13, 133.31, 131.86, 131.08, 128.64, 125.27, 123.72, 117.52, 115.21, 23.75. C₁₃H₉ClN₂O₄S₂, (ESI+, M+1) = 356.90

2-chloro-*N,N*-diethyl-4-oxo-4,5-dihydrothieno[3,2-*c*]quinoline-8-sulfonamide (**6p**)



2,5-dichloro-*N*-(4-(*N,N*-diethylsulfamoyl)phenyl)thiophene-3-carboxamide carboxamide was treated according to the general procedure as starting material. Major product was separated and purified by Combiflash[®] Rf, affording the title compound (15.9 mg, 43%) as beige white solid. $R_f=0.30$ (Hexane: Ethyl acetate =1:1) ¹H NMR (400 MHz, DMSO-*d*₆) δ 12.24 (s,

1H, NH), 8.07 (d, $J = 1.6$ Hz, 1H), 7.89 (dd, $J = 8.7, 1.8$ Hz, 1H), 7.65 (s, 1H), 7.57 (d, $J = 8.7$ Hz, 1H), 3.20 (q, $J = 7.1$ Hz, 4H), 1.06 (t, $J = 7.1$ Hz, 6H). ¹³C NMR (101 MHz, DMSO-*d*₆) δ 157.38, 144.03, 139.38, 134.13, 131.86, 131.10, 128.06, 125.14, 122.50, 117.86, 115.57, 42.35, 14.63. C₁₅H₁₅ClN₂O₃S₂. (ESI+, M+1) =356.05

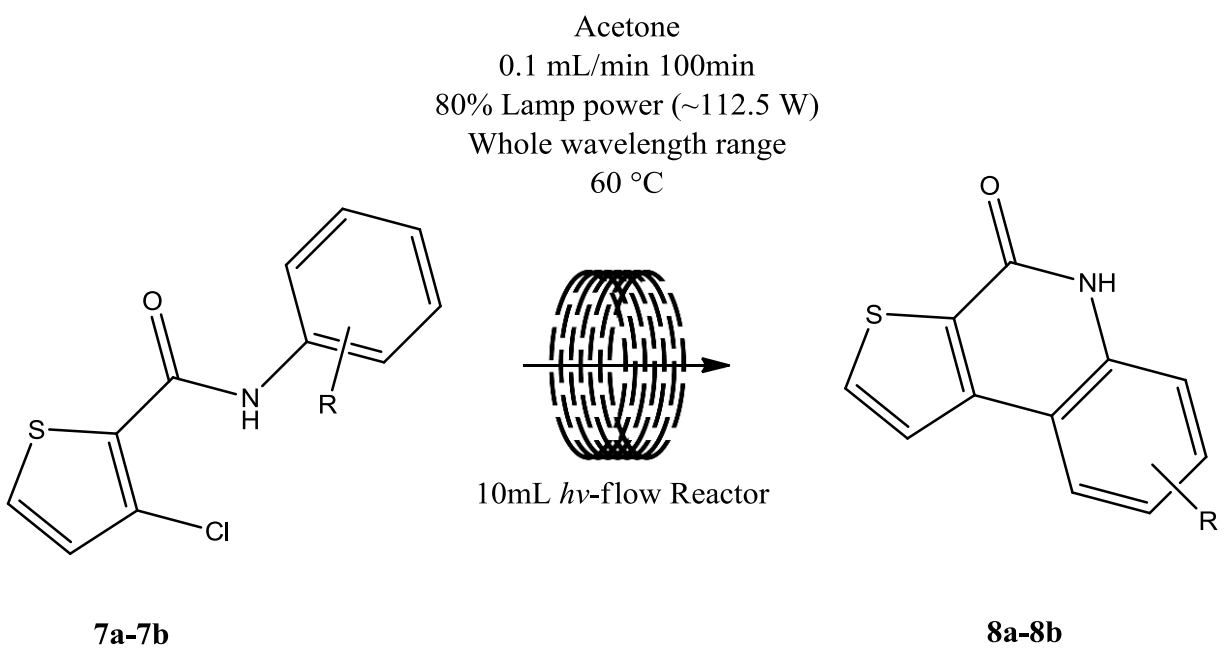
4. Synthesis of Thieno[2,3-*c*]quinolin-4(5H)-ones

a. General Procedure

A summary of the synthesis of thieno[2,3-*c*]quinolin-4(5H)-ones is presented in **Scheme 3.2.4**. A solution of starting material (corresponding 2-chloro-*N*-phenylthiophene-3-carboxamide derivative or 3-chloro-*N*-phenylthiophene-2-carboxamide derivative) (0.1 mmol, 0.005 mmol/mL) in acetone (20mL) was passed continuously through the Vapourtec[®] UV- 150 photochemical flow reactor using a Vapourtec[®] R2+/R4 flow chemistry system at a rate of 0.100 mL/min (reacting time 100min). The UV-150 reactor uses a medium-pressure pure Hg lamp (lamp power 80%, approximately 112.5 watts), a 10mL FEP reactor coil, and a filter (type 1, quartz, whole-wavelength range). The temperature was set and maintained at 60°C using the Vapourtec[®] R4 reactor module, and the UV reactor coil flow stream was passed through an 8 bar

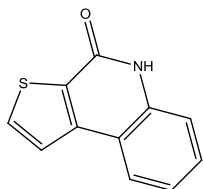
back pressure regulator, with the Vapourtec[®] R2+ pressure limit set at 12 bar. The reaction stream of crude product was collected into a round-bottom flask which was covered by aluminum foil. Solvent acetone was removed by a rotary vacuum and the residue was loaded on silica gel and purified by column chromatography (CombiFlash[®] Rf) using 10% ethyl acetate in hexanes to 50% ethyl acetate in hexanes. The purified product was dried under vacuum and weighed.

Scheme 18. General Synthesis Procedure of Thieno[2,3-*c*]quinolin-4(5H)-ones



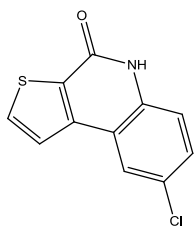
b. Detailed Procedure

Thieno[2,3-*c*]quinolin-4(5H)-one (**8a**)



3-chloro-*N*-phenylthiophene-2-carboxamide was treated according to the general procedure as starting material. Major product was separated and purified by Combiflash[®] Rf, affording the title compound (17.1 mg, 85%) as white solid. $R_f=0.40$ (Hexane: Ethyl acetate =1: 1). ^1H NMR (400 MHz, DMSO- d_6) δ 11.89 (s, 1H, NH), 8.18 (t, $J = 6.8$ Hz, 2H), 8.08 (d, $J = 5.2$ Hz, 1H), 7.53 – 7.47 (m, 1H), 7.45 (d, $J = 7.8$ Hz, 1H), 7.28 (t, $J = 7.4$ Hz, 1H). ^{13}C NMR (101 MHz, DMSO- d_6) δ 158.17, 143.54, 137.85, 134.74, 130.45, 129.47, 124.68, 123.97, 122.65, 117.36, 116.56. $\text{C}_{11}\text{H}_7\text{NOS}$. (ESI+, $M+1$) =202.05.

8-chlorothieno[2,3-*c*]quinolin-4(5H)-one (**8b**)



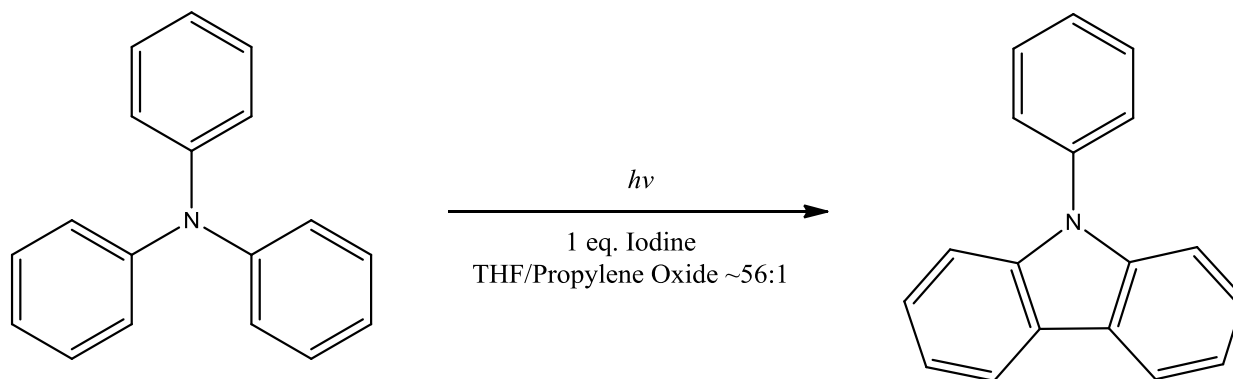
3-chloro-*N*-(4-chlorophenyl)thiophene-2-carboxamide carboxamide was treated according to the general procedure as starting material. Major product was separated and purified by Combiflash[®] Rf, affording the title compound (21.2 mg, 90%) as white solid. $R_f=0.48$ (Hexane: Ethyl acetate =1: 1). ^1H NMR (400 MHz, DMSO- d_6) δ 12.01 (s, 1H, NH), 8.31 (d, $J = 2.2$ Hz, 1H), 8.21 (d, $J = 5.2$ Hz, 1H), 8.14 (d, $J = 5.2$ Hz, 1H), 7.53 (dd, $J = 8.8, 2.2$ Hz, 1H), 7.44 (d, $J = 8.8$ Hz, 1H). ^{13}C NMR (101 MHz, DMSO- d_6) δ 157.96, 142.45, 136.57, 134.97, 131.37, 129.34, 126.79, 124.31, 124.03, 118.61, 118.35. $\text{C}_{11}\text{H}_6\text{ClNOS}$. (ESI+, $M+1$) =235.95.

IV. Results and Discussion

A. Preliminary Reaction and Optimization

We began our research by reproducing a simple photochemical cyclization to test the capability of the flow-photo reactor. Following a previous literature example published by Collins^[67], we purchased commercial-available triphenylamine and used iodine/propylene oxide as the oxidant system to perform this Mallory reaction in THF. The reaction was performed in the presence of 0.1 mmol/mL triphenylamine with 1 equivalent of iodine and 18% propylene oxide. The flow rate was set to 0.2 mL/min so that the solution was irradiated in the 10mL, 50% power (approximately 75 W), whole-wavelength UV reactor for 50 min at 50 °C (**Scheme 19**).

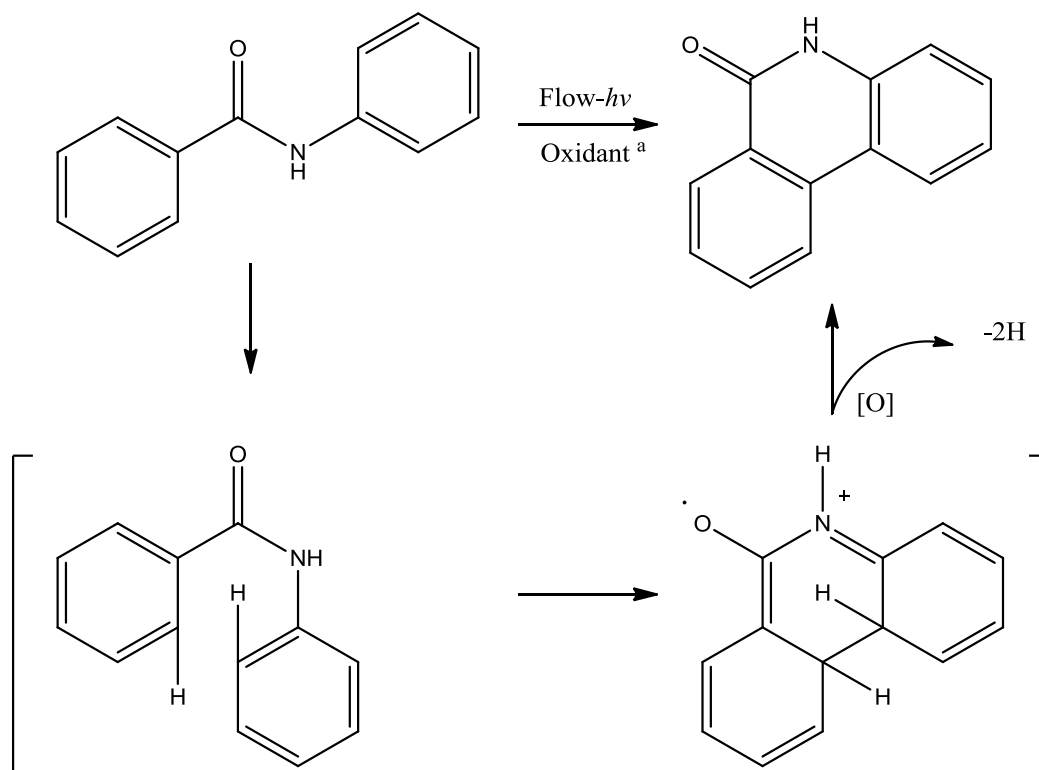
Scheme 19. The Pre-research Test: Photocyclization of Triphenylamine



Once we were satisfied that the flow photochemical reactor was performing well, we decided to develop an alternate method for the flow photochemical cyclization of *N*-phenylbenzamides to produce an expedited route to phenanthridinones (**Scheme 20**). To probe this novel synthesis

method of phenanthridinones and inspired by the Collins's research, we initiated the research by applying the Mallory reaction, as we assumed that the Mallory-type reactions could be used to synthesize phenanthridinone from benzanilide (*N*-phenylbenzamide) as benzanilide had similar structure to diphenylamine, a typical Mallory-reaction starting material. We hypothesized that like the rest of Mallory reactions, UV would excite the substrate to generate a radical first. In the case of benzanilide, the radical might appear first on the amide nitrogen or ketone. The radical might be transferred to the ring system in a short time and form the C–C bond between two corresponding carbon simultaneously. Two supernumerary hydrogens would be cleaved by the oxidant with an oxidation process. The results of our initial attempts are summarized in **Table 1** and describe that our attempts to use a Mallory-type reaction failed and a new method needed to be developed for convert benzanilides to phenanthridinones.

Scheme 20. Potential cyclization of *N*-phenylbenzamides to produce phenanthridinones



a. The oxidant in the reaction will be discussed below.

Table 1. Attempts to perform the Mallory type reaction directly.

| Entry | Oxidant | Solvent | Residence Time | Result |
|-------|---|--------------|----------------|--------|
| 1 | Iodine/ Propylene Oxide System | THF | 50 min | Failed |
| 2 | Iodine/ Propylene Oxide System | Methanol | 50 min | Failed |
| 3 | Iodine/ Propylene Oxide System | DMF | 50 min | Failed |
| 4 | Iodine/ Propylene Oxide System | Acetonitrile | 50 min | Failed |
| 5 | Iodine/ Propylene Oxide System with Oxygen | Acetonitrile | 50 min | Failed |
| 6 | Iodine/ Propylene Oxide System with Oxygen | Methanol | 50 min | Failed |
| 7 | Oxygen | Acetonitrile | 50 min | Failed |

By studying the Mallory-type reaction, we realized that a halogen substituent on ortho-position might create a radical after cleavage/elimination of halogen. Our thoughts were soon verified by a series of tests using 2-chloro-*N*-phenylbenzamide as starting material (**Table 2**). In the reaction screen, we used photoredox catalysts and an oxidant in a desire to accelerate the

reaction. To date, a method that employs the use of a photoredox catalyst to mediate the photocyclization of benzanilides has not appeared in the literature and we set out to develop a method to perform such a reaction using ultraviolet and/or visible light, in combination with a photoredox catalyst. In our initial tests, the reaction produced phenanthridinone with approximately 70% yield.

Table 2. Preliminary Optimization 1 ^a

| Entry | Starting Material | | Product | | Yield ^a |
|-------|-------------------|----------------|-------------------|------------------|--------------------|
| | Amides | | Phenanthridinones | | |
| | R ₁ | R ₂ | R ₁ ' | R ₂ ' | |
| 1 | Cl | H | H | H | 87%-95% |
| 2 | H | Cl | H | H | 51% |
| 3 | Cl | Cl | H | Cl | 50%-61% |
| | | | H | H | 30%-40% |

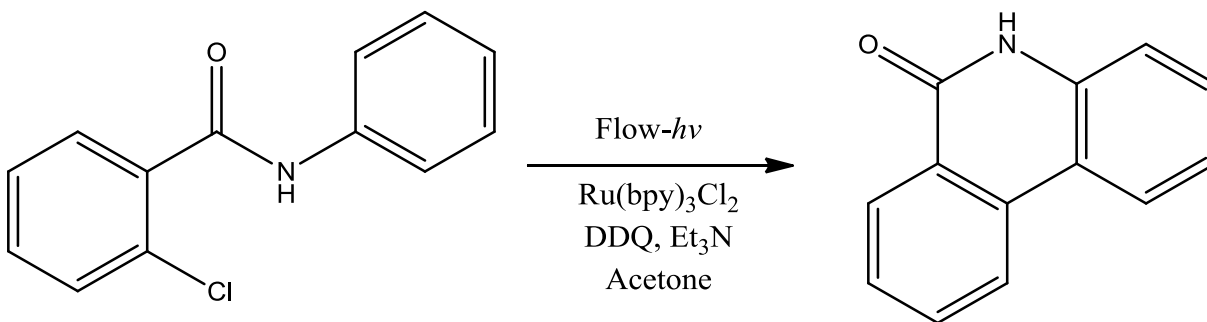
| | | | | | |
|---|----|---|----|---|--------------------|
| | | | Cl | H | Trace ^b |
| 4 | H | I | H | H | Trace |
| 5 | Cl | I | H | H | 81% |
| 6 | Br | H | H | H | Trace |
| 7 | I | H | H | H | Trace |

a. Isolated yields. b. Trace of product is found by LC. The major product is dehalogenated product, which are benzamides.

On the basis of data from our previous reaction screen, we carried out our first optimization procedure focused on the possible influence of halogen substituents at ortho-position. In addition, we aimed to evaluate the scope of the reaction and find out the most suitable starting material motif structure and varied the substituents on the amides with different halogens at the ortho-position as shown in **Table 2**. Originally, we set the flow rate to be 0.2 mL/min again so that the solution would be illuminated for 50 min. The result of this procedure revealed that halogen substituents at R₁ position produced a higher yield than at R₂ position and chloro-substituent amides produced a better yield than other halogen substituents. Iodo- and bromo- substituted starting material didn't work well during the reactions and resulted in the dehalogenated products. Thus, we employed 2-chloro-*N*-phenylbenzamide structure as our motif structure for subsequent research.

To explore the influence of different reaction conditions, an optimization procedure was applied. These reaction conditions included catalyst, oxidant, residence time, concentration, UV

wavelength. For a quick and effective optimizing, we used HPLC with external reference method to determine an approximate yield of each entry after preparing pure phenanthridinone as standard product (99.5% purity, determined by HPLC) with the above mentioned method. The result of the optimization 2 and optimization 3, as shown in **Table 3** and **Table 4**, demonstrated that the usage of oxidant (such as DDQ, which was mentioned by Mallory) or base (such as triethylamine) would decrease the yield significantly and the usage of photoredox catalyst would decrease the yield mildly; we didn't really need any base, oxidant in the reaction. However, the influence of photo catalyst was still confusing.

Table 3. Optimization 2 ^a

| Entry | SM ^c eq. | DDQ ^d eq. | Et_3N ^e eq. | $\text{Ru}(\text{II})$ ^f eq. | Time (min) | Yield ^b (%) |
|-------|---------------------|----------------------|--|---|------------|------------------------|
| 1 | 1 | 1 | 3 | 0.45% | 20 | 51% |
| 2 | 1 | 1 | 0 | 0.45% | 20 | 44% |
| 3 | 1 | 1.5 | 2 | 0.2% | 40 | 50% |
| 4 | 1 | 1.5 | 2 | 0.4% | 40 | 50% |
| 5 | 1 | 1.5 | 2 | 0.6% | 40 | 79% |
| 6 | 1 | 2 | 2 | 0.6% | 40 | 75% |
| 7 | 1 | 2 | 2 | 1.0% | 40 | 81% |

a. All reactions were performed on a 0.1 mmol scale. Yields (%) were obtained after aqueous work-up unless otherwise noted. The reactions were run at 60°C.

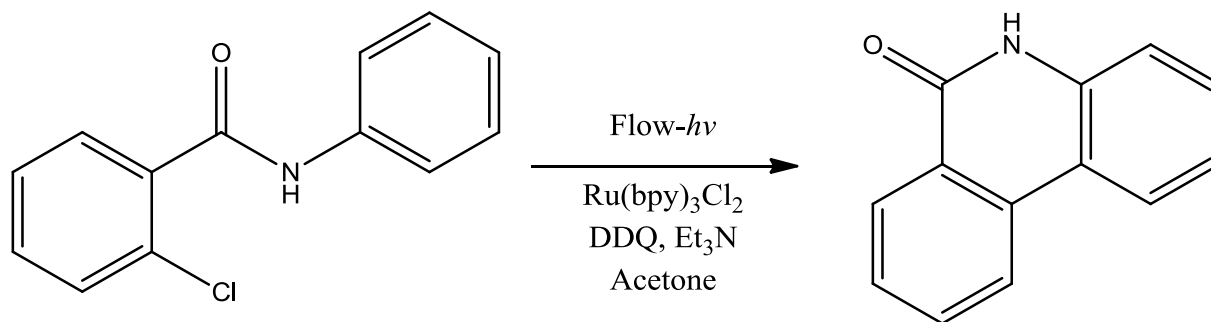
b. Isolated yield (%) after purification by Combi-flash[®] Rf with silica gel.

c. SM: Starting material; eq.:equivalent

d. DDQ: 2,3-Dichloro-5,6-dicyano-1,4-benzoquinone

e. Et_3N : Triethylamine

f. $\text{Ru}(\text{II})$: $\text{Ru}(\text{bpy})_3\text{Cl}_2$. The photocatalyst's solubility in acetone is approximately 2.5×10^{-5} mmol/mL.

Table 4. Optimization 3 ^a

| Entry | SM ^c eq. | DDQ ^d eq. | Et ₃ N ^e eq. | Ru(II) ^f eq. | O ₂ removed or not | Yield (%) ^b |
|-------|---------------------|----------------------|------------------------------------|-------------------------|-------------------------------|------------------------|
| 1 | 1 | 0 | 0 | 1.0% | No | 95 |
| 2 | 1 | 0 | 0 | 1.0% | Yes | 87 |

a. All reactions were performed on a 0.1 mmol scale. Yields (%) were obtained after aqueous work-up unless otherwise noted. The reactions were run at 60°C.

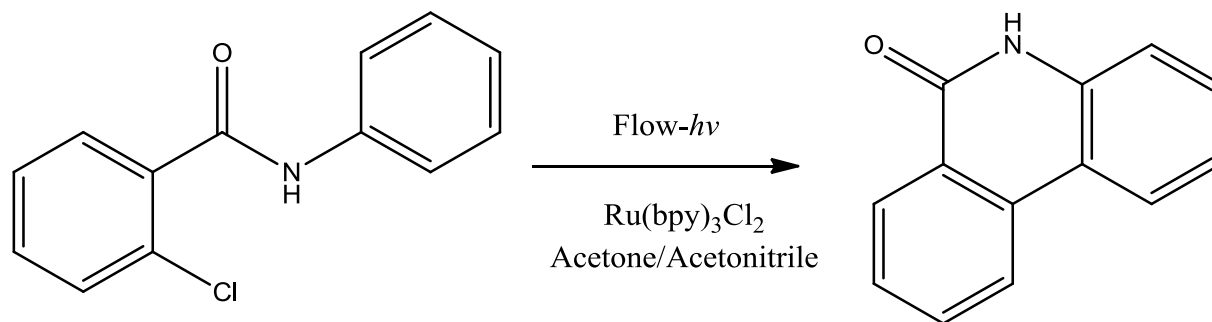
b. Isolated yield (%) after purification by Combi-flash[®] rf with silica gel.

c. SM: Starting material; eq.:equivalent

d. DDQ: 2,3-Dichloro-5,6-dicyano-1,4-benzoquinone

e. Et₃N: Triethylamine

f. Ru(II): Ru(bpy)₃Cl₂. The photocatalyst's solubility in acetone is approximately 2.5*10⁻⁵ mmol/mL

Table 5. Optimization 4 ^a

| Entry | SM C ^a | Catalyst | C eq ^b | RT ^c | Solvent | WI ^d | Yield ^e |
|-------|-------------------|--------------------------------|-------------------|-----------------|---------|--------------------|--------------------|
| 1 | 0.05 | Cl ^{-f} | 0.2% | 50 | Acetone | Whole ^g | 37% |
| 2 | 0.05 | Cl ⁻ | 0.4% | 50 | Acetone | Whole | 34% |
| 3 | 0.05 | Cl ⁻ | 0.6% | 50 | Acetone | Whole | 28% |
| 4 | 0.05 | Cl ⁻ | 1.0% | 50 | Acetone | Whole | 26% |
| 5 | 0.05 | Cl ⁻ | 5.0% | 50 | Acetone | Whole | 10% |
| 6 | 0.05 | Cl ⁻ | 1.0% | 60 | Acetone | Whole | 30% |
| 7 | 0.05 | Cl ⁻ | 2.0% | 90 | Acetone | Whole | 26% |
| 8 | 0.05 | Cl ⁻ | 1.0% | 90 | Acetone | Whole | 26% |
| 9 | 0.017 | Cl ⁻ | 1.0% | 50 | Acetone | Whole | 69% |
| 10 | 0.01 | Cl ⁻ | 1.0% | 50 | Acetone | Whole | 69% |
| 11 | 0.01 | Cl ⁻ | 2.4% | 50 | Acetone | Whole | 66% |
| 12 | 0.05 | PO ₄ ^{3-h} | 1.0% | 50 | Acetone | Whole | 31% |

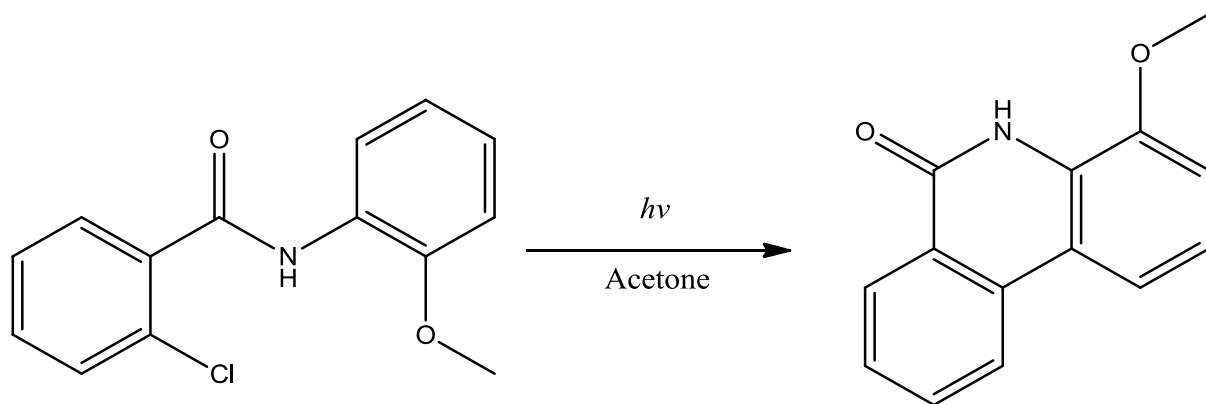
| | | | | | | | |
|----|---------|-------------------------------|------|----|-------------------|------------------------|-----|
| 13 | 0.05 | PO ₄ ³⁻ | 5.4% | 50 | Acetone | Whole | 22% |
| 14 | 0.017 | PO ₄ ³⁻ | 1.0% | 50 | Acetone | Whole | 65% |
| 15 | 0.01 | PO ₄ ³⁻ | 0.6% | 50 | Acetone | Whole | 81% |
| 16 | 0.01 | PO ₄ ³⁻ | 1.1% | 50 | Acetone | Whole | 73% |
| 17 | 0.01 | PO ₄ ³⁻ | 5.0% | 50 | Acetone | Whole | 81% |
| 18 | 0.00625 | PO ₄ ³⁻ | 1.0% | 50 | Acetone | Whole | 93% |
| 19 | 0.005 | PO ₄ ³⁻ | 1.0% | 7 | Acetone | Whole | 60% |
| 20 | 0.005 | PO ₄ ³⁻ | 1.0% | 10 | Acetone | Whole | 78% |
| 21 | 0.005 | PO ₄ ³⁻ | 1.0% | 30 | Acetone | Whole | 88% |
| 22 | 0.005 | PO ₄ ³⁻ | 1.0% | 50 | Acetone | Whole | 94% |
| 23 | 0.005 | PO ₄ ³⁻ | 1.0% | 50 | MeCN ⁱ | Whole | 88% |
| 24 | 0.005 | Cl ⁻ | 0.1% | 50 | Acetone | Whole | 99% |
| 25 | 0.005 | N/A | N/A | 50 | Acetone | Whole | 99% |
| 26 | 0.005 | N/A | N/A | 30 | Acetone | Whole | 97% |
| 27 | 0.005 | N/A | N/A | 10 | Acetone | Whole | 93% |
| 28 | 0.005 | N/A | N/A | 50 | Acetone | Filter2 ^(j) | 90% |
| 29 | 0.01 | N/A | N/A | 50 | Acetone | Whole | 90% |

a. SMC: Starting Material Concentration, mmol/mL

b. C eq²: Catalyst equivalent

- c. RT: Residence Time (Reacting Time), minutes
- d. Wl: Wavelength
- e. Determined by HPLC with external standard method
- f. Cl: Tris(bipyridine)ruthenium(II) chloride, $\text{Ru}(\text{bpy})_3\text{Cl}_2$
- g. Whole: Whole wavelength range, 200 nm ~ 600 nm
- h. PO_4^{3-} : Tris(2,2'-bipyridine)ruthenium(II) hexafluorophosphate, $\text{Ru}(\text{bpy})_3(\text{PF}_6)_2$
- i. MeCN: Acetonitrile
- j. Filter2: 300 nm ~ 400 nm

Table 6. Optimization 5



| Entry | Residence Time (Minutes) | Yield (Isolated Yield) |
|-------|--------------------------|------------------------|
| 1 | 50 | 17.3 mg, 80% |
| 2 | 30 | 8.1 mg, 36% |
| 3 | 10 | 6.6 mg, 29% |

The result of optimization 4 and optimization 5 aimed to disclose the influence of residence time, concentration, solvent, UV wavelength, as well as the influence of photoredox catalyst, (**Table 5**) (**Table 6**). We were not surprised to find that photoredox catalyst would definitely decrease the yield despite of which species it was. We also found that by increasing the irradiation time and decreasing the reagent concentration would benefit the yield significantly. We assumed that this might be related to the photon absorption. In addition, acetone seemed to be the best solvent to choose in this case. By comparing the optimization results and well-known theory, we conclude the following:

1. The concentration of starting material amide has significant influence on the yield: The lower the concentration, the better the yield. This conclusion can be explained by the Grotthuss-Draper law and the Stark-Einstein law, as efficiency of the reaction depends on the equivalent of received photons and the total quantity of chemical compound. As the solution is more diluted, the opportunity for each chemical compound to receive a photon increases so that the reaction becomes more efficient.
2. There is no need for oxidant (DDQ) or base (triethylamine) in the reaction.
3. A catalyst is not needed in this photochemical reaction. Rather than helping transfer electrons or energy, the catalyst actually slows down the reacting rate. The reason for this may also be related with Grotthuss-Draper Law as the catalyst may have better ability to absorb photons, which results in fewer photons are received by chemical compounds.
4. The longer the residence time, the better the yield. It is apparent that prolonging the residence time increases the opportunity for each chemical compound to receive a photon, which can be rationalized by Grotthuss-Draper law and the Stark-Einstein law as well. As

we change the starting material from 2-chloro-*N*-phenylbenzamide to 2-chloro-*N*-(2-methoxyphenyl)benzamide, it makes the influence of residence time even more obvious

5. Radiation lying in the ultraviolet range is the major energy source of this reaction.
6. In addition to acetone, acetonitrile can also be the solvent, which indicates that the ketone group is not involved in the reaction. However, the reaction in acetonitrile produces more side products than in acetone. Although DMSO and toluene were also used in other cases, acetone is much easier to be removed.

In the meantime, even though prolonging the residence time made the yield better, we were aware of that the reaction itself would be less efficient with a longer reacting time. Therefore, we employed 50 minutes as residence time in the following research. That is to say, the flow rate is set to be 0.2 mL/min, for a 10 mL UV-150 reactor. Here is the optimized reaction condition for single-step flow-photochemical reaction:

1. Solvent: Acetone
2. Reagent concentration: 0.005 mmol/mL
3. No catalyst
4. No oxidant
5. No base or acid
6. Flow rate: 0.2 mL/min; Residence time: 50 minutes. Depending on the actual yield, flow rate can be decreased for a longer residence time.
7. Lamp output: 75%: The lamp power is approximately 112 W. Depending on the actual yield, lamp power can be increased for better photon intensity.

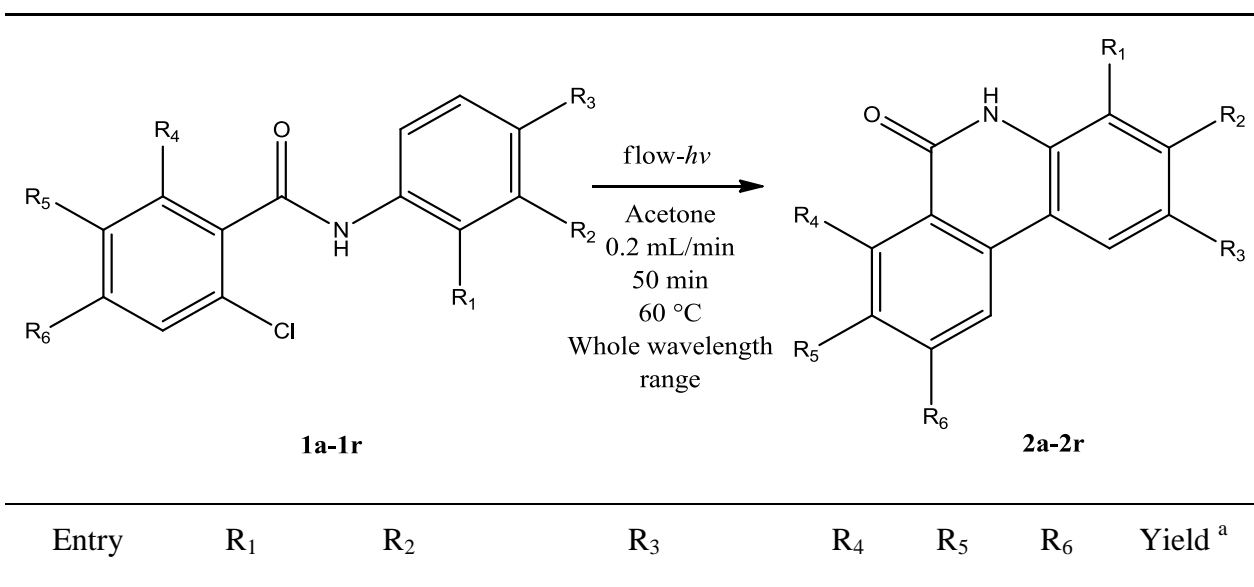
8. Temperature: 60 °C. We don't have a cooling system and 60 °C is the lowest temperature we can get when lamp power is approximately 112 W. The highest temperature the reactor/lamp can tolerate is 80 °C, which indicates that adjustable range is limited.
9. Whole wavelength range: 200 nm ~ 600 nm

B. Research Results and Conclusion

1. Synthesis of Phenanthridinones

To probe the feasibility and robustness of flow-photochemical method for the synthesis of phenanthridinones, we considered to employ amides with different substituents to perform the cyclization reaction. The result of single-step synthesis of phenanthridinones, along with a summary of the reaction scheme, is shown in **Table 7**.

Table 7. The result of single-step synthesis of phenanthridinones.



| | | | | | | | |
|-------|-----|------|-----------------|----|-----------------|----|-----|
| 1a-2a | H | H | H | H | H | H | 99% |
| 1b-2b | Cl | H | H | H | H | H | 74% |
| 1c-2c | H | H | Cl | H | H | H | 93% |
| 1d-2d | H | H | F | H | H | H | 80% |
| 1e-2e | H | H | CF ₃ | H | H | H | 86% |
| 1f-2f | OMe | H | H | H | H | H | 80% |
| 1g-2g | Me | H | H | H | H | H | 21% |
| 1h-2h | H | H | Sulfacetamide | H | H | H | 91% |
| 1i-2i | H | H | Sulfonamide | H | H | H | 30% |
| 1j-2j | H | COMe | H | H | H | H | 76% |
| 1k-2k | H | Cl | Me | H | H | H | 13% |
| 1l-2l | H | H | H | Cl | H | H | 67% |
| 1m-2m | H | H | Cl | Cl | H | H | 74% |
| 1n-2n | H | H | F | Cl | H | H | 67% |
| 1o-2o | H | H | H | H | H | Cl | 85% |
| 1p-2p | H | H | Cl | H | H | Cl | 83% |
| 1q-2q | H | H | H | H | CF ₃ | H | 26% |
| 1r-2r | H | H | F | H | H | F | 84% |

a. Isolated Yield.

As shown in the **Table 7**, we successfully produced a series of phenanthridinones via flow-photocyclization of corresponding amides. By comparing different products from different entries, we found that:

- a. Comparing **Entry 1g-2g** and a failed result that para-NH₃ on the amide nitrogen component to **Entry 1b-2b** and **Entry 1c-2c** generally, the amides with electron-donating substituents give lower yields than the ones with electron withdrawing substituents.
- b. Substituents on the para-position of the amide nitrogen component have greater influence on the reaction. This influence may result from electron effect of substituents (Comparing **Entry 1c-2c** to **Entry 1k-2k**), or the size of substituents. (Comparing **Entry 1c-2c** to **Entry 1h-1h** and **Entry 1i-2i**)
- c. Substituents on the carbonyl side aromatic ring have less effect on the reaction, compared to ones on the amide nitrogen component. However, a strong electron-withdrawing group is not preferred. (Comparing the last 7 entries to the others)
- d. It is also possible that positions, electron effect and sizes of substituents affect the reaction cooperatively, which rationalizes that **Entry 1m-2m** has a high yield and **Entry 1k-2k** has a low yield.

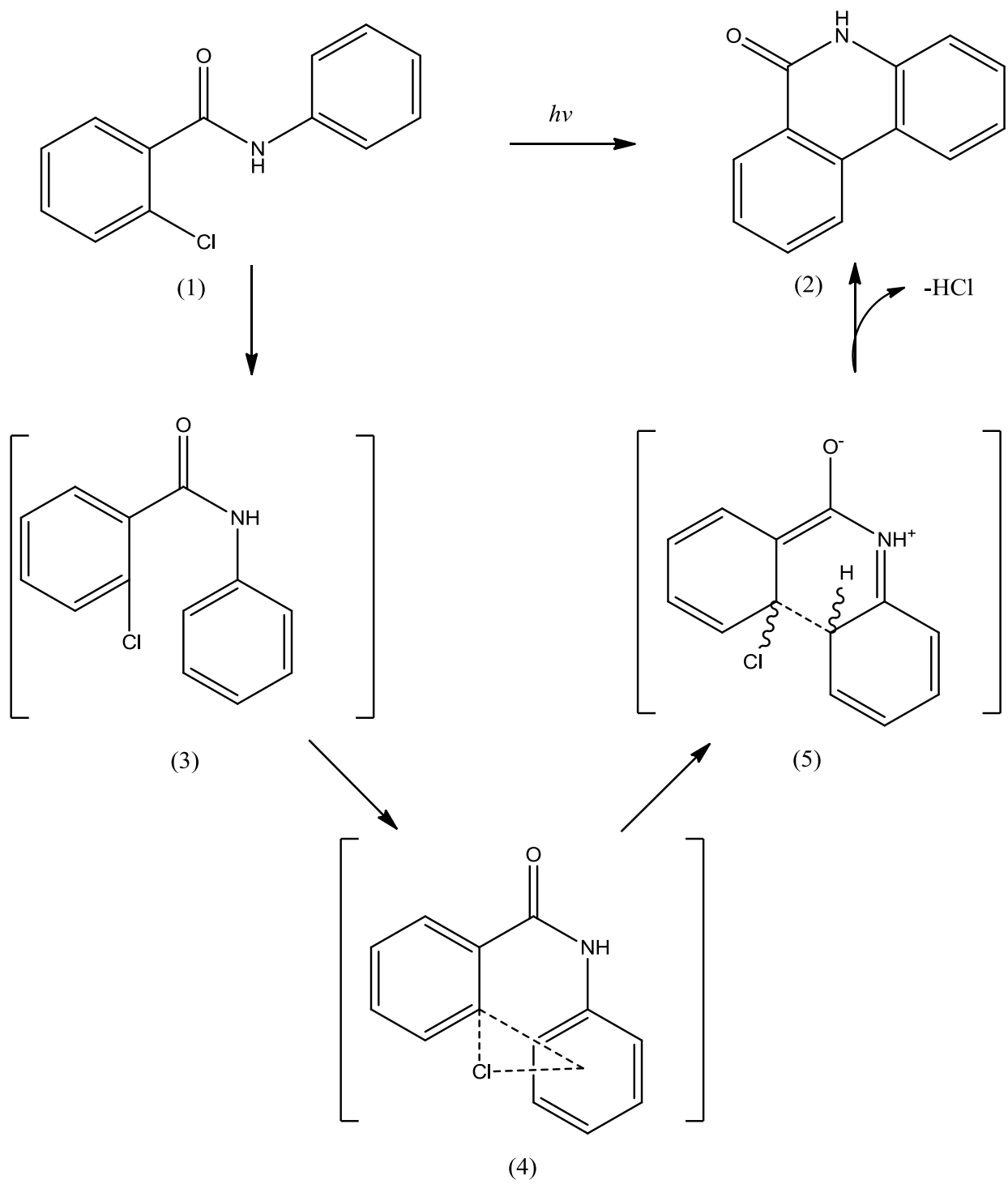
An unexpected result was the synthesis of 1-(2-(2-chlorophenyl)benzo[d]oxazol-5-yl)ethanone from the flow-photocyclization reaction of 2-chloro-2'-bromoanilides, rather than desired product.

The greatest issue remaining in the reaction was appearance of a side-reaction. We found yellowish byproducts in the crude product. The yellowish byproducts showed long retention time

on the column and they could not be eluted by the ethyl acetate/hexane solvent system. The byproducts were liquid at room temperature. Meanwhile, as we had tried using NMR to characterize the byproducts, we only found unidentified peaks, mixed with remaining solvent peaks. As it was really hard to separate the desired product from the byproducts completely, we developed a practical purification procedure. We found that, the byproducts, as well as starting material, had good solubility in methanol while the desired product, phenanthridinones, didn't dissolve well in methanol. We dried the crude product and added a very small amount of methanol into it. Removing yellowish solution after centrifugation afforded the desired product with high purity. However, even though we believed that the side reaction might be photo-decomposition or photo-Fries reaction, we didn't find a way to reduce the prevalence of side-reactions or byproducts.

A potential mechanism is shown as below (**Scheme 21**). When (1) is excited by UV light, the starting material is excited. The reaction starts from the cis- configuration (3), which may provide anchimeric assistance. The interaction of the phenyl ring through its π -cloud and stretching C–Cl bond with developing radical center of the amide nitrogen component generate transition state complex (4). Further reaction of (4) forms C–C bond in (5) which is drawn in resonance form. The cleavage of H–Cl of (5) leads to the final product (2) ^[130].

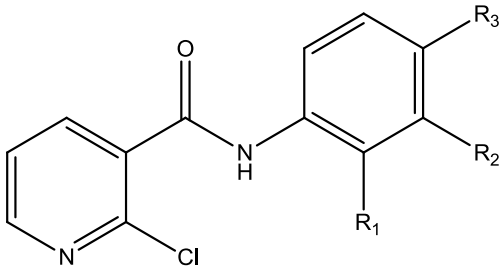
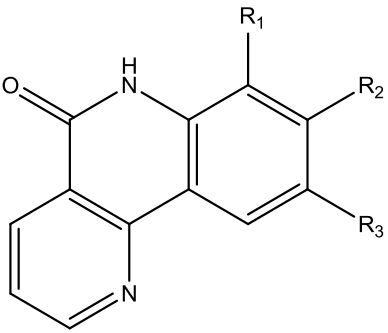
Scheme 21. A potential mechanism of the photocyclization



2. Synthesis of Naphthyridinones

To continue exploring the application of flow-photochemical method for the synthesis of phenanthridinone-type compounds, we decided to use this method to synthesize naphthridinones with different substituents. The results, along with the summary of the reaction condition are shown in **Table 8**.

Table 8. The result of single-step synthesis of naphthyridinones

|  3a-3e | $\xrightarrow{\text{flow-}h\nu}$ Acetone 0.1 mL/min 100 min 1% Ru(bpy) ₃ (PF ₆) ₂ 60 °C Whole wavelength range |  4a-4e | | |
|--|--|--|-----------------|--------------------|
| Entry | R ₁ | R ₂ | R ₃ | Yield ^a |
| 3a-4a | Cl | H | H | 47% |
| 3b-4b | H | H | Cl | 24% |
| 3c-4c | H | H | F | 26% |
| 3d-4d | H | H | CF ₃ | 50% |
| 3e-4e | H | H | Sulfacetamide | 52% |

a. Isolated Yield.

This part of research employed the previous reaction condition to produce **4a** and **4b**. The results were not as good as previous phenanthridinone examples as conversion rates were rather low. We prolonged the reaction time by decreasing the flow rate to 0.1 mL/min. We found the conversion rate increased, but still not satisfying. We added ruthenium catalyst to the reaction and we found the conversion rate increased to 83% (determined by LC). We assumed that metal complex catalyst might benefit the reaction, but we were not sure if it acted as a photocatalyst or not. To probe the mechanism, we used two kinds of ruthenium catalyst ($\text{Ru}(\text{bpy})_3\text{Cl}_2$ and $\text{Ru}(\text{bpy})_3(\text{PF}_6)_2$), copper(II) acetate and Iron(III) acetylacetonate respectively. The two ruthenium catalyst gave similar conversion rates while Fe(II) catalyst gave 77% conversion rate and copper complex gave 64% conversion rate. In addition, 1 % equivalent of the Ru catalyst gave the best conversion rate, compared to 5%, 10% 0.1% 0.5% equivalent of the Ru catalyst. Meanwhile, if base or acid was added to the system, the reaction didn't work. Those findings suggested metal complex might act as a Lewis acid, which might chelate to the pyridine component, or the amide nitrogen (considering metal catalyst didn't work when we tried to synthesize phenanthridinones, it was less likely that metal complex would chelate to the amide nitrogen).

We had only produced 5 compounds and we found yields of the naphthyridinones are quite low and the one without any substituents failed. According to the results, it was revealed that a para-position substituent influenced the reaction the most.

Generally, this reaction was problematic. As we had achieved near a quantitative conversion rate (**Entry 3d-4d** and **Entry 3e-4e**, determined by isolated unreacted starting materials), it was quiet disappointing that the highest yield was 52%. We suggested that the major problem was side-reactions. The naphthyridinones had slightly better solubility in methanol than the phenanthridinones. It was highly possible that we washed away a slightly higher portion of the

desired product while purifying. The only where the purification procedure was avoided was **Entry 3e-4e**. The bulky, high-polarity substituent made the final product have the highest polarity among all the products. When we used column to separate the desired product from the byproduct, we used 3% methanol/DCM solvent system. The byproduct was eluted quickly from the column because of the solvent we used and in which way we obtained a comparable purer product.

As a conclusion, the method we developed can be used to produce naphthyridinones. However the low yields didn't make it the best pathway. Compared to traditional coupling reaction we mentioned above, the tolerance of bulky substituent makes it a cheaper and convenient way to develop novel naphthyridinones. In addition, a more polar, bulky substituent made it easy to separate, which indicate that the photocyclization can be used as the last step when synthesizing other large compounds.

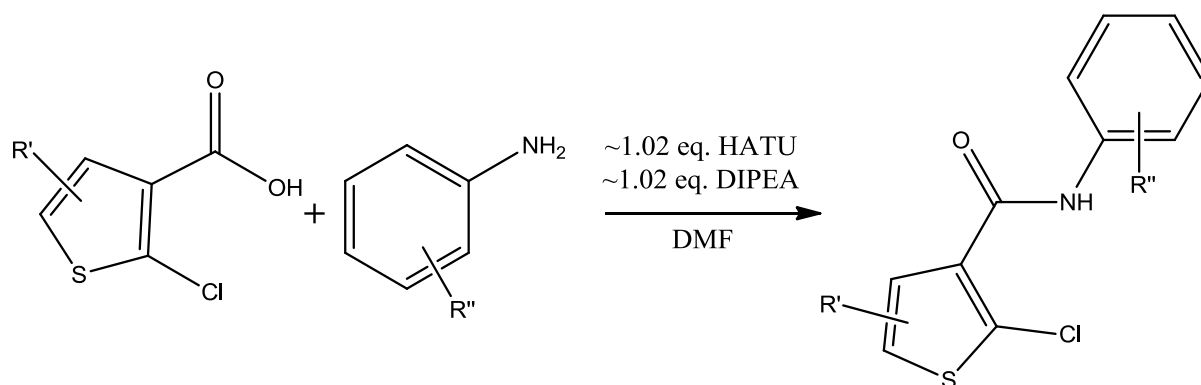
3. Synthesis of Thieno-quinolinones

Herein, we present the result of synthesizing thieno[3,2-*c*]quinolin-4(5H)-one and its analogues directly from *N*-phenylthiophene-3-carboxamides through a single-step photocyclization within the 10 mL continuous flow reactor equipped with a medium-pressure mercury lamp.

We applied 2-chloro-*N*-phenylthiophene-3-carboxamides as the starting materials, as we assumed this type of photocyclization reaction shared the same feature, i.e. a 2-chlorine substituent was essential. An amide coupling reaction was used to make 2-chloro-*N*-phenylthiophene-3-carboxamides started from the corresponding 2-chlorothiophene-3-carboxylic

acids and anilines, with the presence of approximately 1 eq. of HATU and DIPEA, in DMF (**Scheme 22**). Another pathway to make the starting material used carboxylic acids, involving the synthesis of acyl chlorides, from corresponding amides, utilizing oxalyl chloride. The former one was more effective in this case.

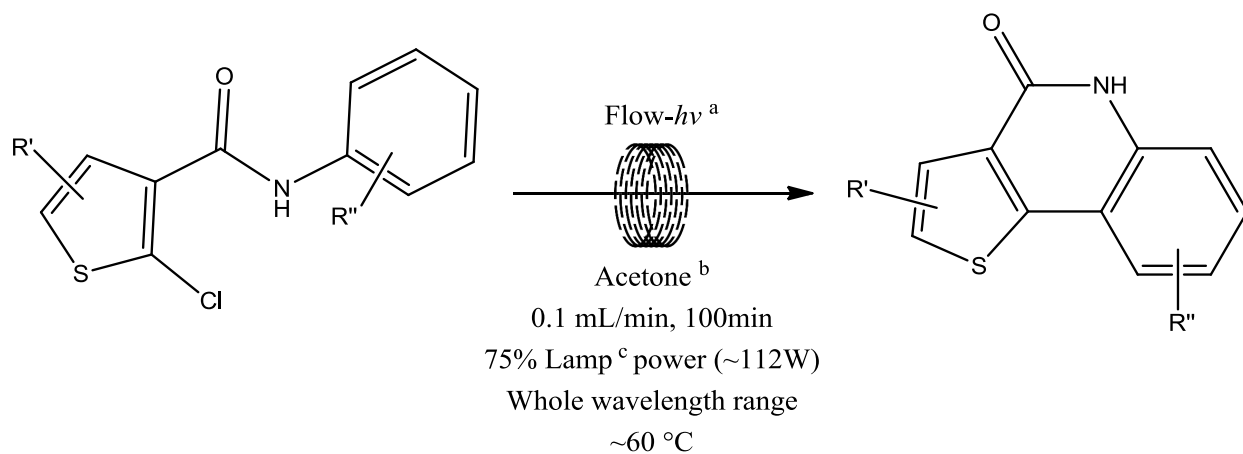
Scheme 22. Synthesis of 2-chloro-*N*-phenylthiophene-3-carboxamides



To perform the photochemical cyclization in flow, we employed the flow reactor mentioned above. However, we found 2-chloro-*N*-phenylthiophene-3-carboxamide was only converted partially during a preliminary test reaction in 50 min, employing the reaction condition mentioned above, which revealed that this thiophene motif might be less photo-reactive. One adjustment of the established reaction condition was done for this reason. We prolonged the residence time from 50 min to 100 min, which indicated that the flow rate was 0.1 mL/min as well. The proposed reaction, along with the reaction condition, is displayed below (**Scheme 23**). Same reaction condition was applied for the synthesis of thieno[2,3-*c*]quinolin-4(5H)-ones. Using this adjusted reaction conditions, we were able to synthesize a series of thieno[3,2-

c]quinolin-4(5H)-ones, as well as two examples of thieno[2,3-*c*]quinolin-4(5H)-ones, for comparison. (Table 9 & Table 10)

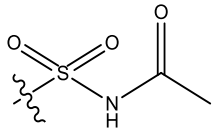
Scheme 23: Synthesis of thieno[3,2-*c*]quinolin-4(5H)-ones

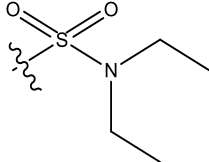
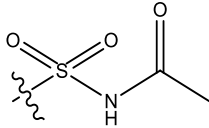
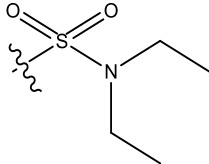


a. 10 mL fluorinated ethylene propylene (FEP) coil. b. The concentration of the reagent is 0.005 mmol/mL. c. Vapourtec UV-150 medium pressure Hg lamp

Table 9. Results of the synthesis of thieno[3,2-*c*]quinolin-4(5H)-ones

5a-5p $\xrightarrow[\text{Acetone}]{h\nu}$ **6a-6p**

| Entry | R ₁ | R ₂ | R ₃ | R ₄ | Yield ^a |
|-------|----------------|----------------|--|----------------|--------------------|
| 5a-6a | H | H | H | H | 64% |
| 5b-6b | Cl | H | H | H | 54% |
| 5c-6c | H | H | Cl | H | 72% |
| 5d-6d | H | H | F | H | 65% |
| 5e-6e | H | H | CF ₃ | H | 77% |
| 5f-6f | OMe | H | H | H | 50% |
| 5g-6g | H | H | OMe | H | 23% |
| 5h-6h | Me | H | H | H | 39% |
| 5i-6i | H | H |  | H | 41% |

| | | | | | |
|-------|----|------|---|----|------------------|
| 5j-6j | H | H |  | H | 29% |
| 5k-6k | H | COMe | H | H | 50% ^b |
| 5l-6l | H | H | H | Cl | 41% |
| 5m-6m | Cl | H | H | Cl | 30% |
| 5n-6n | H | H | Cl | Cl | 45% |
| 5o-6o | H | H |  | Cl | 43% |
| 5p-6p | H | H |  | Cl | 43% |

a. Isolated Yield; b. A mixture of two products

According to the results, generally, the synthesis of thieno[3,2-*c*]quinolin-4(5H)-ones was practical using the developed flow-photocyclization method; The yields of photocyclization were satisfying, up to 77%; Substitution was permitted on the both ring components based on our results. Meta-substituted starting material produced two kinds of products as a mixture. Comparing each entry, it was revealed that para-substituent products had better yields over ortho-substituent ones, except the para-methoxy product; Electron-withdrawing-substituent (such as halogen) products had better yields over electron-donating-substituent (such as methyl) ones;

Bulky-substituent (such as sulfonamide) products had lower yield than small ones; 2-chlorothiено[3,2-*c*]quinolin-4(5H)-ones has lower yields than thieno[3,2-*c*]quinolin-4(5H)-ones, which did not have chloro-substituents on the thiophene component.

The results illustrated that electron-withdrawing substituents on the amide nitrogen component were preferable, especially the ones on the para-position. However, the chloro-substituent on the thiophene component might lead to a decrease on reaction rate. As shown in **Entry 5m-6m**, the yield of the product is 30%. However, approximately 30% of unreacted starting material was isolated from the crude product (**Entry 5m-6m**), which manifested a low conversion rate. It was possible that the substituent decreased the photo-activity of the starting material, or introducing steric hindrance to the reaction. Since 2-chlorothiено version was our only example with (a) substituent(s) on the thiophene ring, it was hard to tell if the electron withdrawing property of halogen has anything to do with the rate. Further exploration is necessary.

We had also synthesized two examples of thieno[2,3-*c*]quinolin-4(5H)-ones in flow, i.e. 8-chlorothiено[2,3-*c*]quinolin-4(5H)-one and thieno[2,3-*c*]quinolin-4(5H)-one. We had approximately 90% yields of these two product. Comparing our results of thieno[2,3-*c*]quinolin-4(5H)-ones to previous results mentioned above, it was apparent that the flow-photocyclization method is much more effective, and the yields were comparably higher. To achieve high yields, the reactions carried out within the flow reactor equipped with the mercury lamp only takes 100 min while others always take several hours.

Table 10. Results of the synthesis of thieno[2,3-*c*]quinolin-4(5H)-ones

| Entry | R ₁ | R ₂ | R ₃ | R ₄ | Yield ^a |
|-------|----------------|----------------|----------------|----------------|--------------------|
| 7a-8a | H | H | H | H | 85% |
| 7b-8b | H | H | Cl | H | 90% |

a. Isolated Yield

Using the flow reactor equipped with the UV lamp would benefit the photocyclization reaction of thieno-quinolinones synthesis and we were able to produce a sequence of different derivatives via a similar protocol in a much shorter period of time than conventional batch reactions. This pathway was proved to be robust enough to produce two types of thieno-quinolinones, and one of them demonstrated the superiority of flow-photo pathway. Even though the yields were not extraordinarily good, we could still have 50%+ yields when producing halogenated products. These halogenated products could be used as a basis to develop other thieno-quinolinone-containing compounds through derivatization using alternate existing literature methods, such as substitution reactions or coupling reactions. The remaining problems, aside from low conversion

rate because of the substituents, existed in possible side-reactions which had been mentioned before in the synthesis of phenanthridinones and naphthyridinones.

C. Overall Conclusion and Discussion

Using flow chemistry system equipped with the UV reactor, we have successfully developed a synthesis pathway to produce phenanthridinone-type compounds. It is revealed that this method can produce four different kinds of cyclic compounds, including phenanthridinones, naphthyridinones and two kinds of thieno-quinolinones. The method gives comparably high yields in most cases.

Comparing our method to conventional coupling reactions, it is cheaper and more efficient. The photocyclization reaction only requires a chloro-substituted amide as the starting material rather than expensive Pd catalyst and boronic acid, or any other coupling reagents. With UV illumination the reaction can be carried out at 60 °C, under a mild reaction condition, which is much safer, compared to high pressure, high temperature reaction conditions. The photocyclization takes 100 minutes to accomplish with mostly decent yields, which is more efficient than those coupling reactions we have reviewed above.

We have also tried to scale up two reactions starting from **1b** and **1d** to produce corresponding phenanthridinones. The results are satisfying as both entries give more than 50% yields. It is noted that for mass production, the concentration of the starting material is critical as the solubility of the product is poor. To prevent the product from precipitating in the tubing which blocks the system, a low concentration (<0.01 mmol/mL) is necessary. Furthermore, we

notice that a column separation is not necessary. Washing the crude product with methanol under vacuum filtration gives a high-purity product, which has been determined by HPLC. These attempts demonstrate the possibility of direct transition from lab to industry using flow chemistry, of which traditional batch reaction is not capable.

However, the problem remains as yields are “irregular” and it’s hard to conclude a certain pattern. As well as the method cannot be applied when there are $-NH_2$ substituents, most cases demonstrate that an electron-donating substituent may induce low yields. However, a few examples strongly oppose this conclusion, such as **Entry 1f-2f**, **Entry 5f-6f**. Para- and ortho-substituted compounds give different yields, despite of electron effect of the substituent. (Comparing **Entry 1b-2b** to **Entry 1c-2c**, **Entry 5b-6b** to **Entry 5c-6c**, **Entry 5f-6f**).

Before we understand the real mechanism of the reaction, we assume that the influence of yields results from the electron effects (considering the substituent as a whole), the size (or spatial hindrance), the substituted position.

The other problem with this method is the generation of a byproduct that is difficult to purify by conventional column chromatography. It is obvious that four types of compounds carry out a similar type(s) of side-reaction(s), giving the same yellowish byproduct(s). We have tried to isolate the byproduct and analyze it to determine its structure, and potential source. The NMR results show similar but unidentified peaks appearing at upfield chemical shift. The byproducts do affect the research method as they cannot be separated completely from desired products with column chromatography. During this research we found that the byproduct(s) have good solubility in solvents with high polarity such as methanol while the desired cyclic products do

not, so that we managed to wash the crude product with methanol after column-separation to give a high purity product.

We have developed a method to produce different types of tricyclic phenanthridinone-like compounds. The method uses a flow chemistry reactor with a UV lamp. The results reveal that this method is more efficient and economic, in contrast to traditional coupling/cyclization route. In addition, this method is able to produce some compounds which cannot be synthesized in conventional ways, as we have developed some novel compounds. Even though the method has some shortcomings, it has shown its robustness handling photocyclization reactions.

In the future, this method will be used to produce more phenanthridinone-like compounds. Encouraged by the positive result that this method is able to produce different phenanthridinone-like tricyclic compounds, we will look into diverse combination of aromatic rings to make various motifs in the next stage of development via this newly established synthetic pathway. Further biological evaluation will be applied on these novel phenanthridinone-like compounds, including thieno[3,2-*c*]quinolin-4(5H)-one, to investigate their actions on tumor cells, such as RDM4 murine lymphoma cells ^[96]. In addition, we plan to evaluate potential synergistic effect with antitumor drugs, such as topoisomerase poisons camptothecin on tumor cells, such as L1210 cells ^{[88] [131]}, as well as synergistic effect with ionizing radiation on cultured tumor cells ^[95]. Ideally, we would obtain structure–activity relationship through biological evaluation, which will be of crucial importance for further study.

V. References

1. Kirschning, A. (2011). Chemistry in flow systems II. *Beilstein journal of organic chemistry*, 7(1), 1046-1047.
2. Pastre, J. C., Browne, D. L., & Ley, S. V. (2013). Flow chemistry syntheses of natural products. *Chemical Society Reviews*, 42(23), 8849-8869.
3. e.g. Hopkin, M. D., Baxendale, I. R., & Ley, S. V. (2013). An expeditious synthesis of imatinib and analogues utilising flow chemistry methods. *Organic & biomolecular chemistry*, 11(11), 1822-1839.
4. Mason, B. P., Price, K. E., Steinbacher, J. L., Bogdan, A. R., & McQuade, D. T. (2007). Greener approaches to organic synthesis using microreactor technology. *Chemical reviews*, 107(6), 2300-2318.
5. e.g. (a) Polyzos, A., O'Brien, M., Petersen, T. P., Baxendale, I. R., & Ley, S. V. (2011). The continuous-flow synthesis of carboxylic acids using CO₂ in a tube-in-tube gas permeable membrane reactor. *Angewandte Chemie International Edition*, 50(5), 1190-1193. (b) Kasinathan, S., Bourne, S. L., Tolstoy, P., Koos, P., O'brien, M., Bates, R. W., & Ley, S. V. (2011). Syngas-Mediated C—C Bond Formation in Flow: Selective Rhodium-catalysed Hydroformylation of Styrenes. *Synlett*, (18), 2648-2651.
6. Qian, Z., Baxendale, I. R., Ley, S. V., (2010). A flow process using microreactors for the preparation of a quinolone derivative as a potent 5HT(1B) antagonist. *Synlett*. (4), 505–508
7. Wegner, J., Ceylan, S., & Kirschning, A. (2011). Ten key issues in modern flow chemistry. *Chemical Communications*, 47(16), 4583-4592.

8. Jas, G., & Kirschning, A. (2003). Continuous flow techniques in organic synthesis. *Chemistry—A European Journal*, 9(23), 5708-5723.
9. Book, G. (2014). Compendium of Chemical Terminology, 293.
10. Gold, V., Loening, K. L., McNaught, A. D., & Shemi, P. (1997). IUPAC Compendium of Chemical Terminology. *Blackwell Science, Oxford*.
11. e.g. (a)Carter, C. F., Baxendale, I. R., O'Brien, M., Pavey, J. B., & Ley, S. V. (2009). Synthesis of acetal protected building blocks using flow chemistry with flow IR analysis: preparation of butane-2, 3-diacetal tartrates. *Organic & biomolecular chemistry*, 7(22), 4594-4597. (b) Lange, H., Carter, C. F., Hopkin, M. D., Burke, A., Goode, J. G., Baxendale, I. R., & Ley, S. V. (2011). A breakthrough method for the accurate addition of reagents in multi-step segmented flow processing. *Chemical Science*, 2(4), 765-769
12. Baxendale, I. R., Griffiths-Jones, C. M., Ley, S. V., & Tranmer, G. K. (2006). Preparation of the neolignan natural product grossamide by a continuous-flow process. *Synlett*, (3), 427-430.
13. Baumann, M., Baxendale, I. R., Ley, S. V., Smith, C. D., & Tranmer, G. K. (2006). Fully automated continuous flow synthesis of 4, 5-disubstituted oxazoles. *Organic letters*, 8(23), 5231-5234.
14. Tokmakoff, A., Fayer, M. D., & Dlott, D. D. (1993). Chemical reaction initiation and hot-spot formation in shocked energetic molecular materials. *The Journal of Physical Chemistry*, 97(9), 1901-1913.
15. He, P., Haswell, S. J., & Fletcher, P. D. (2004). Microwave-assisted Suzuki reactions in a continuous flow capillary reactor. *Applied Catalysis A: General*, 274(1), 111-114.

16. Eynde, J. J. V., Mayence, A., Johnson, M. T., Huang, T. L., Collins, M. S., Rebholz, S., ... & Donkor, I. O. (2005). Antitumor and anti-Pneumocystis carinii activities of novel bisbenzamidines. *Medicinal Chemistry Research*, *14*(3), 143-157.
17. e.g. (a) Alza, E., Rodríguez-Esrich, C., Sayalero, S., Bastero, A., & Pericàs, M. A. (2009). A Solid-Supported Organocatalyst for Highly Stereoselective, Batch, and Continuous-Flow Mannich Reactions. *Chemistry—A European Journal*, *15*(39), 10167-10172. (b) Puglisi, A., Benaglia, M., & Chirolì, V. (2013). Stereoselective organic reactions promoted by immobilized chiral catalysts in continuous flow systems. *Green Chemistry*, *15*(7), 1790-1813.
18. Poehlauer, P., Manley, J., Broxterman, R., Gregertsen, B., & Ridemark, M. (2012). Continuous processing in the manufacture of active pharmaceutical ingredients and finished dosage forms: an industry perspective. *Organic Process Research & Development*, *16*(10), 1586-1590.
19. e.g. McQuade, D. T., & Seeberger, P. H. (2013). Applying flow chemistry: Methods, materials, and multistep synthesis. *The Journal of organic chemistry*, *78*(13), 6384-6389.
20. Lévesque, F., & Seeberger, P. H. (2012). Continuous-Flow Synthesis of the Anti-Malaria Drug Artemisinin. *Angewandte Chemie International Edition*, *51*(7), 1706-1709.
21. Book, G. (2014). Compendium of Chemical Terminology, 1218.
22. Jaboski, A. (1933). Efficiency of anti-Stokes fluorescence in dyes. *Nature*, *131*(839-840), 21.
23. Book, G. (2014). Compendium of Chemical Terminology, 800.
24. Royer, C. A. (1995). Approaches to teaching fluorescence spectroscopy. *Biophysical journal*, *68*(3), 1191.

25. Xu, H., Chen, R., Sun, Q., Lai, W., Su, Q., Huang, W., & Liu, X. (2014). Recent progress in metal–organic complexes for optoelectronic applications. *Chemical Society Reviews*, 43(10), 3259-3302.
26. Pitts Jr, J. N., & Blacet, F. E. (1950). Methyl ethyl ketone photochemical processes. *Journal of the American Chemical Society*, 72(6), 2810-2811.
27. Barton, D. H. R., Beaton, J. M., Geller, L. E., & Pechet, M. M. (1960). A new photochemical reaction. *Journal of the American Chemical Society*, 82(10), 2640-2641.
28. Syamala, M. S., & Ramamurthy, V. (1988). Modification of photochemical reactivity by cyclodextrin complexation: selectivity in photo-claisen rearrangement. *Tetrahedron*, 44(23), 7223-7233.
29. Kalmus, C. E., & Hercules, D. M. (1974). Mechanistic study of the photo-Fries rearrangement of phenyl acetate. *Journal of the American Chemical Society*, 96(2), 449-456.
30. Morrison, H., Bernasconi, C., & Pandey, G. (1984). A wavelength effect on urocanic acid E/Z photoisomerization. *Photochemistry and photobiology*, 40(4), 549-550.
31. Book, G. (2014). Compendium of Chemical Terminology, 1010
32. Griesbeck, A. G., & Heckroth, H. (2002). Stereoselective synthesis of 2-aminocyclobutanols via photocyclization of α -amido alkylaryl ketones: Mechanistic implications for the Norrish/Yang reaction. *Journal of the American Chemical Society*, 124(3), 396-403.
33. Li, J. J. (2003). Paterno-Büchi reaction. In *Name Reactions* (pp. 299-299). Springer Berlin Heidelberg.
34. Li, J. J. (2009). de Mayo reaction. *Name Reactions*, 173-174.

35. Evenzahav, A., & Turro, N. J. (1998). Photochemical rearrangement of enediynes: is a “photo-Bergman” cyclization a possibility?. *Journal of the American Chemical Society*, *120*(8), 1835-1841.
36. Bigot, B., Sevin, A., & Devaquet, A. (1978). Photochemical extrusion of nitrogen in azo compounds. An ab initio SCF-cI study. *Journal of the American Chemical Society*, *100*(9), 2639-2642.
37. Mondal, R., Okhrimenko, A. N., Shah, B. K., & Neckers, D. C. (2008). Photodecarbonylation of α -diketones: a mechanistic study of reactions leading to acenes. *The Journal of Physical Chemistry B*, *112*(1), 11-15.
38. Budac, D., & Wan, P. (1992). Photodecarboxylation: mechanism and synthetic utility. *Journal of Photochemistry and Photobiology A: Chemistry*, *67*(2), 135-166.
39. Rohatgi-Mukherjee, K. K. (1978). *Fundamentals of photochemistry*. New Age International.
40. e.g. Xu, J., Atme, A., Martins, A. F. M., Jung, K., & Boyer, C. (2014). Photoredox catalyst-mediated atom transfer radical addition for polymer functionalization under visible light. *Polymer Chemistry*, *5*(10), 3321-3325.
41. e.g. Xu, J., Jung, K., & Boyer, C. (2014). Oxygen tolerance study of photoinduced electron transfer–reversible addition–fragmentation chain transfer (PET-RAFT) polymerization mediated by Ru (bpy)₃Cl₂. *Macromolecules*, *47*(13), 4217-4229.
42. Knowles, J. P., Elliott, L. D., & Booker-Milburn, K. I. (2012). Flow photochemistry: Old light through new windows. *Beilstein journal of organic chemistry*, *8*(1), 2025-2052.
43. Horváth, O. (1994). Photochemistry of copper (I) complexes. *Coordination Chemistry Reviews*, *135*, 303-324.

44. Prier, C. K., Rankic, D. A., & MacMillan, D. W. (2013). Visible light photoredox catalysis with transition metal complexes: applications in organic synthesis. *Chemical reviews*, 113(7), 5322-5363.
45. Hari, D. P., & König, B. (2011). Eosin Y catalyzed visible light oxidative C–C and C–P bond formation. *Organic letters*, 13(15), 3852-3855.
46. Akaba, R., Sakuragi, H., & Tokumaru, K. (1991). Triphenylpyrylium-salt-sensitized electron transfer oxygenation of adamantylideneadamantane. Product, fluorescence quenching, and laser flash photolysis studies. *J. Chem. Soc., Perkin Trans. 2*, (3), 291-297.
47. Caspar, J. V., & Meyer, T. J. (1983). Photochemistry of MLCT excited states. Effect of nonchromophoric ligand variations on photophysical properties in the series cis-Ru (bpy)₂L₂₂₊. *Inorganic Chemistry*, 22(17), 2444-2453.
48. Indelli, M. T., Bignozzi, C. A., Scandola, F., & Collin, J. P. (1998). Design of long-lived Ru (II) terpyridine MLCT states. Tricyano terpyridine complexes. *Inorganic chemistry*, 37(23), 6084-6089.
49. Fischer, H. E., & Horster, H. (1992). *U.S. Patent No. 5,109,181*. Washington, DC: U.S. Patent and Trademark Office.
50. Bouguer, P. (1729). *Essai d'optique sur la gradation de la lumière*. Jombert.
51. Lambert, J. H. (1892). *Photometrie: Photometria, sive De mensura et gradibus luminis, colorum et umbrae (1760)* (Vol. 31). W. Engelmann.
52. Beer, A. (1852). Determination of the absorption of red light in colored liquids. *Ann. Phys. Chem*, 86, 78-88.
53. Crouch, J. D. J. (1988). Ingle and SR “Spectrochemical Analysis.”

54. Hook, B. D., Dohle, W., Hirst, P. R., Pickworth, M., Berry, M. B., & Booker-Milburn, K. I. (2005). A practical flow reactor for continuous organic photochemistry. *The Journal of organic chemistry*, 70(19), 7558-7564.
55. Lipinski, C. A. (2004). Lead-and drug-like compounds: the rule-of-five revolution. *Drug Discovery Today: Technologies*, 1(4), 337-341.
56. Ritchie, T. J., & Macdonald, S. J. (2009). The impact of aromatic ring count on compound developability—are too many aromatic rings a liability in drug design?. *Drug discovery today*, 14(21), 1011-1020.
57. Ward, Simon E., and Paul Beswick. "What does the aromatic ring number mean for drug design?." *Expert opinion on drug discovery* 9.9 (2014): 995-1003.
58. Wender, P. A., Takahashi, H., & Witulski, B. (1995). Transition metal catalyzed [5+ 2] cycloadditions of vinylcyclopropanes and alkynes: A homolog of the Diels-Alder reaction for the synthesis of seven-membered rings. *Journal of the American Chemical Society*, 117(16), 4720-4721.
59. Miyaura, N., & Suzuki, A. (1995). Palladium-catalyzed cross-coupling reactions of organoboron compounds. *Chemical reviews*, 95(7), 2457-2483.
60. HATU: 1-[Bis(dimethylamino)methylene]-1H-1,2,3-triazolo[4,5-b]pyridinium 3-oxid hexafluorophosphate) and Hydroxybenzotriazole
61. Lopez-Macia, A., Jiménez, J. C., Royo, M., Giralt, E., & Albericio, F. (2000). Kahalalide B. Synthesis of a natural cyclodepsipeptide. *Tetrahedron Letters*, 41(50), 9765-9769.
62. Mallory, F. B., Wood, C. S., Gordon, J. T., Lindquist, L. C., & Savitz, M. L. (1962). Photochemistry of Stilbenes. I. *Journal of the American Chemical Society*, 84(22), 4361-4362.

63. Mallory, F. B., & Mallory, C. W. (1984). Photocyclization of stilbenes and related molecules. *Organic reactions*.
64. Giles, R. G., & Sargent, M. V. (1974). Photochemical synthesis of phenanthrenes from 2-methoxystilbenes. *Journal of the Chemical Society, Perkin Transactions 1*, 2447-2450.
- Sargent, M. V., & Timmons, C. J. (1964). 1063. Studies in photochemistry. Part I. The stilbenes. *Journal of the Chemical Society (Resumed)*, 5544-5552.
65. Lapouyade, R., Koussini, R., & Rayez, J. C. (1975). Photocyclisation of 1, 1-diarylethylenes; the novel formation of a five-membered ring. *Journal of the Chemical Society, Chemical Communications*, (16), 676-677.
66. Hernandez-Perez, A. C., & Collins, S. K. (2013). A visible-light-mediated synthesis of carbazoles. *Angewandte Chemie*, 125(48), 12928-12932
67. Caron, A., Hernandez-Perez, A. C., & Collins, S. K. (2014). Synthesis of a Carprofen Analogue Using a Continuous Flow UV-Reactor. *Organic Process Research & Development*, 18(11), 1571-1574.
68. Bennett, C., Hankenson, K., Harrison, S., Longo, K., MacDougald, O., & Wagman, A. (2004). *U.S. Patent Application No. 10/917,707*.
69. McQuade, D. T., O'Brien, A. G., Dörr, M., Rajaratnam, R., Eisold, U., Monnanda, B., Nobuta, T., Lohmannsroben, H., Meggers, H., & Seeberger, P. H. (2013). Continuous synthesis of pyridocarbazoles and initial photophysical and bioprobe characterization. *Chemical Science*, 4(10), 4067-4070.
70. Hernandez-Perez, A. C., Vlassova, A., & Collins, S. K. (2012). Toward a visible light mediated photocyclization: Cu-based sensitizers for the synthesis of [5] helicene. *Organic letters*, 14(12), 2988-2991.

71. Maskill, K. G., Knowles, J. P., Elliott, L. D., Alder, R. W., & Booker-Milburn, K. I. (2013). Complexity from simplicity: tricyclic aziridines from the rearrangement of pyrroles by batch and flow photochemistry. *Angewandte Chemie International Edition*, 52(5), 1499-1502.
72. Joule, J. A., & Mills, K. (2008). *Heterocyclic chemistry*. John Wiley & Sons.
73. Sperry, J. B., & Wright, D. L. (2005). Furans, thiophenes and related heterocycles in drug discovery. *Current opinion in drug discovery & development*, 8(6), 723-740.
74. Ylijoki, Kai EO, and Jeffrey M. Stryker. "[5 + 2] cycloaddition reactions in organic and natural product synthesis." *Chemical reviews* 113.3 (2012): 2244-2266.
75. Lainchbury, M. D., Medley, M. I., Taylor, P. M., Hirst, P., Dohle, W., & Booker-Milburn, K. I. (2008). A protecting group free synthesis of (±)-neostenine via the [5+ 2] photocycloaddition of maleimides. *The Journal of organic chemistry*, 73(17), 6497-6505.
76. Kumarasamy, E., Raghunathan, R., Jockusch, S., Ugrinov, A., & Sivaguru, J. (2014). Tailoring Atropisomeric Maleimides for Stereospecific [2+ 2] Photocycloaddition Photochemical and Photophysical Investigations Leading to Visible-Light Photocatalysis. *Journal of the American Chemical Society*, 136(24), 8729-8737.
77. Liao, H. H., Hsiao, C. C., Sugiono, E., & Rueping, M. (2013). Shedding light on Brønsted acid catalysis—a photocyclization–reduction reaction for the asymmetric synthesis of tetrahydroquinolines from aminochalcones in batch and flow. *Chemical Communications*, 49(72), 7953-7955.
78. Beatty, J. W., & Stephenson, C. R. (2014). Synthesis of (–)-pseudotabersonine, (–)-pseudovincadifformine, and (+)-coronaridine enabled by photoredox catalysis in flow. *Journal of the American Chemical Society*, 136(29), 10270-10273.

79. Martin, V. I., Goodell, J. R., Ingham, O. J., Porco Jr, J. A., & Beeler, A. B. (2014). Multidimensional reaction screening for photochemical transformations as a tool for discovering new chemotypes. *The Journal of organic chemistry*, 79(9), 3838-3846.
80. Grube, K., & Bürkle, A. (1992). Poly (ADP-ribose) polymerase activity in mononuclear leukocytes of 13 mammalian species correlates with species-specific life span. *Proceedings of the National Academy of Sciences*, 89(24), 11759-11763.
81. Amé, J. C., Spenlehauer, C., & de Murcia, G. (2004). The PARP superfamily. *Bioessays*, 26(8), 882-893.
82. Virág, L., & Szabó, C. (2002). The therapeutic potential of poly (ADP-ribose) polymerase inhibitors. *Pharmacological reviews*, 54(3), 375-429.
83. Caiafa, P., Guastafierro, T., & Zampieri, M. (2009). Epigenetics: poly (ADP-ribosyl) ation of PARP-1 regulates genomic methylation patterns. *The FASEB Journal*, 23(3), 672-678.
84. Curtin, N. J. (2012). Poly (ADP-ribose) polymerase (PARP) and PARP inhibitors. *Drug Discovery Today: Disease Models*, 9(2), e51-e58.
85. Riccio, A. A., Cingolani, G., & Pascal, J. M. (2015). PARP-2 domain requirements for DNA damage-dependent activation and localization to sites of DNA damage. *Nucleic acids research*, gkv1376.
86. Scheer, U., & Benavente, R. (1990). Nucleolus structure and function. *Cell Biology International Reports*, 14, 14.
87. Amé, J. C., Rolli, V., Schreiber, V., Niedergang, C., Apiou, F., Decker, P., & de Murcia, G. (1999). PARP-2, A novel mammalian DNA damage-dependent poly (ADP-ribose) polymerase. *Journal of Biological Chemistry*, 274(25), 17860-17868.

88. Curtin, N. J. (2005). PARP inhibitors for cancer therapy. *Expert reviews in molecular medicine*, 7(04), 1-20.
89. Ishida, J., Yamamoto, H., Kido, Y., Kamijo, K., Murano, K., Miyake, H., & Mihara, K. (2006). Discovery of potent and selective PARP-1 and PARP-2 inhibitors: SBDD analysis via a combination of X-ray structural study and homology modeling. *Bioorganic & medicinal chemistry*, 14(5), 1378-1390.
90. Loseva, O., Jemth, A. S., Bryant, H. E., Schüler, H., Lehtiö, L., Karlberg, T., & Helleday, T. (2010). PARP-3 is a mono-ADP-ribosylase that activates PARP-1 in the absence of DNA. *Journal of Biological Chemistry*, 285(11), 8054-8060.
91. Lehtiö, L., Jemth, A. S., Collins, R., Loseva, O., Johansson, A., Markova, N., ... & Helleday, T. (2009). Structural Basis for Inhibitor Specificity in Human Poly (ADP-ribose) Polymerase-3[†]. *Journal of medicinal chemistry*, 52(9), 3108-3111.
92. Scott, C. L., Swisher, E. M., & Kaufmann, S. H. (2015). Poly (ADP-ribose) polymerase inhibitors: recent advances and future development. *Journal of Clinical Oncology*, JCO-2014.
93. Johannes, Jeffrey W., et al. "Discovery of AZ0108, an orally bioavailable phthalazinone PARP inhibitor that blocks centrosome clustering." *Bioorganic & medicinal chemistry letters* 25.24 (2015): 5743-5747.
94. Vedadi, M., Niesen, F. H., Allali-Hassani, A., Fedorov, O. Y., Finerty, P. J., Wasney, G. A., Hui, R., et al. (2006). Chemical screening methods to identify ligands that promote protein stability, protein crystallization, and structure determination. *Proceedings of the National Academy of Sciences*, 103(43), 15835-15840.

95. Weltin, D., Holl, V., Hyun, J. W., Dufour, P., Marchal, J., Bischoff, P., (1997). Effect of 6 (5H)-phenanthridinone, a poly (ADP-ribose) polymerase inhibitor, and ionizing radiation on the growth of cultured lymphoma cells. *International journal of radiation biology*, 72(6), 685-692.
96. Weltin, D., Marchal, J., Dufour, P., Potworowski, E., Oth, D., & Bischoff, P. (1993). Effect of 6 (5H)-phenanthridinone, an inhibitor of poly (ADP-ribose) polymerase, on cultured tumor cells. *Oncology research*, 6(9), 399-403.
97. Richardson, D. S., Allen, P. D., Kelsey, S. M., & Newland, A. C. (1999). Effects of PARP inhibition on drug and Fas-induced apoptosis in leukaemic cells. In *Drug Resistance in Leukemia and Lymphoma III* (pp. 267-279). Springer US.
98. Jagtap, P., & Szabó, C. (2005). Poly (ADP-ribose) polymerase and the therapeutic effects of its inhibitors. *Nature reviews Drug discovery*, 4(5), 421-440.
99. Niesen, F. H., Berglund, H., & Vedadi, M. (2007). The use of differential scanning fluorimetry to detect ligand interactions that promote protein stability. *Nature protocols*, 2(9), 2212-2221.
100. Wahlberg, E., Karlberg, T., Kouznetsova, E., Markova, N., Macchiarulo, A., Thorsell, A. G. & Kull, B. (2012). Family-wide chemical profiling and structural analysis of PARP and tankyrase inhibitors. *Nature biotechnology*, 30(3), 283-288.
101. Mayo, M., Grosskurth, S., Wang, X., Wang, W., Petteruti, P., Wen, S., Scott, D, *et al.* (2013). Novel PARP6 Inhibitors Demonstrate In vivo Efficacy in Xenograft Models. *Lung*, 21(4.635), 0-040.
102. Johannes, J. W., Almeida, L., Daly, K., Ferguson, A. D., Grosskurth, S. E., Guan, H., Larsen, N. A. *et al.* (2015). Discovery of AZ0108, an orally bioavailable

- phthalazinone PARP inhibitor that blocks centrosome clustering. *Bioorganic & medicinal chemistry letters*, 25(24), 5743-5747.
103. Kirby, C. A., Cheung, A., Fazal, A., Shultz, M. D., & Stams, T. (2012). Structure of human tankyrase 1 in complex with small-molecule inhibitors PJ34 and XAV939. *Acta Crystallographica Section F: Structural Biology and Crystallization Communications*, 68(2), 115-118.
104. Kirubakaran, P., Kothandan, G., Cho, S. J., & Muthusamy, K. (2014). Molecular insights on TNKS1/TNKS2 and inhibitor-IWR1 interactions. *Molecular BioSystems*, 10(2), 281-293.
105. Karlberg, T., Markova, N., Johansson, I., Hammarström, M., Schütz, P., Weigelt, J., & Schüler, H. (2010). Structural basis for the interaction between tankyrase-2 and a potent Wnt-signaling inhibitor. *Journal of medicinal chemistry*, 53(14), 5352-5355.
106. Bregman, H., Gunaydin, H., Gu, Y., Schneider, S., Wilson, C., DiMauro, E. F., & Huang, X. (2013). Discovery of a class of novel tankyrase inhibitors that bind to both the nicotinamide pocket and the induced pocket. *Journal of medicinal chemistry*, 56(3), 1341-1345.
107. Li, J. H., Serdyuk, L., Ferraris, D. V., Xiao, G., Tays, K. L., Kletzly, P. W., & Kalish, V. J. (2001). Synthesis of substituted 5 [h] phenanthridin-6-ones as potent poly (ADP-ribose) polymerase-1 (PARP1) inhibitors. *Bioorganic & medicinal chemistry letters*, 11(13), 1687-1690.
108. Tanimoto, K., Nakagawa, N., Takeda, K., Kirihata, M., & Tanimori, S. (2013). A convenient one-pot access to phenanthridinones via Suzuki–Miyaura cross-coupling reaction. *Tetrahedron Letters*, 54(28), 3712-3714.

109. Dubost, E., Magnelli, R., Cailly, T., Legay, R., Fabis, F., & Rault, S. (2010). General method for the synthesis of substituted phenanthridin-6 (5H)-ones using a KOH-mediated anionic ring closure as the key step. *Tetrahedron*, 66(27), 5008-5016.
110. Banwell, M. G., Lupton, D. W., Ma, X., Renner, J., & Sydnese, M. O. (2004). Synthesis of Quinolines, 2-Quinolones, Phenanthridines, and 6 (5 H)-Phenanthridinones via Palladium [0]-Mediated Ullmann Cross-coupling of 1-Bromo-2-nitroarenes with β -Halo-enals,-enones, or-esters. *Organic letters*, 6(16), 2741-2744.
111. Lu, C., Dubrovskiy, A. V., & Larock, R. C. (2012). Palladium-catalyzed Annulation of Arynes by o-Halobenzamides: Synthesis of Phenanthridinones. *The Journal of organic chemistry*, 77(19), 8648-8656.
112. Chen, Y. F., Wu, Y. S., Jhan, Y. H., & Hsieh, J. C. (2014). An efficient synthesis of (NH)-phenanthridinones via ligand-free copper-catalyzed annulation. *Organic Chemistry Frontiers*, 1(3), 253-257.
113. Lu, S. M., & Alper, H. (2005). Intramolecular carbonylation reactions with recyclable palladium-complexed dendrimers on silica: Synthesis of oxygen, nitrogen, or sulfur-containing medium ring fused heterocycles. *Journal of the American Chemical Society*, 127(42), 14776-14784.
114. Fang, Y., & Tranmer, G. K. (2016). Continuous flow photochemistry as an enabling synthetic technology: synthesis of substituted-6 (5 H)-phenanthridinones for use as poly (ADP-ribose) polymerase inhibitors. *MedChemComm*, 7(4), 720-724.
115. Bhakuni, B. S., Kumar, A., Balkrishna, S. J., Sheikh, J. A., Konar, S., & Kumar, S. (2012). KO^tBu Mediated Synthesis of Phenanthridinones and Dibenzoazepinones. *Organic letters*, 14(11), 2838-2841.

116. Grimshaw, J., & de Silva, A. P. (1980). Photocyclisation of 2-halogenobenzanilides: an extreme example of halogen atom, solvent, and isomer dependence. A practical phenanthridine synthesis. *Journal of the Chemical Society, Chemical Communications*, (7), 302-303.
117. Cailly, T., Fabis, F., & Rault, S. (2006). A new, direct, and efficient synthesis of benzonaphthyridin-5-ones. *Tetrahedron*, 62(25), 5862-5867.
118. Ferraris, D., Ko, Y. S., Pahutski, T., Ficco, R. P., Serdyuk, L., Alemu, C., & Lautar, S. (2003). Design and synthesis of poly ADP-ribose polymerase-1 inhibitors. 2. Biological evaluation of aza-5 [h]-phenanthridin-6-ones as potent, aqueous-soluble compounds for the treatment of ischemic injuries. *Journal of medicinal chemistry*, 46(14), 3138-3151.
119. Feng, B. B., Lu, L., Li, C., & Wang, X. S. (2016). Iodine-catalyzed synthesis of dibenzo [b, h][1, 6] naphthyridine-11-carboxamides via a domino reaction involving double elimination of hydrogen bromide. *Organic & biomolecular chemistry*, 14(9), 2774-2779.
120. Kumar, A. K. M. M. S., Rajkumar, R., Rajendran, S. P. (2016). Efficient synthesis of fused benzo[b] indazolo[6,7-h] [1,6] naphthyridines. *Archives of Applied Science Research*, 7(10), 60-64.
121. Ibrahim, M. A., El-Gohary, N. M., & Said, S. (2015). Synthesis of Heteroannulated Chromeno [2, 3-b] Pyridines: DBU Catalyzed Reactions of 2-Amino-6-methylchromone-3-Carboxaldehyde with Some Heterocyclic Enols and Enamines. *Journal of Heterocyclic Chemistry*.

122. Meanwell, N. A. (2011). Synopsis of some recent tactical application of bioisosteres in drug design. *Journal of medicinal chemistry*, 54(8), 2529-2591.
123. Patani, G. A., & LaVoie, E. J. (1996). Bioisosterism: a rational approach in drug design. *Chemical reviews*, 96(8), 3147-3176.
124. Dogan Koruznjak, J., Grdiša, M., Slade, N., Zamola, B., Pavelic, K., & Karminski-Zamola, G. (2003). Novel derivatives of benzo [b] thieno [2, 3-c] quinolones: synthesis, photochemical synthesis, and antitumor evaluation. *Journal of medicinal chemistry*, 46(21), 4516-4524.
125. Aleksić, M., Bertoša, B., Nhili, R., Depauw, S., Martin-Kleiner, I., David-cordonnier, M. H., Karminski-Zamola, G., *et al.* (2014). Anilides and quinolones with nitrogen-bearing substituents from benzothiophene and thienothiophene series: Synthesis, photochemical synthesis, cytostatic evaluation, 3D-derived QSAR analysis and DNA-binding properties. *European journal of medicinal chemistry*, 71, 267-281.
126. Sović, I., Viskiće, M., Bertoša, B., Ester, K., Kralj, M., Hranjec, M., & Karminski-Zamola, G. (2015). Exploring antiproliferative activity of heteroaromatic amides and their fused derivatives using 3D-QSAR, synthesis, and biological tests. *Monatshefte für Chemie-chemical Monthly*, 146(9), 1503-1517.
127. Liscio, P., Carotti, A., Ascitti, S., Ferri, M., Pires, M. M., Valloscuro, S., Pellicciari, R., *et al.* (2014). Scaffold hopping approach on the route to selective tankyrase inhibitors. *European journal of medicinal chemistry*, 87, 611-623.
128. Gorlitzer, K., Gabriel, B., Jomaa, H., & Wiesner, J. (2006). Synthesis of thieno [3, 2-c] quinolin-4-ylamines and antimalarial activity. *Pharmazie*, 61, 278-284.

129. Chatterjee, A., Cutler, S. J., Khan, I. A., & Williamson, J. S. (2014). Efficient synthesis of 4-oxo-4, 5-dihydrothieno [3, 2-c] quinoline-2-carboxylic acid derivatives from aniline. *Molecular diversity*, 18(1), 51-59.
130. Park, Y. T., Jung, C. H., Kim, M. S., Kim, K. W., Song, N. W., & Kim, D. (2001). Photoreaction of 2-Halo-N-pyridinylbenzamide: Intramolecular Cyclization Mechanism of Phenyl Radical Assisted with n-Complexation of Chlorine Radical. *The Journal of organic chemistry*, 66(7), 2197-2206.
131. Mattern, M. R., Mong, S. M., Bartus, H. F., Mirabelli, C. K., Crooke, S. T., & Johnson, R. K. (1987). Relationship between the intracellular effects of camptothecin and the inhibition of DNA topoisomerase I in cultured L1210 cells. *Cancer research*, 47(7),

The application of flow chemistry techniques in medicinal chemistry programs: The development of flow-photocyclization methods for the synthesis of phenanthridinone-type compounds.

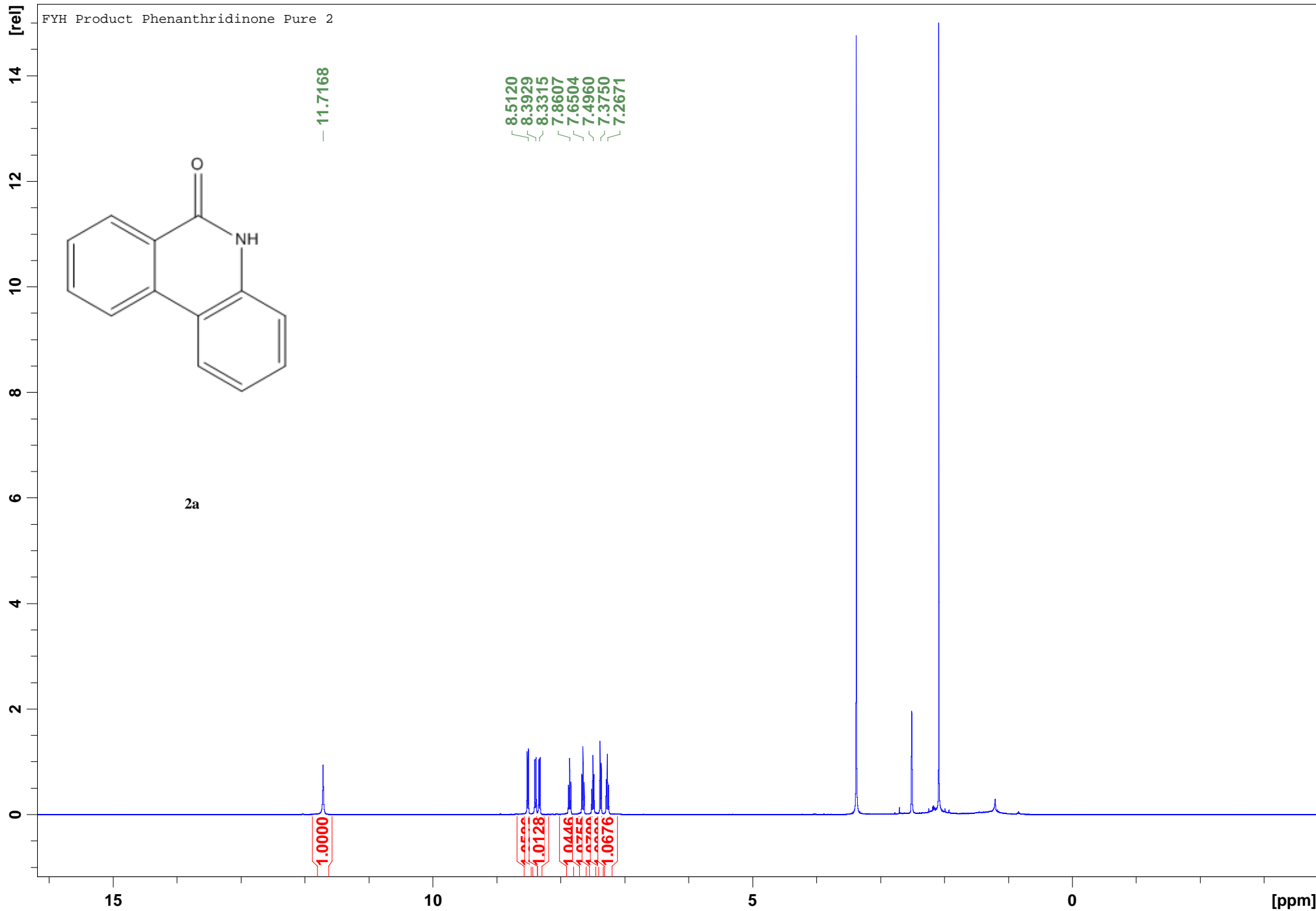
by

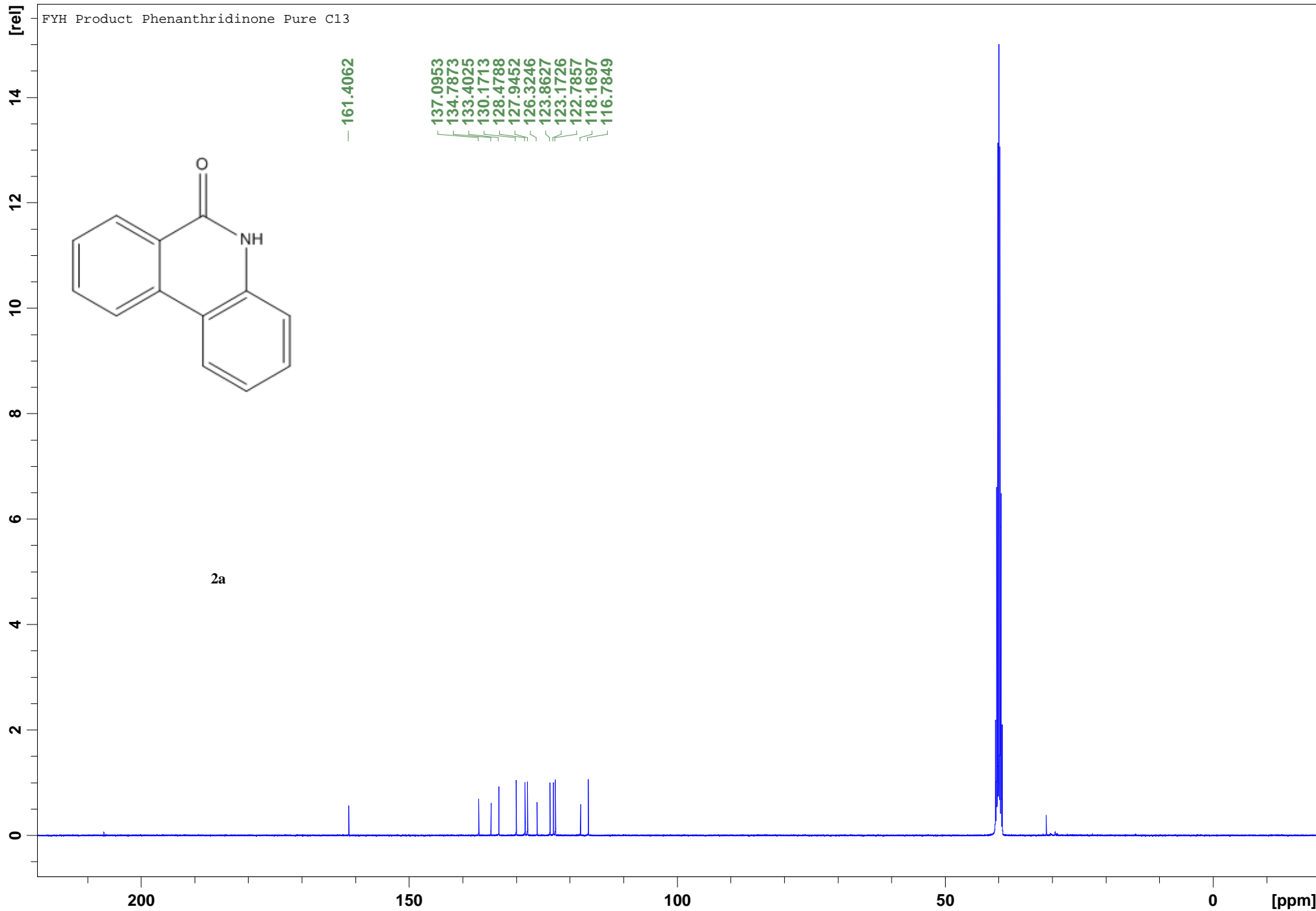
Yuhua Fang

Supplemental Appendix

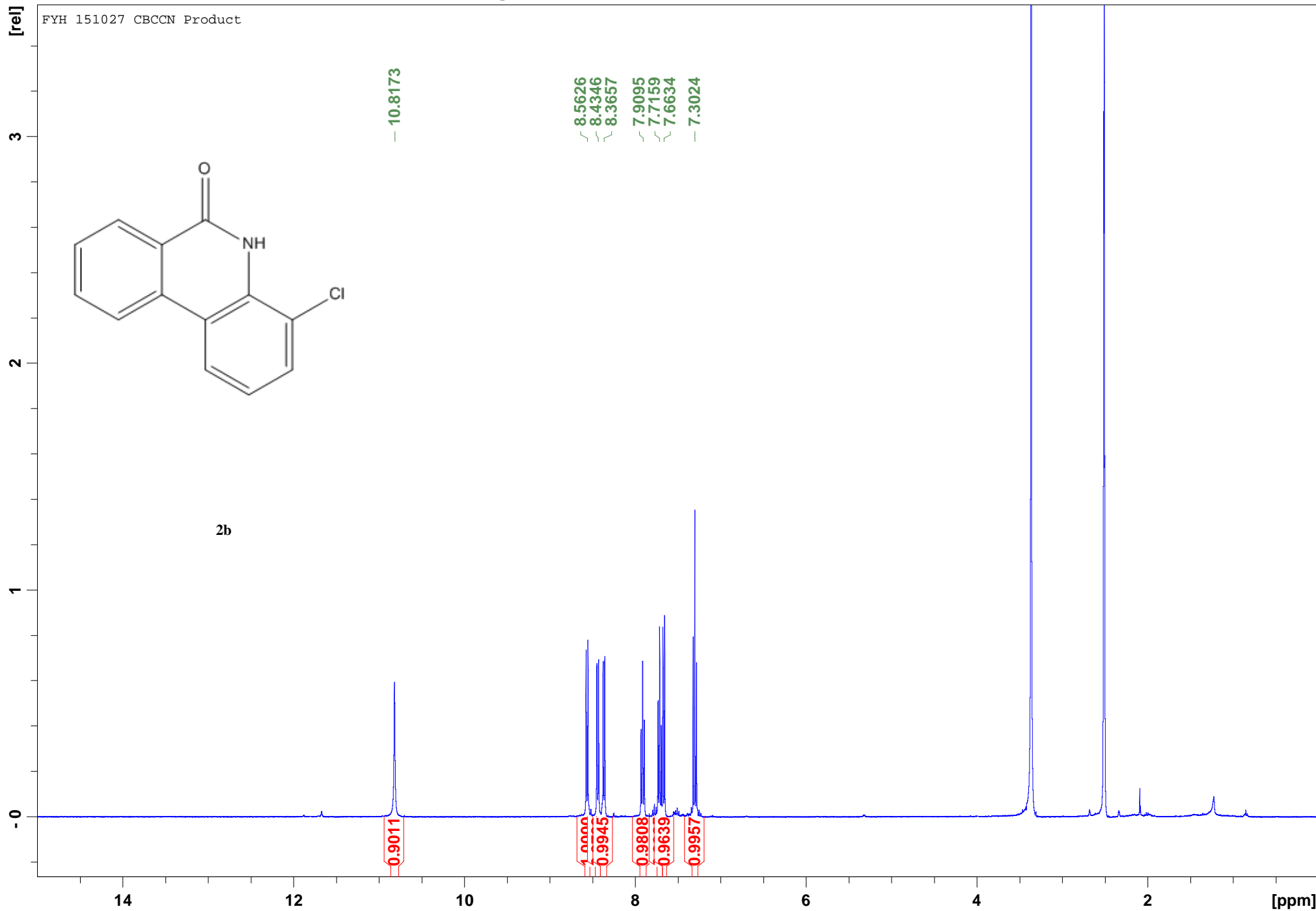
NMR Spectra

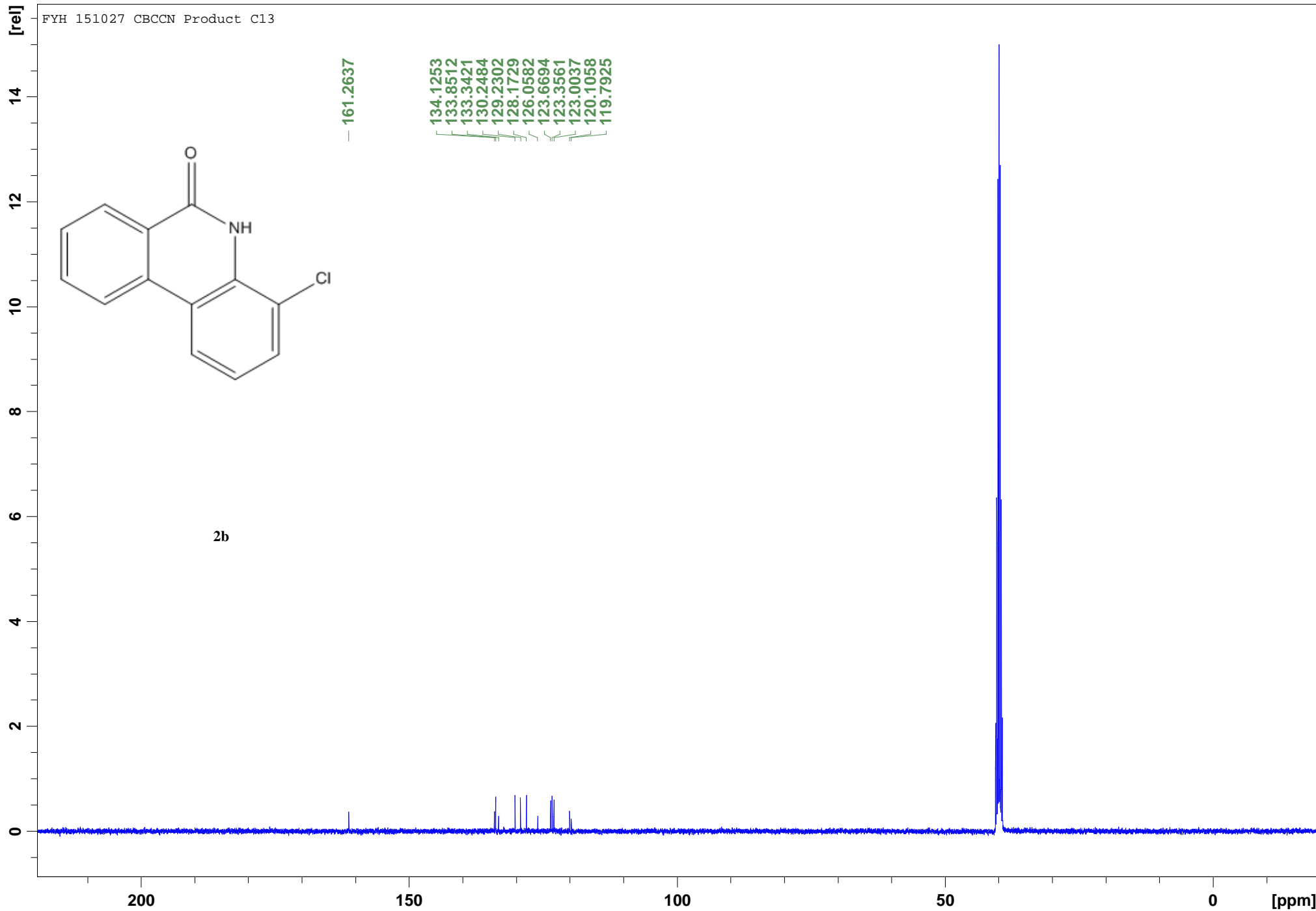
FYH Product Phenanthridinone Pure 2



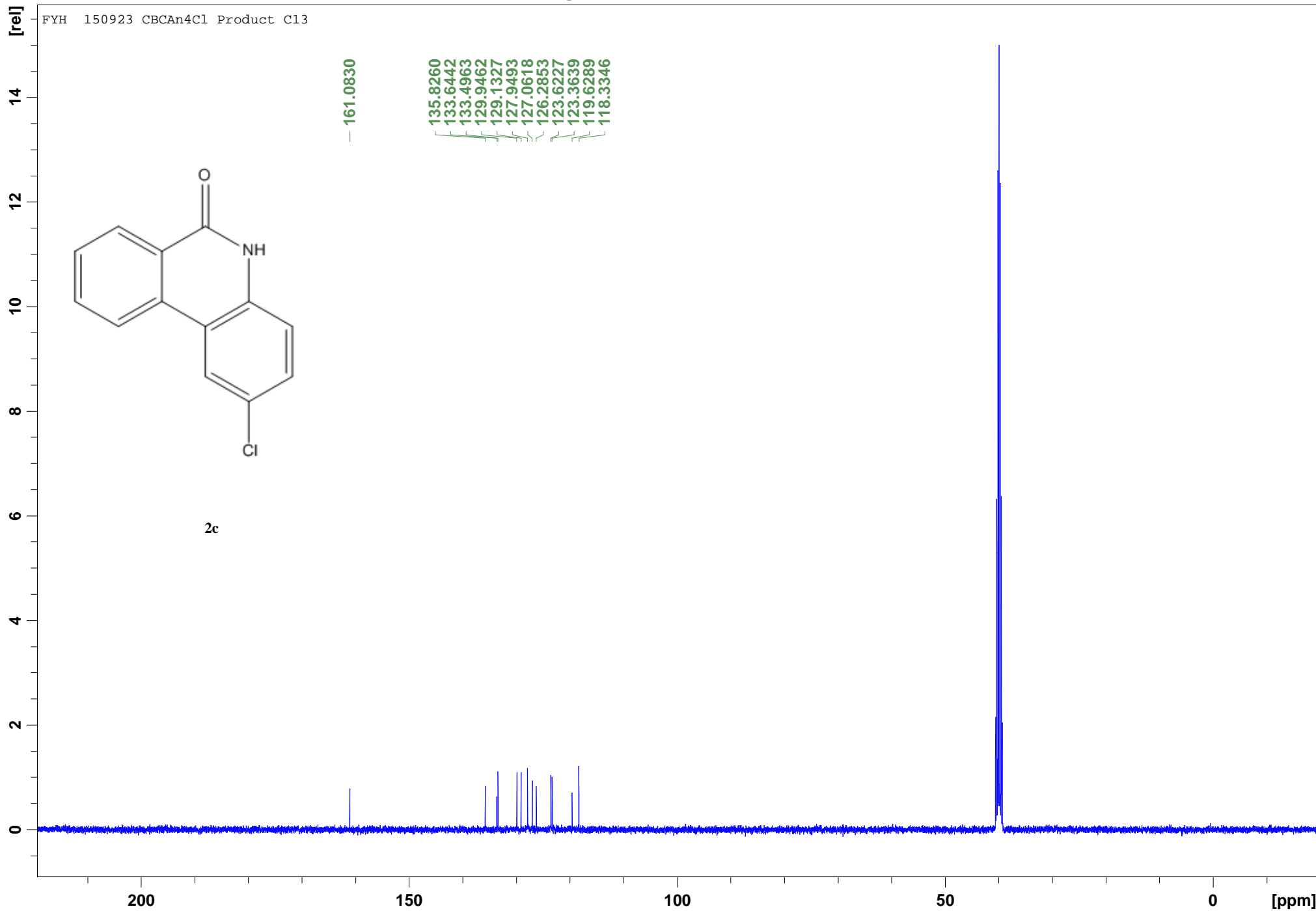


FYH 151027 CBCCN Product

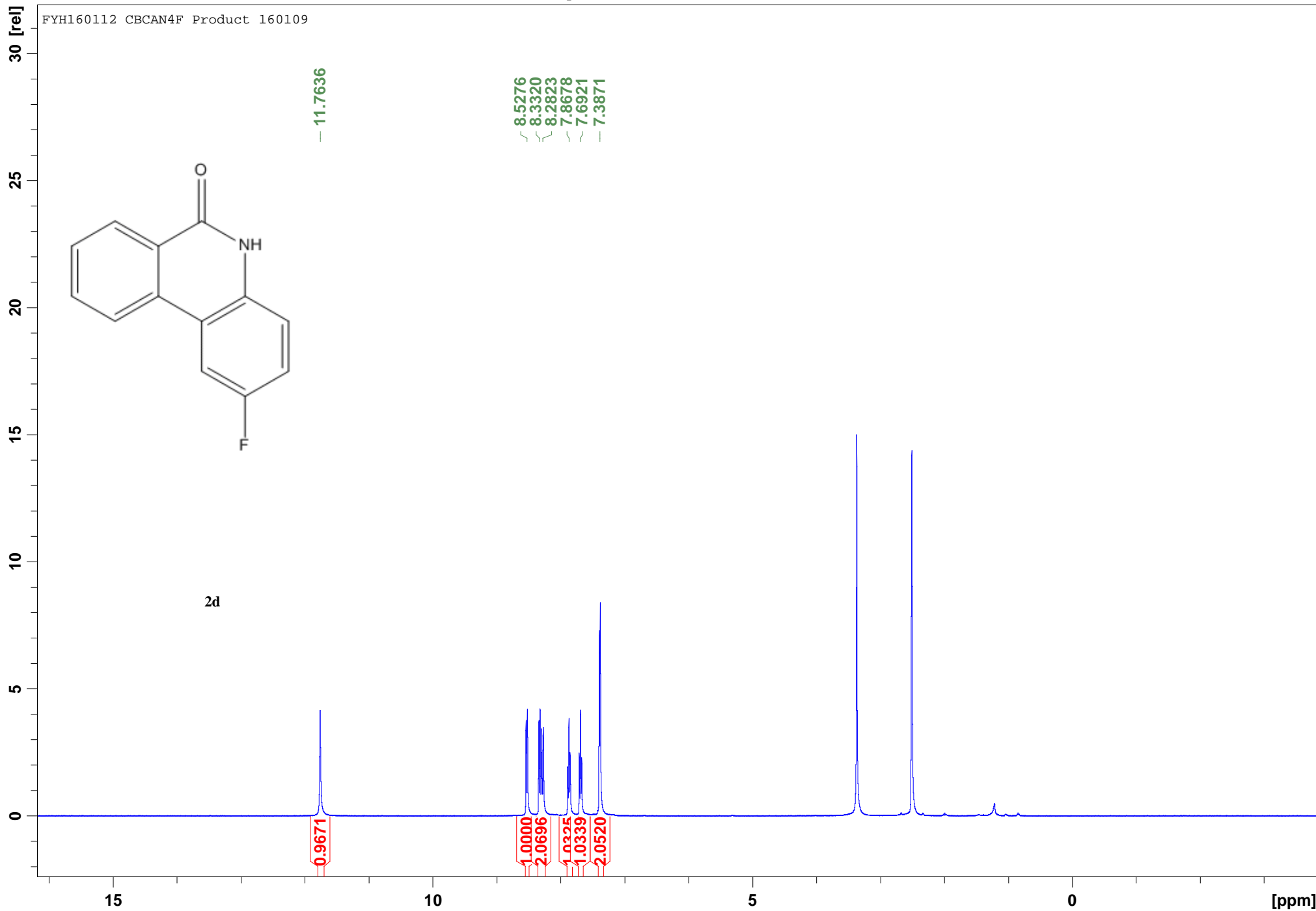




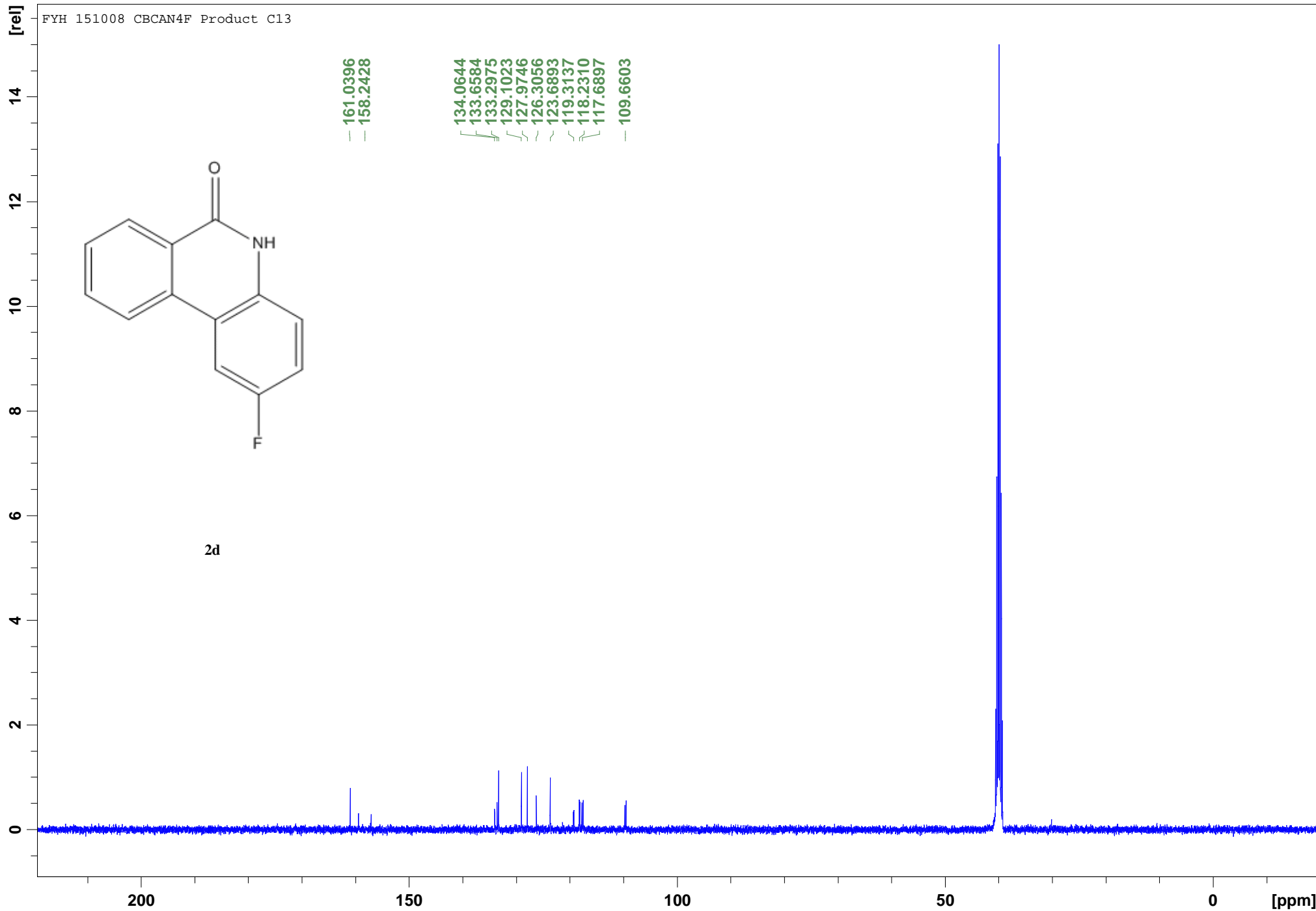
FYH 150923 CBCAn4Cl Product C13



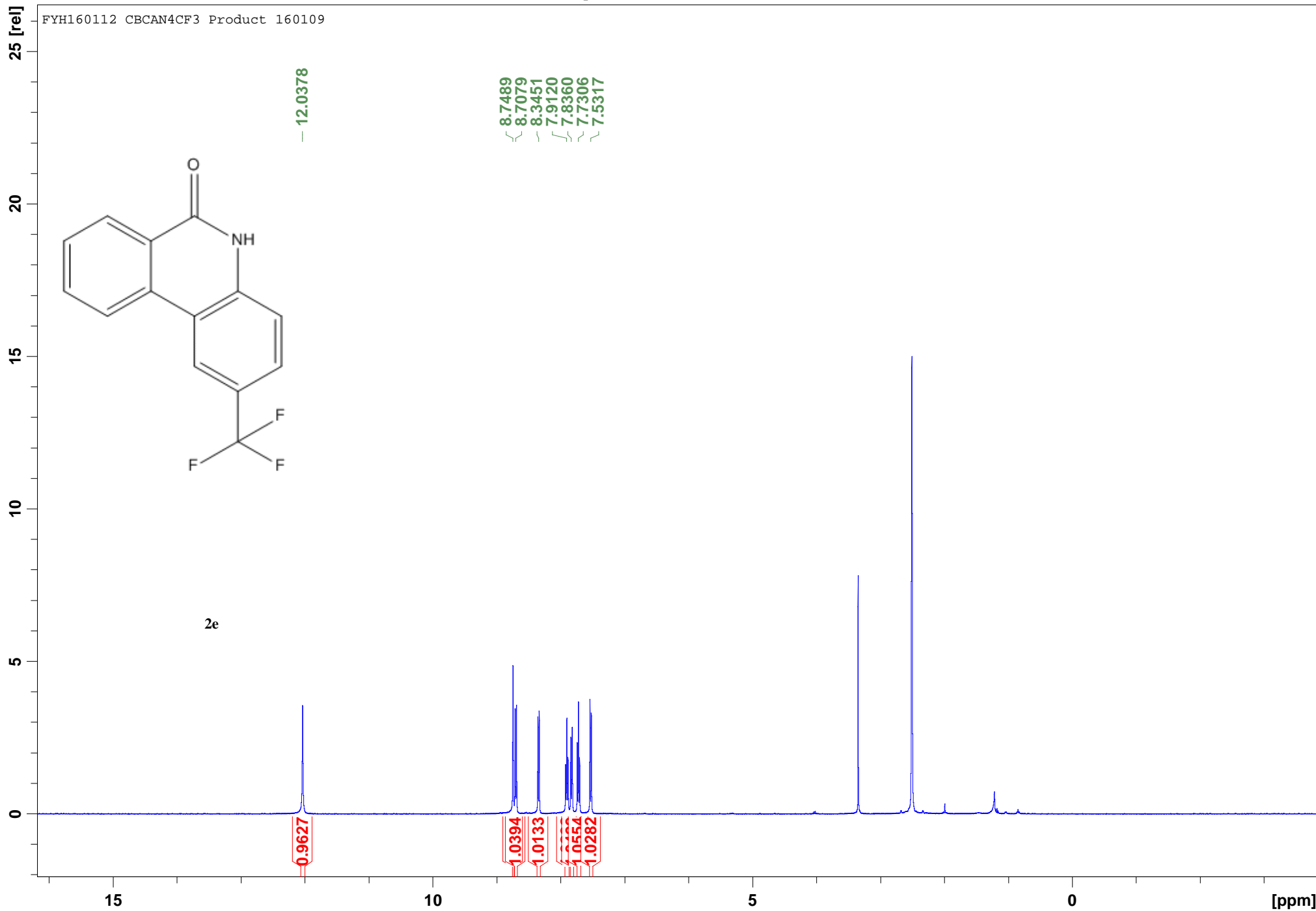
FYH160112 CBCAN4F Product 160109

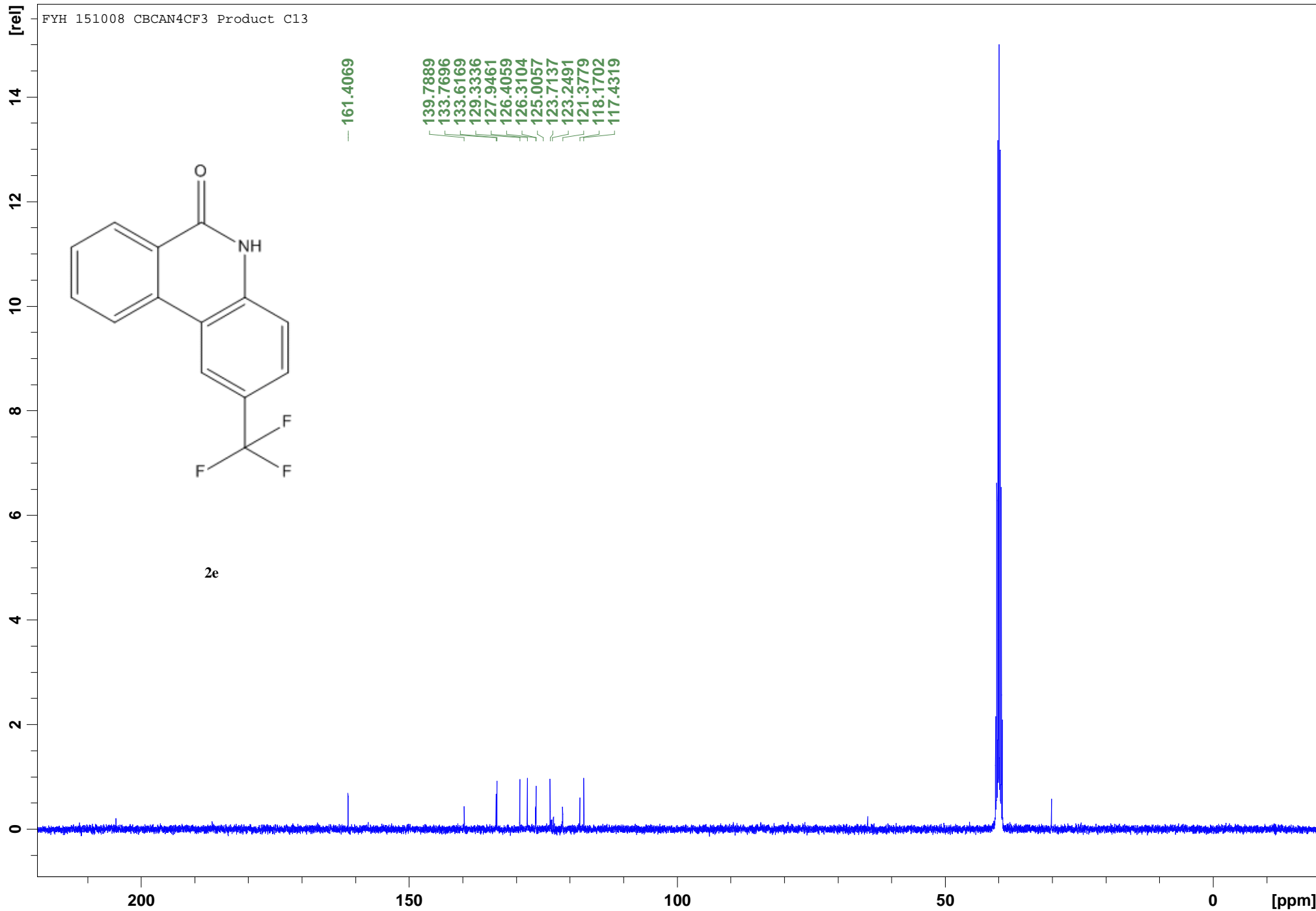


FYH 151008 CBCAN4F Product C13

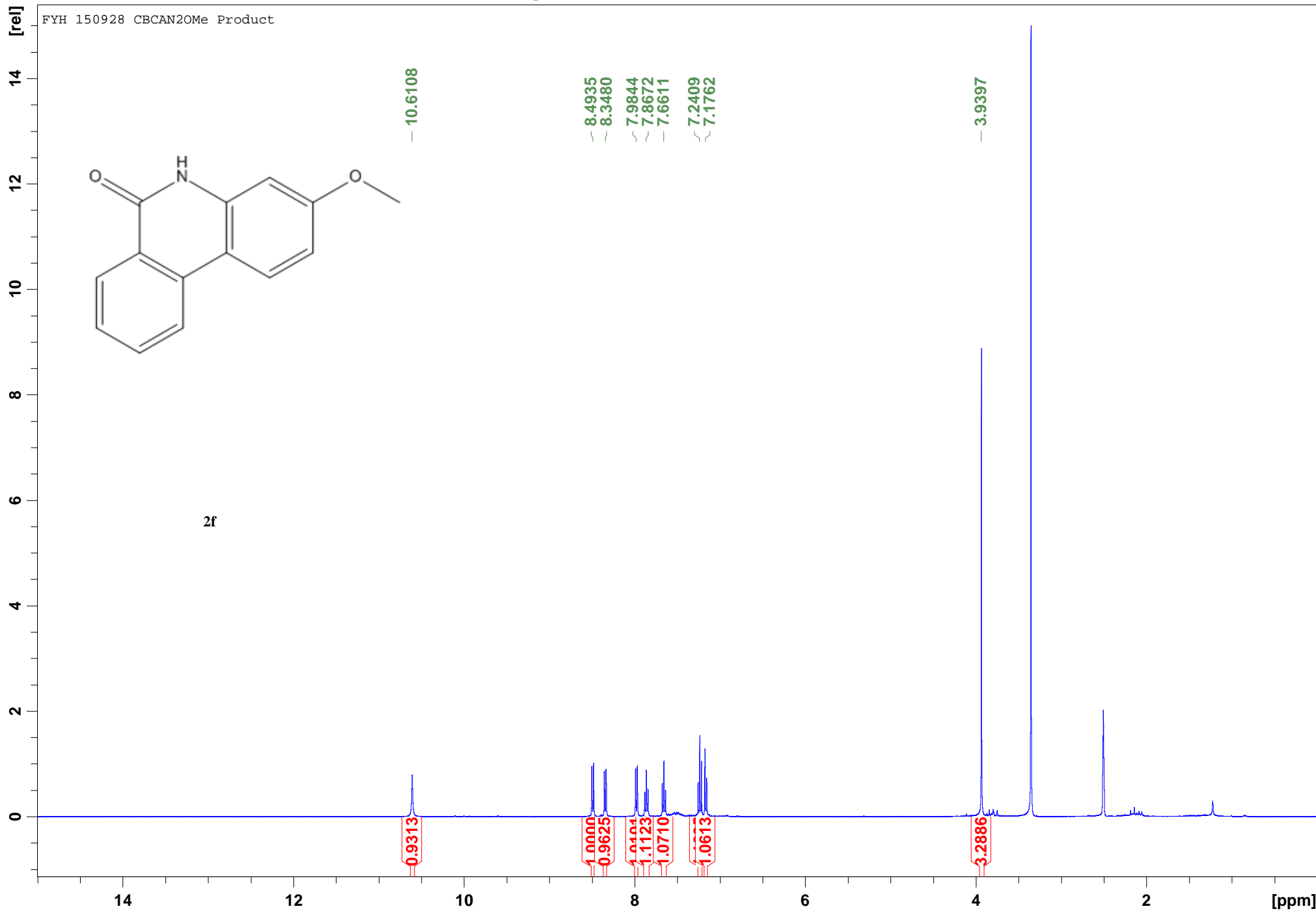


FYH160112 CBCAN4CF3 Product 160109

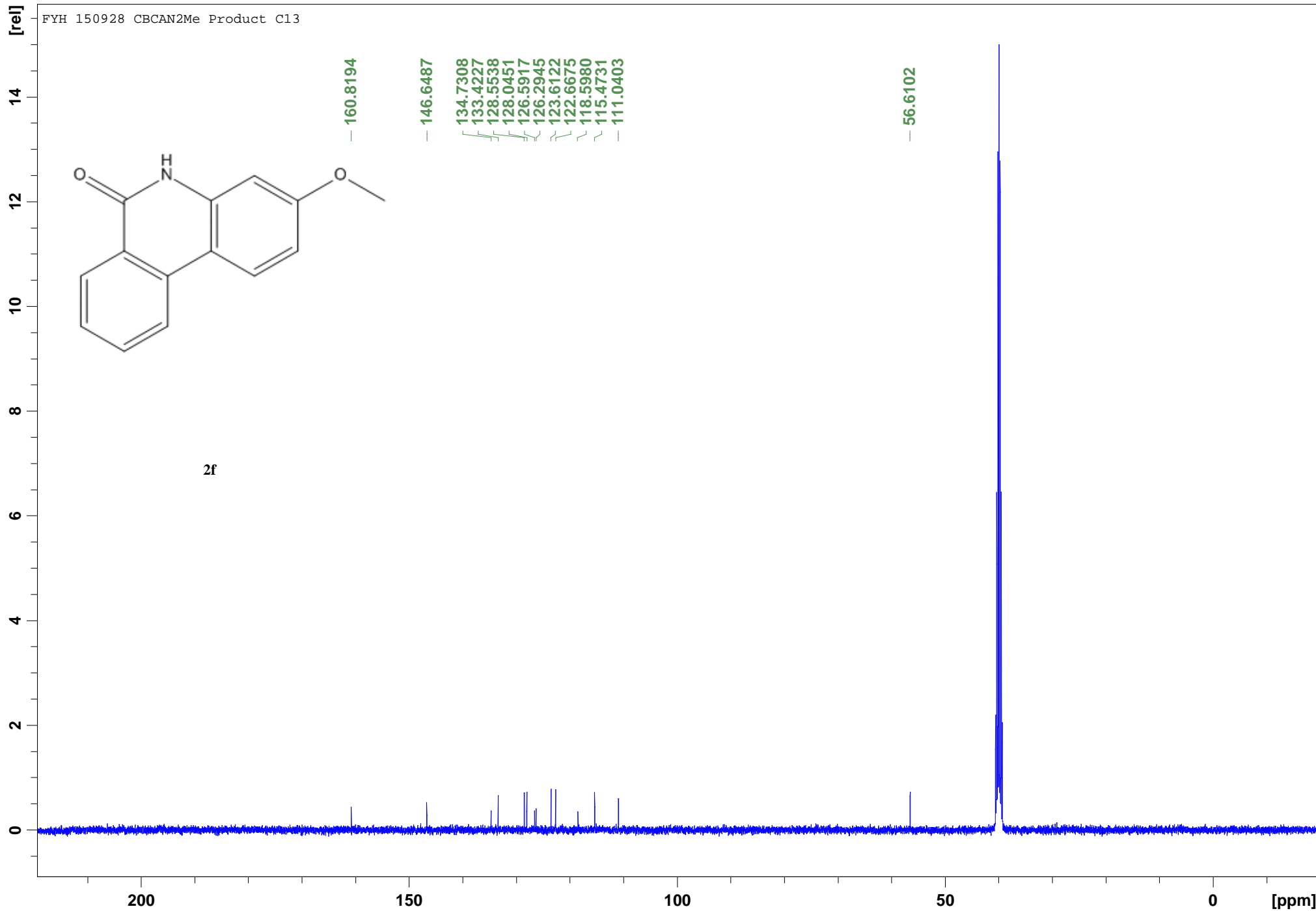




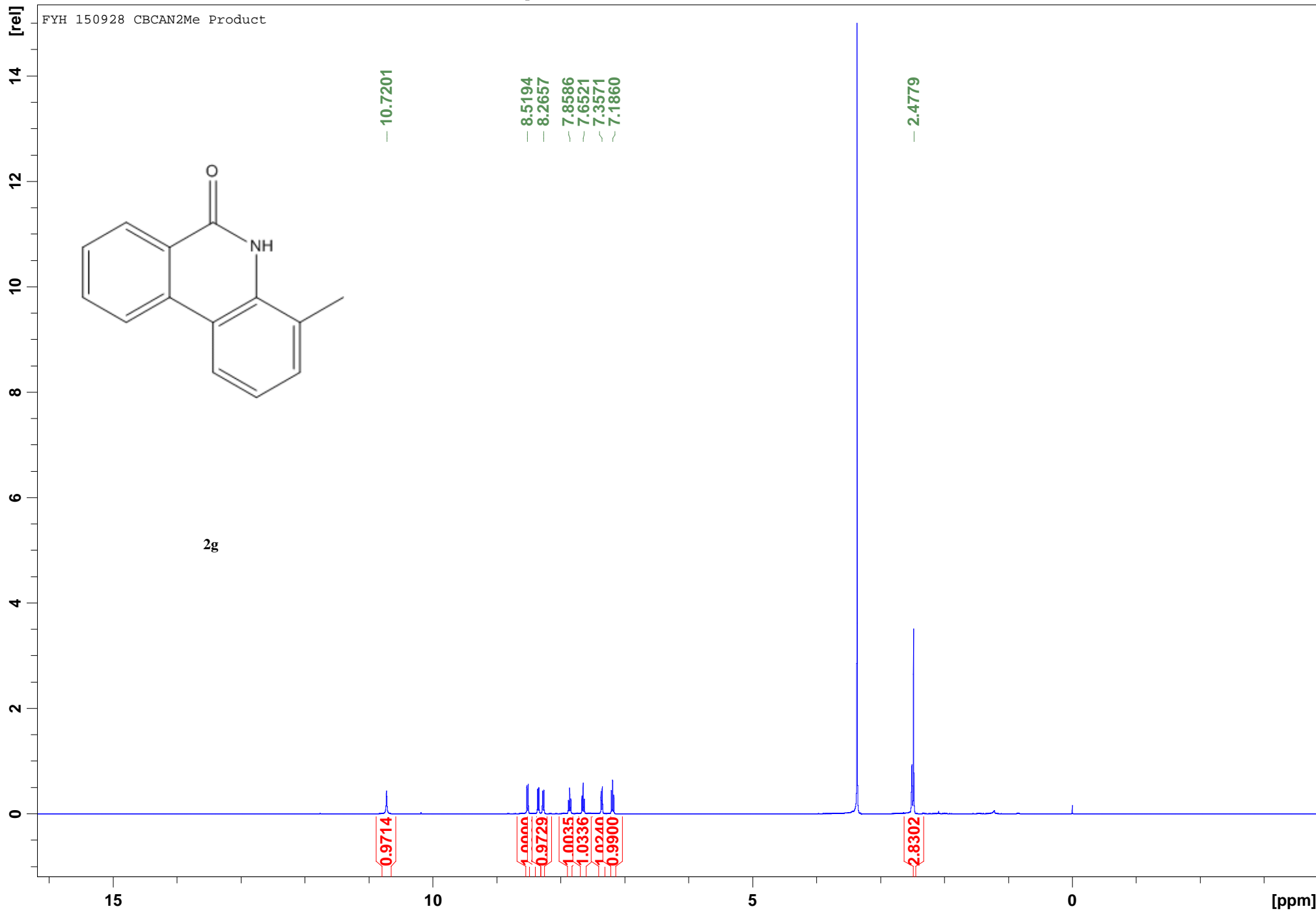
FYH 150928 CBCAN2OMe Product



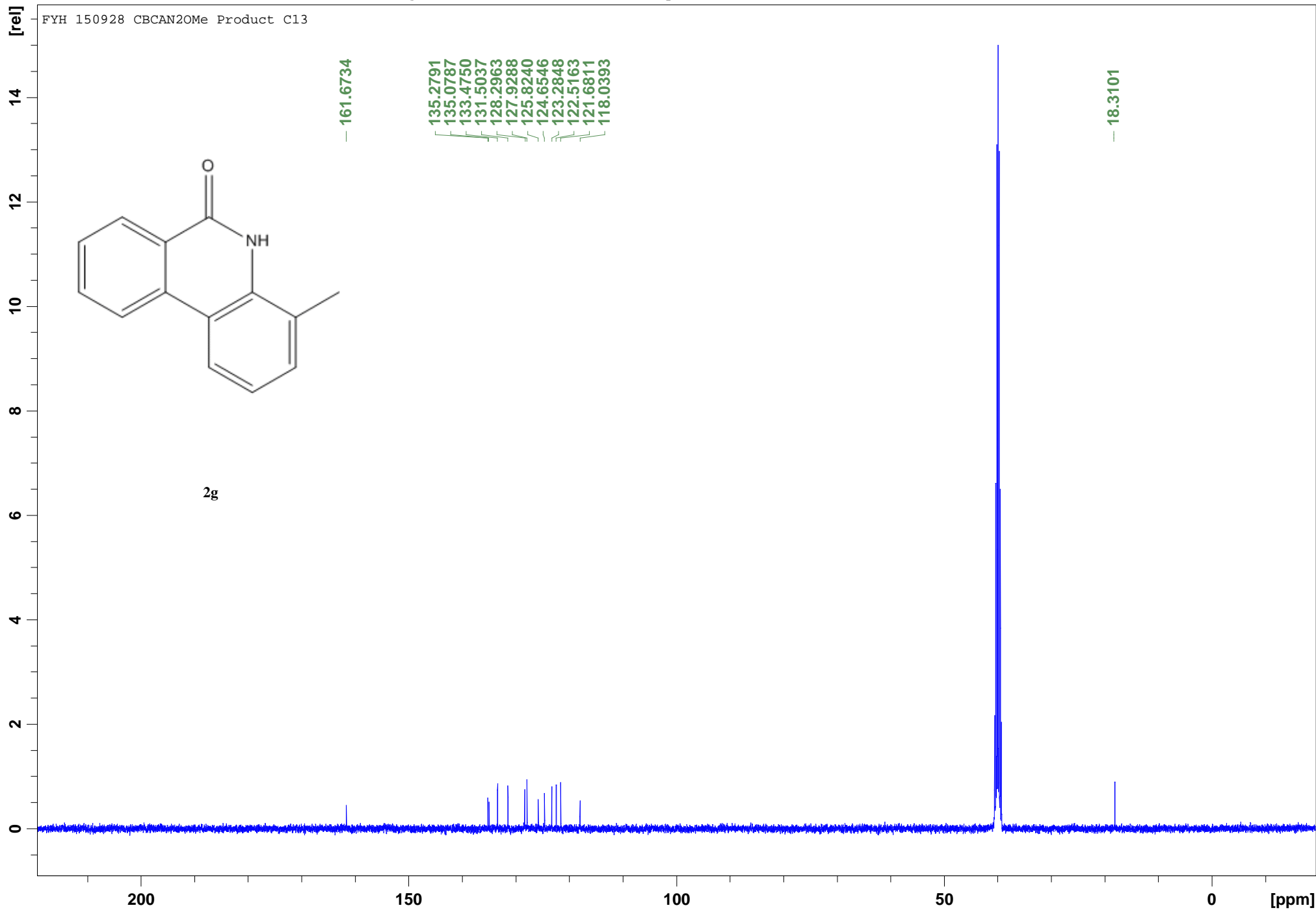
FYH 150928 CBCAN2Me Product C13



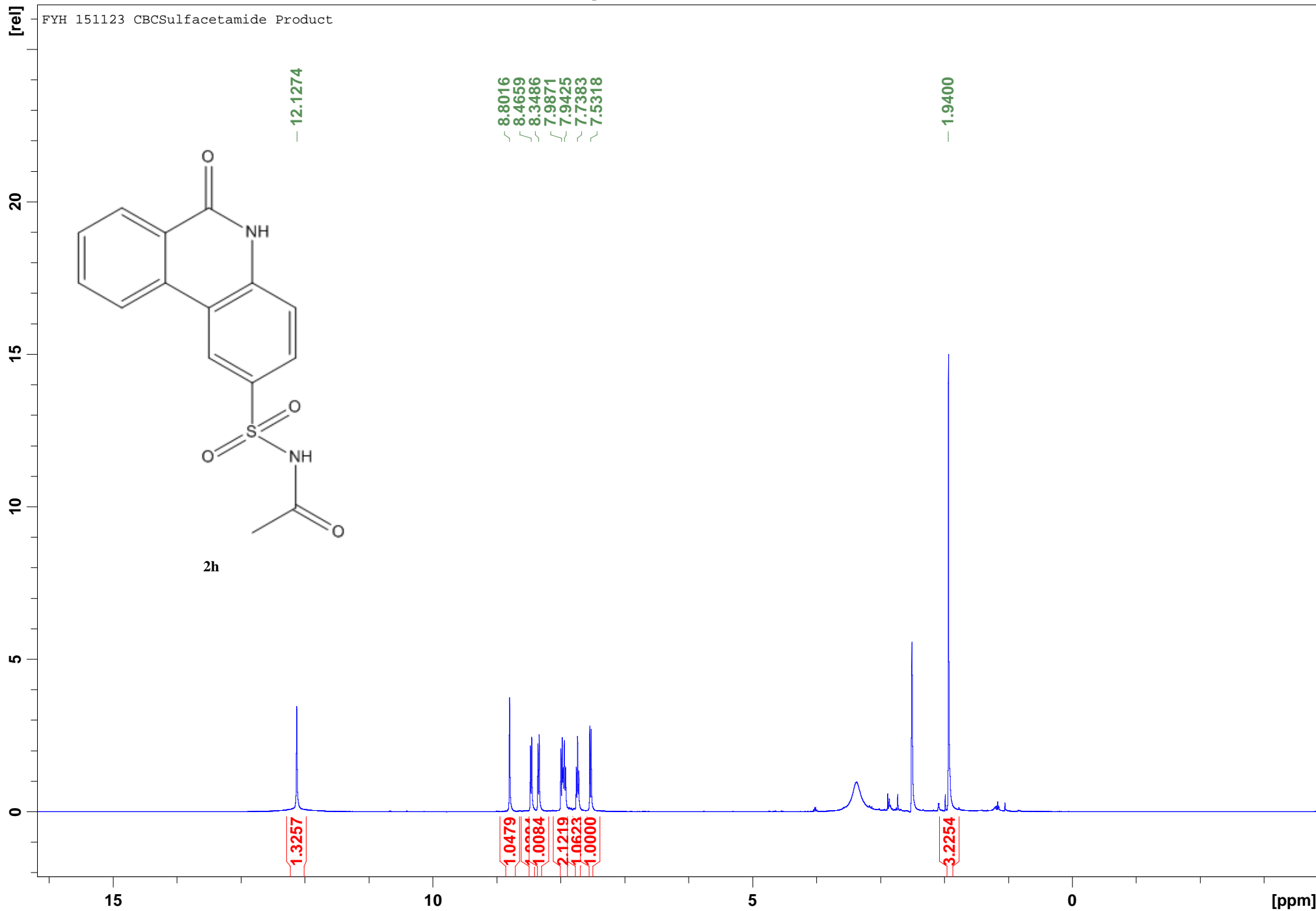
FYH 150928 CBCAN2Me Product



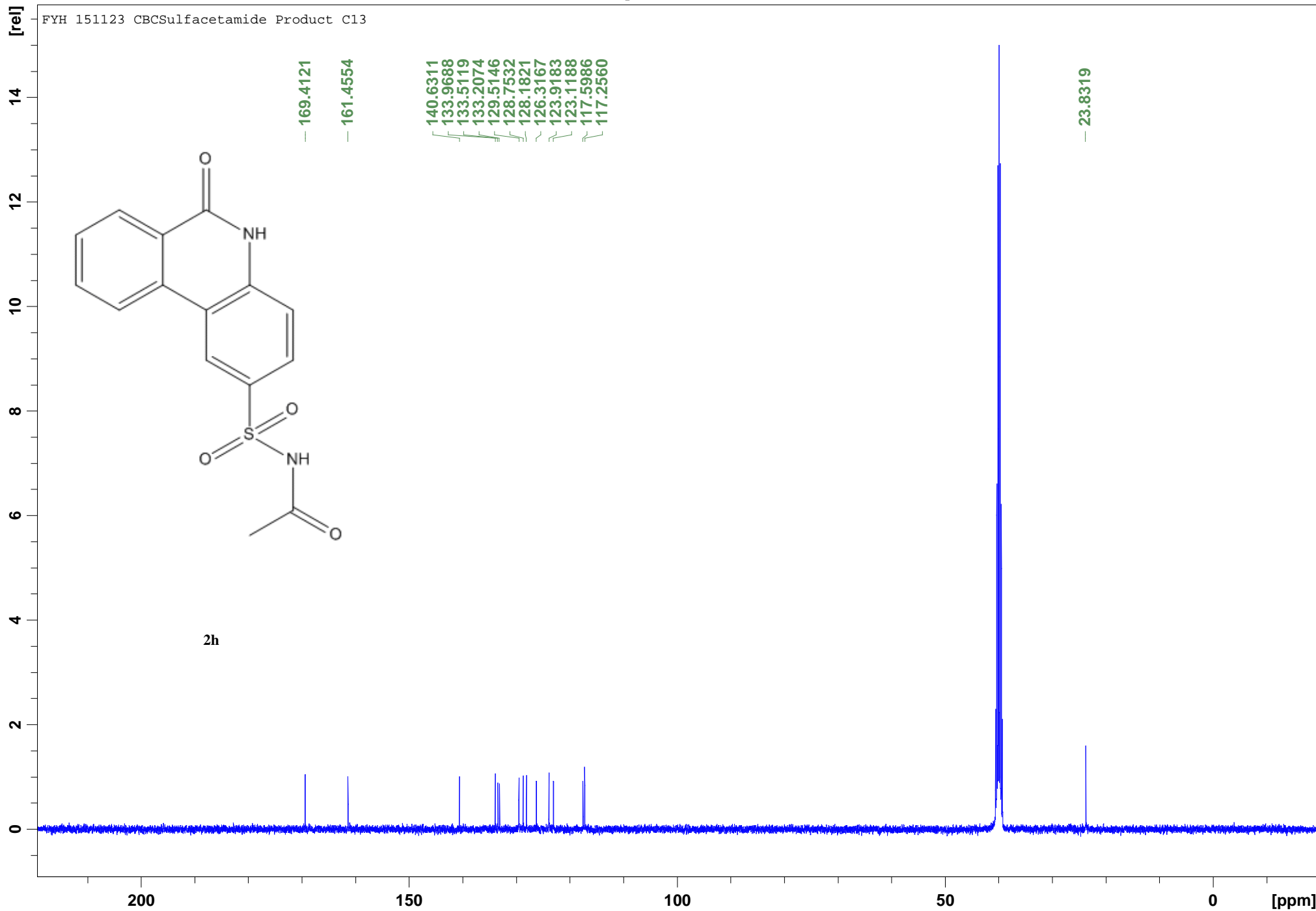
FYH 150928 CBCAN20Me Product C13

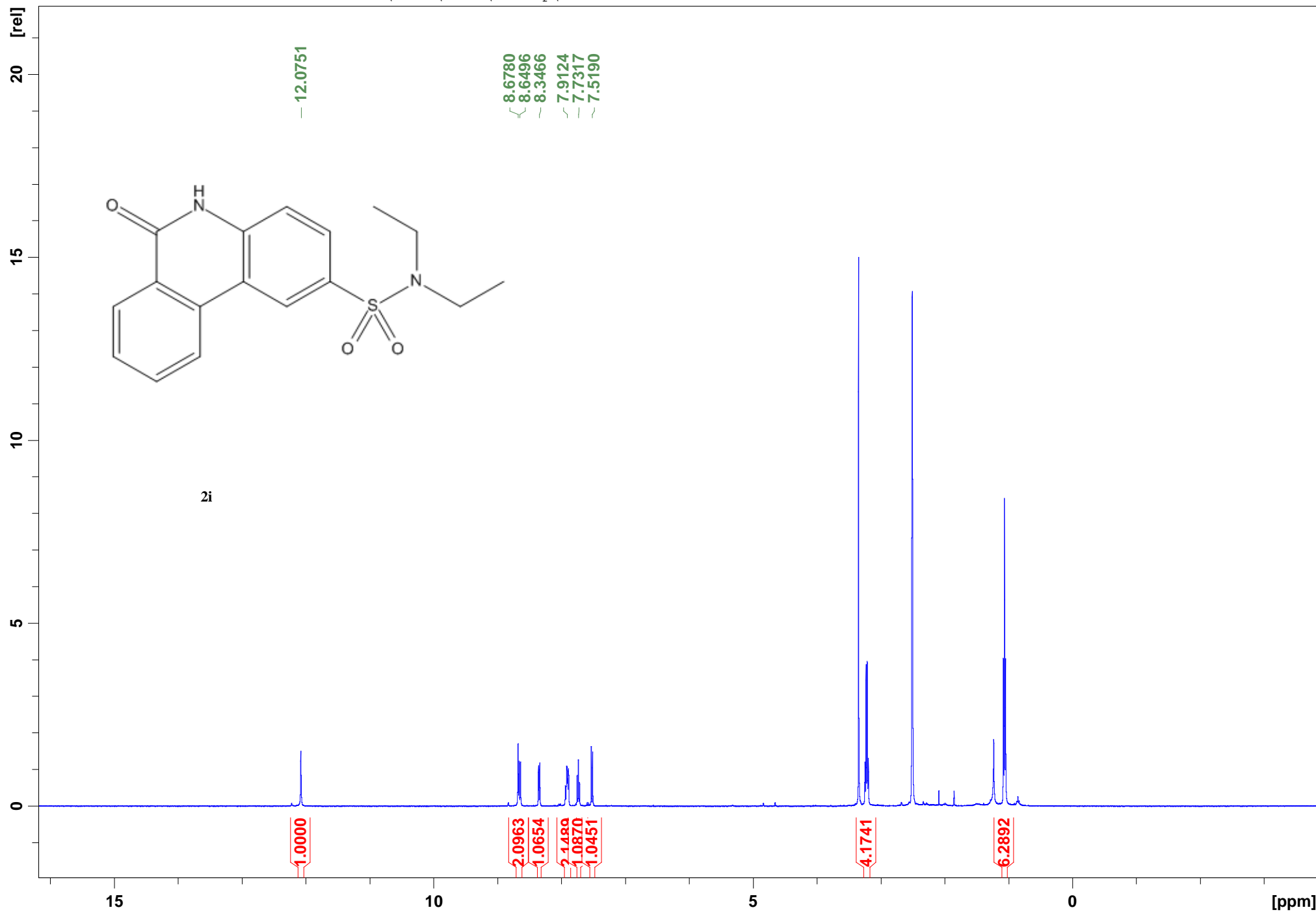


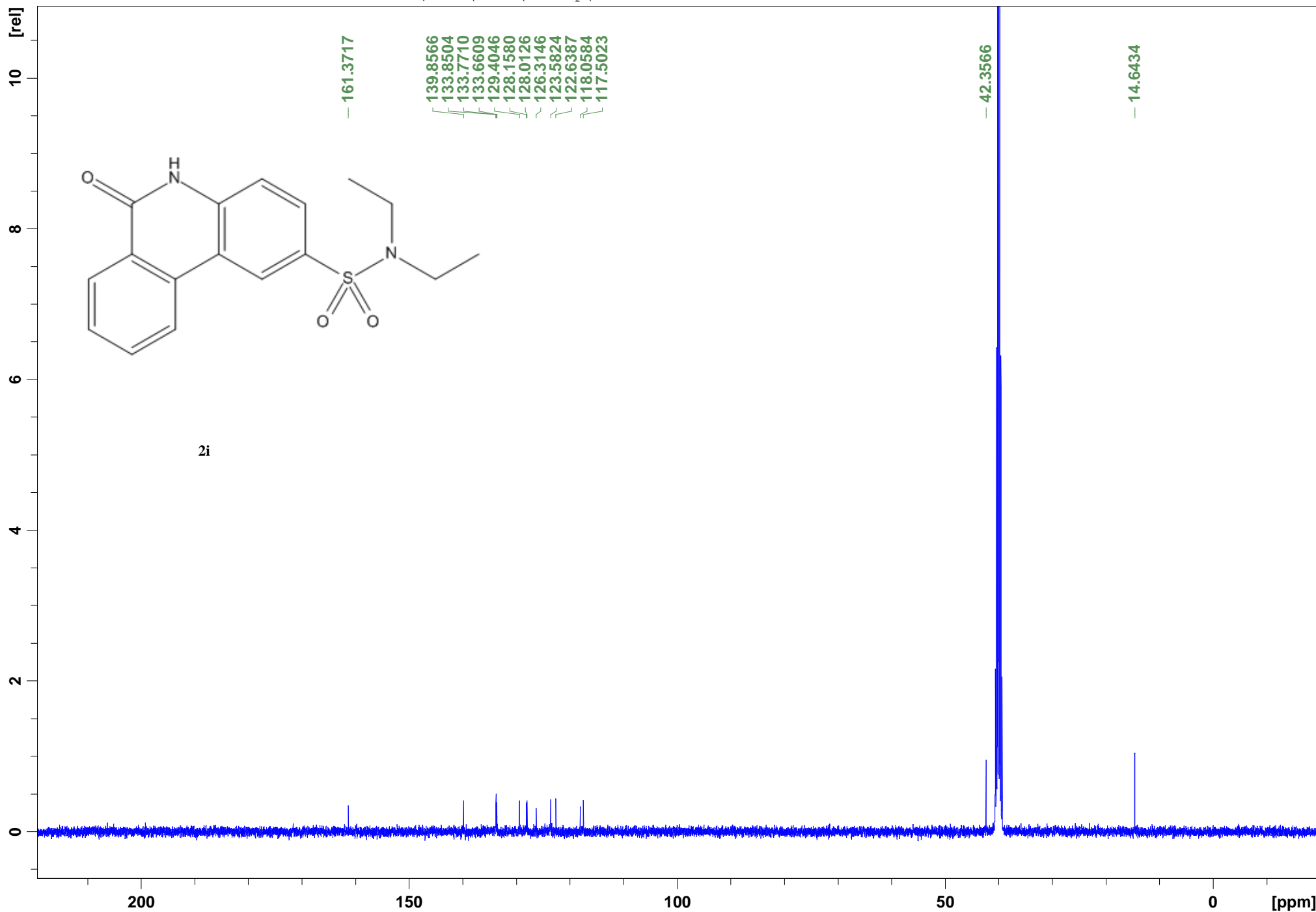
FYH 151123 CBCSulfacetamide Product



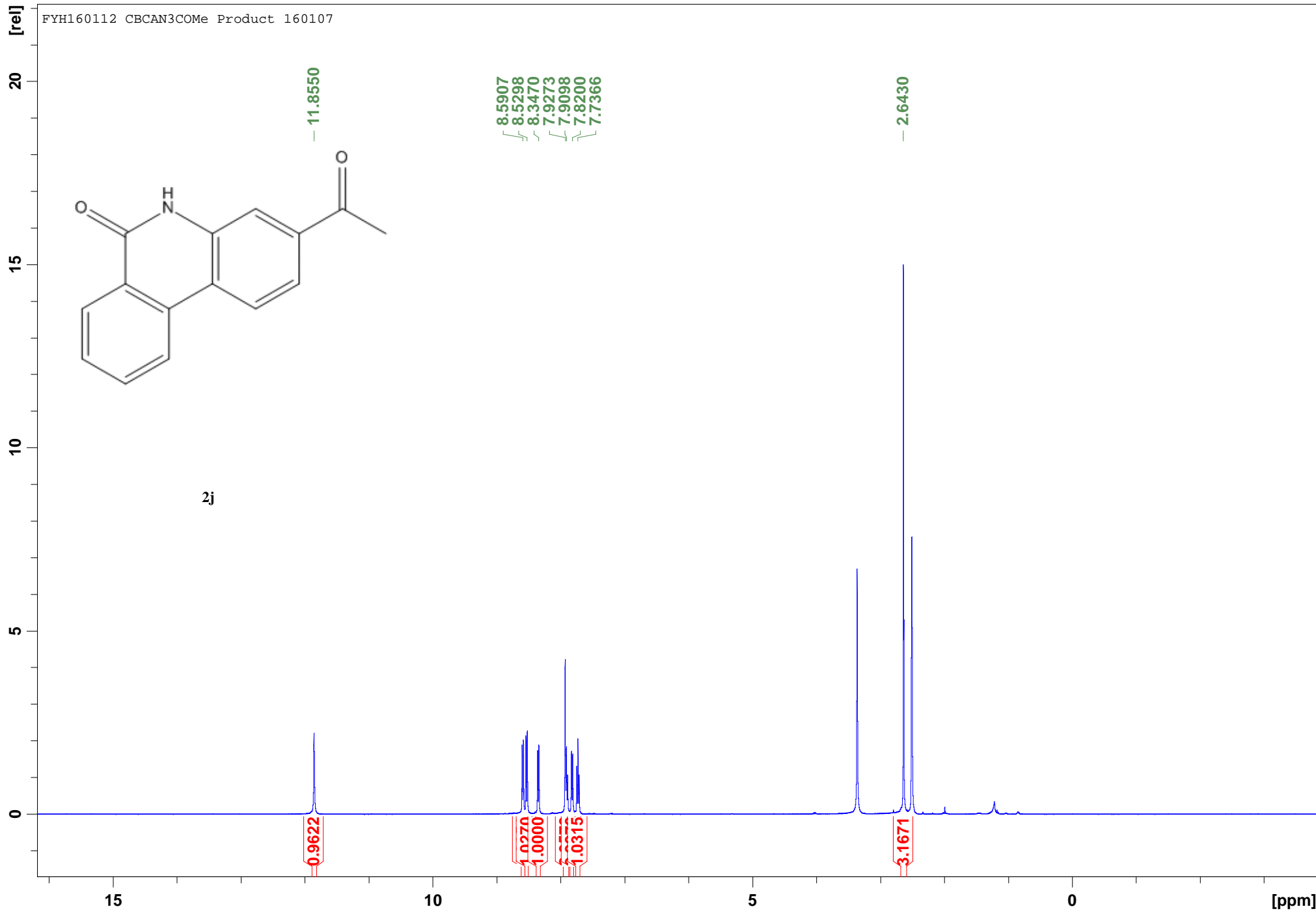
FYH 151123 CBCSulfacetamide Product C13



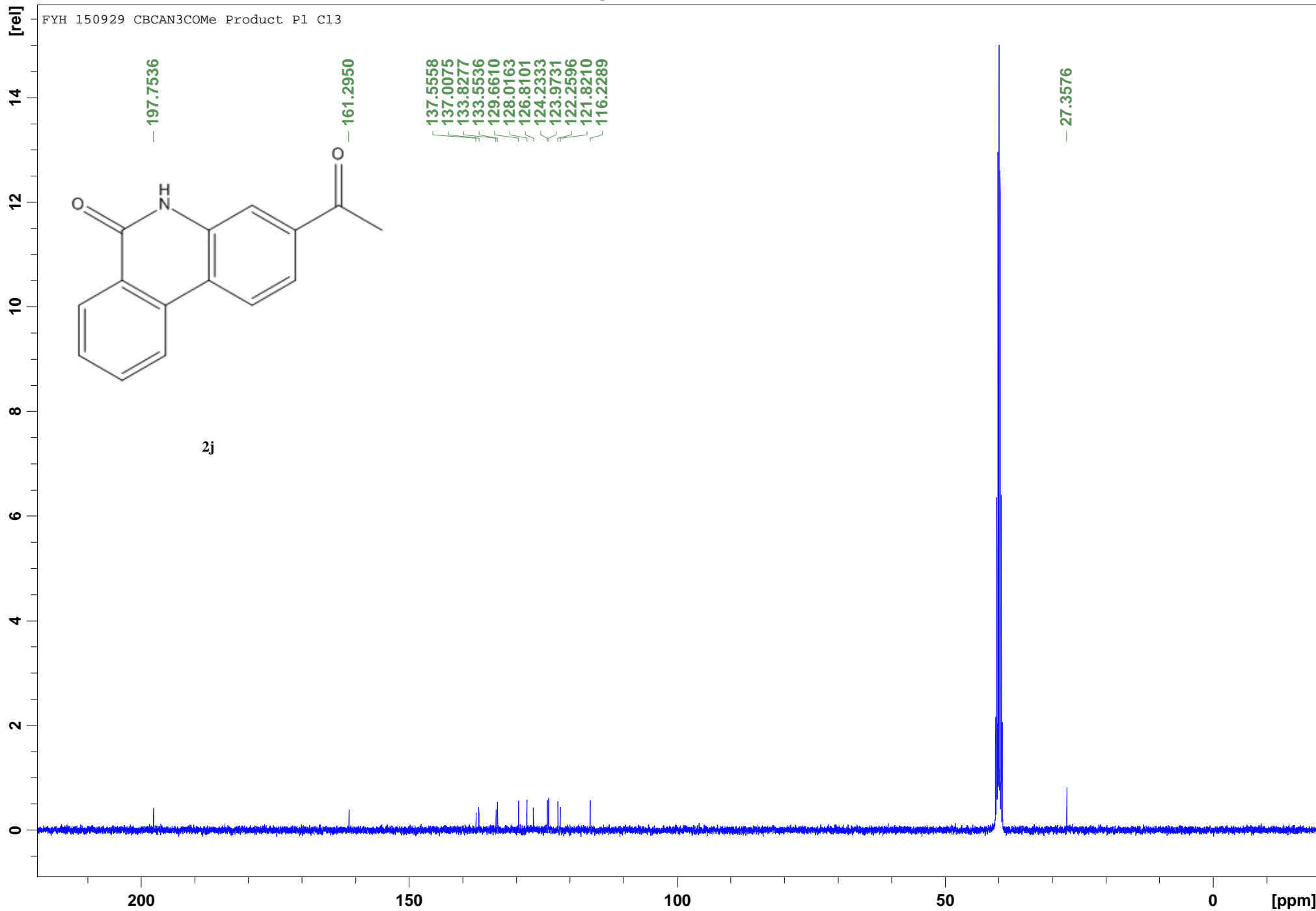




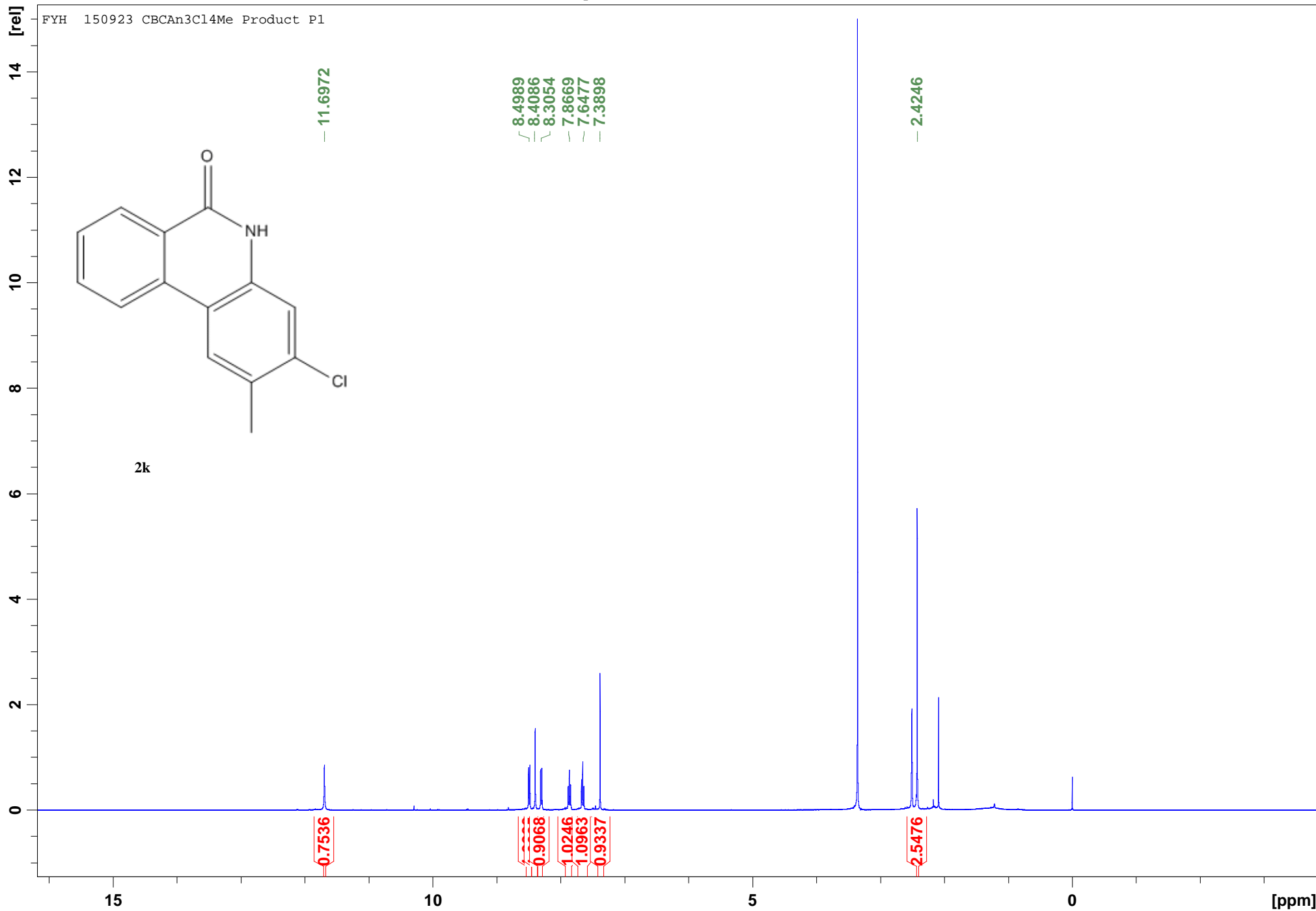
FYH160112 CBCAN3COMe Product 160107

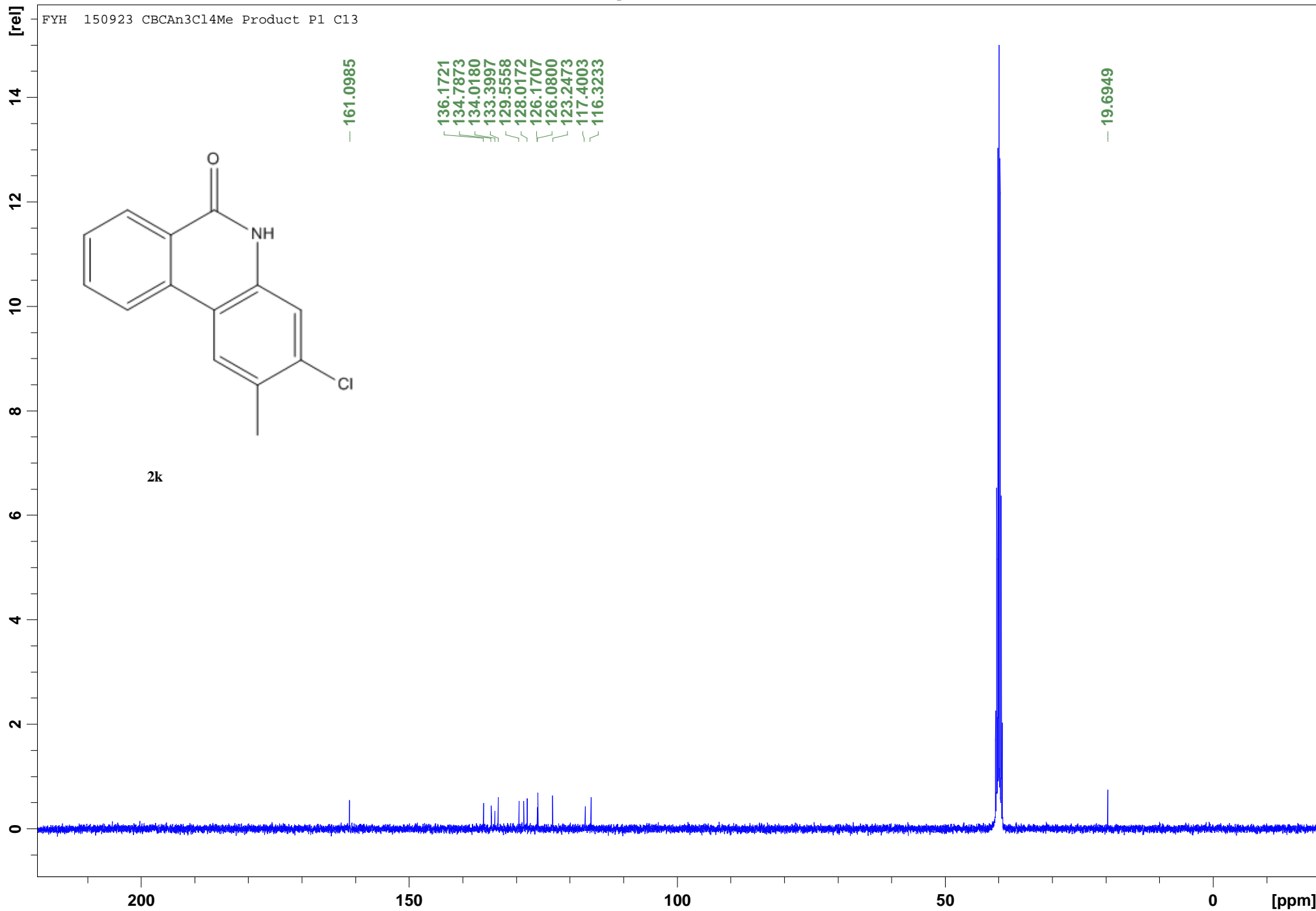


FYH 150929 CBCAN3COMe Product P1 C13

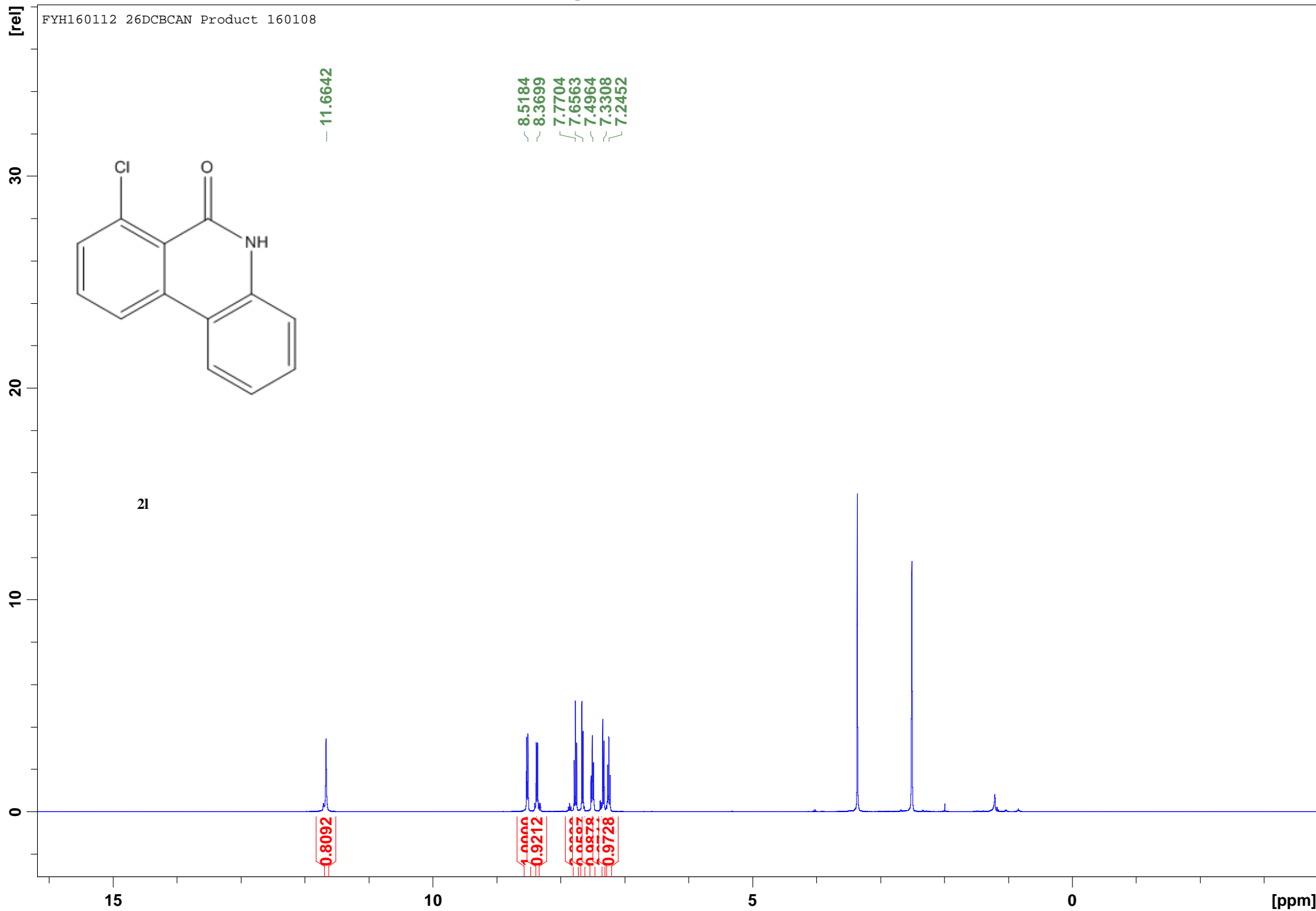


FYH 150923 CBCAn3Cl4Me Product P1

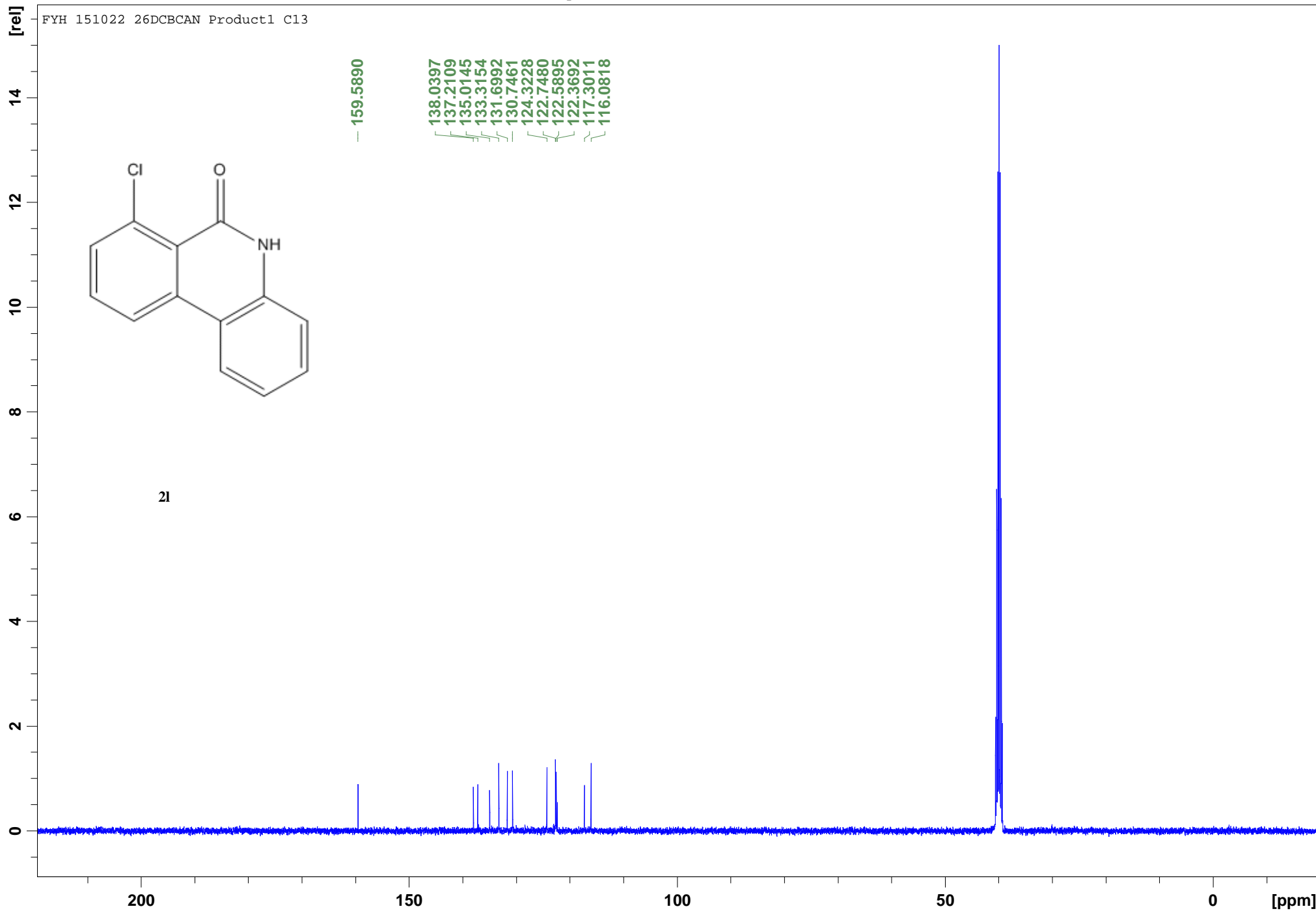




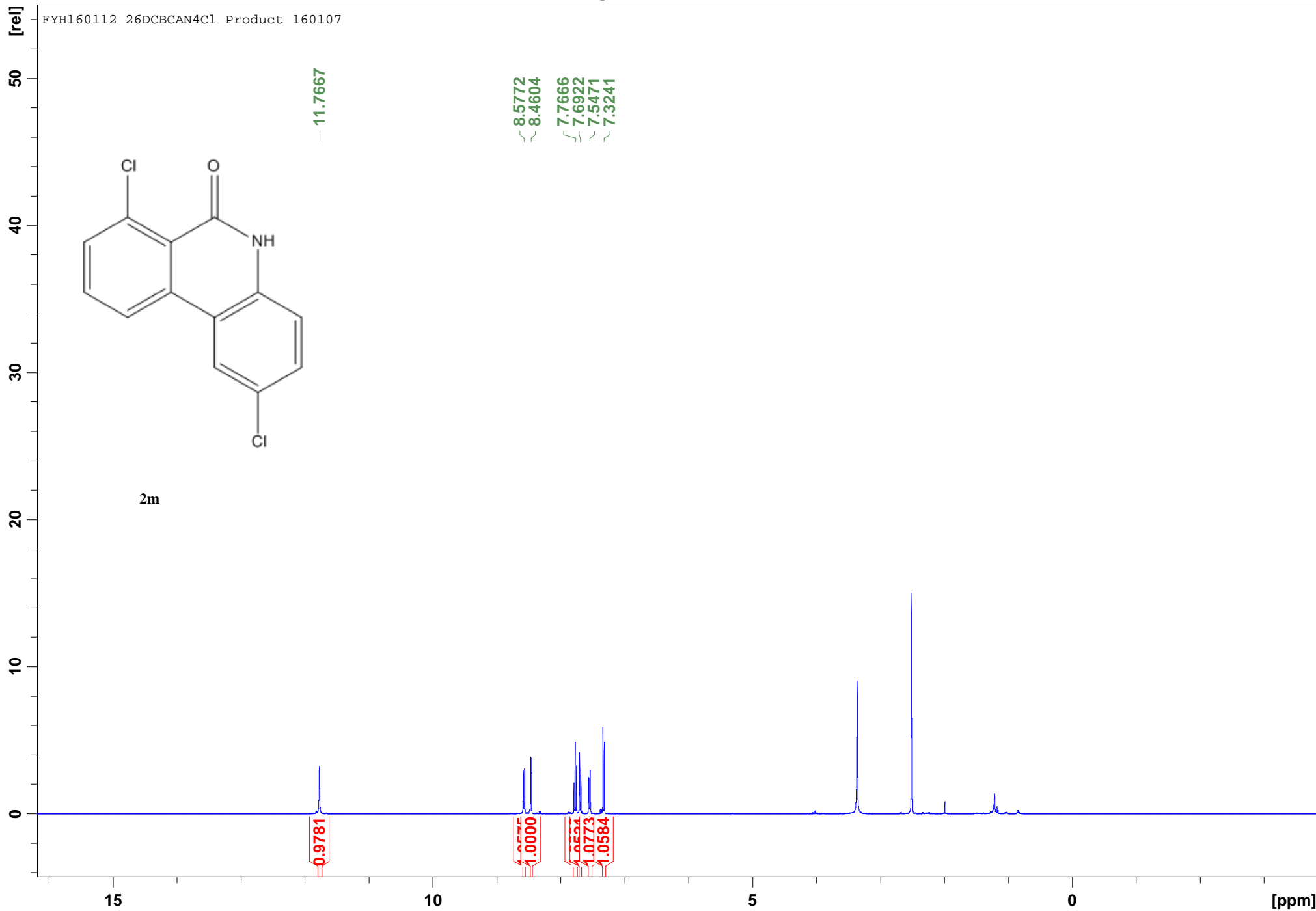
FYH160112 26DCBCAN Product 160108



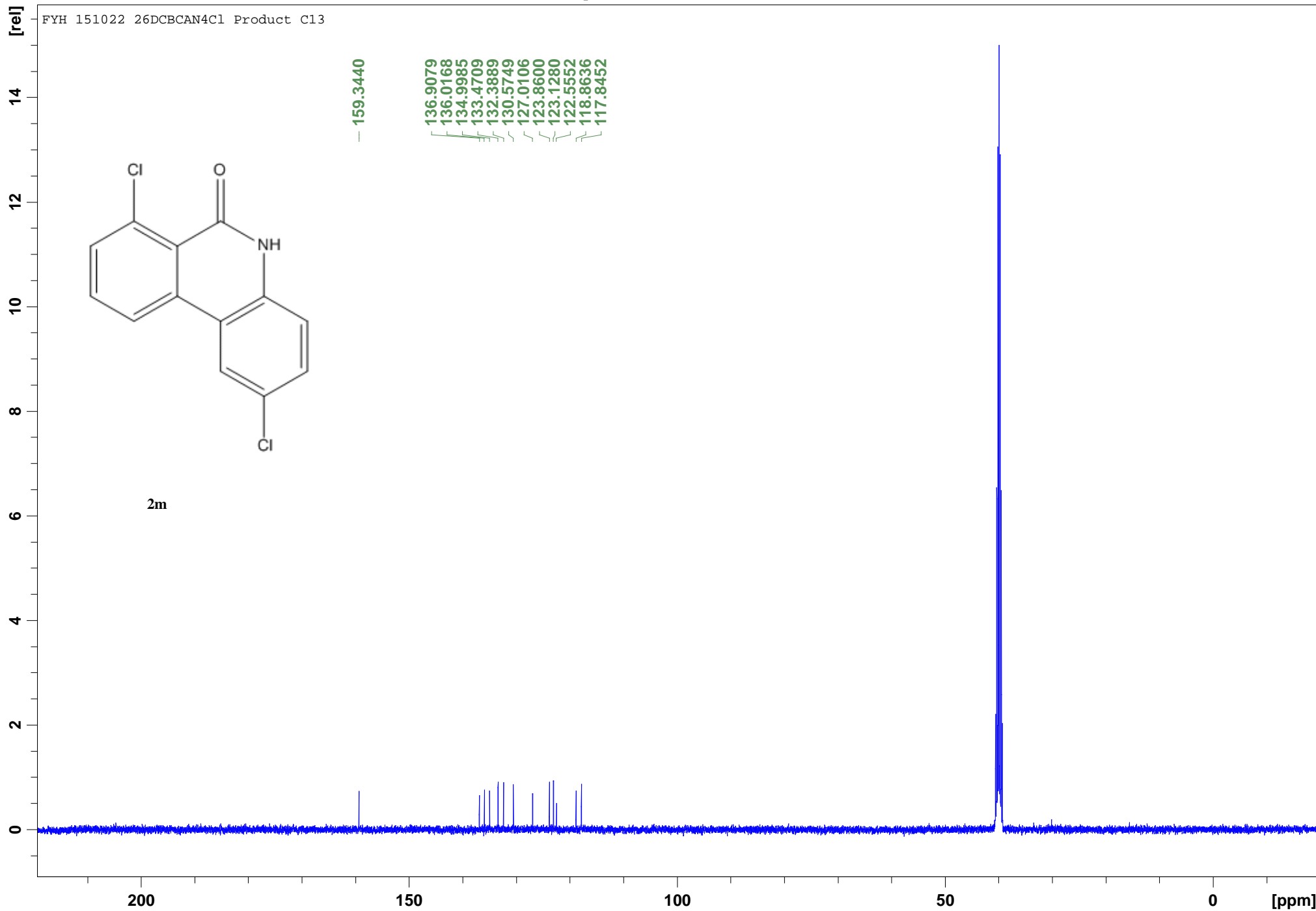
FYH 151022 26DCBCAN Product1 C13



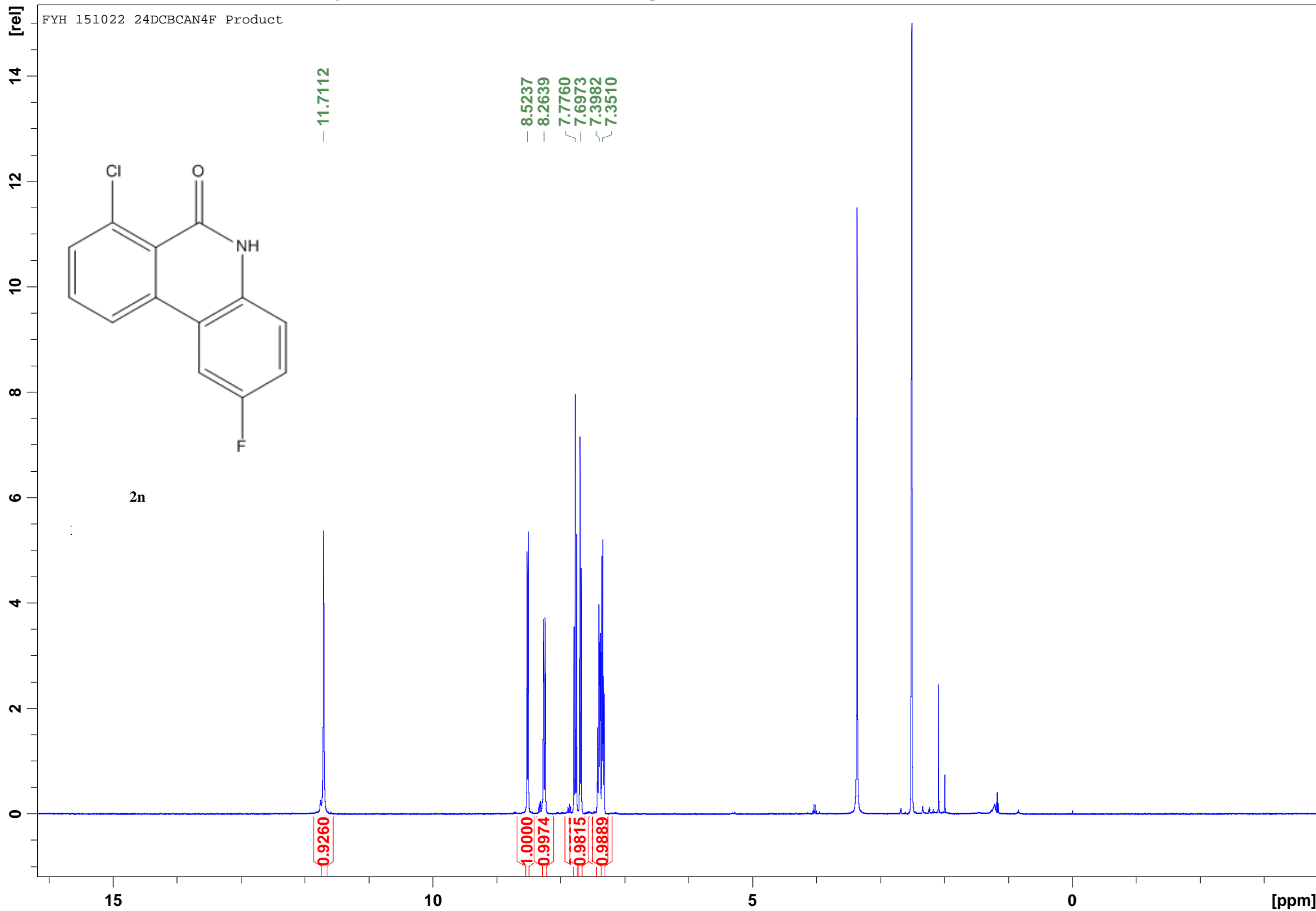
FYH160112 26DCBCAN4Cl Product 160107



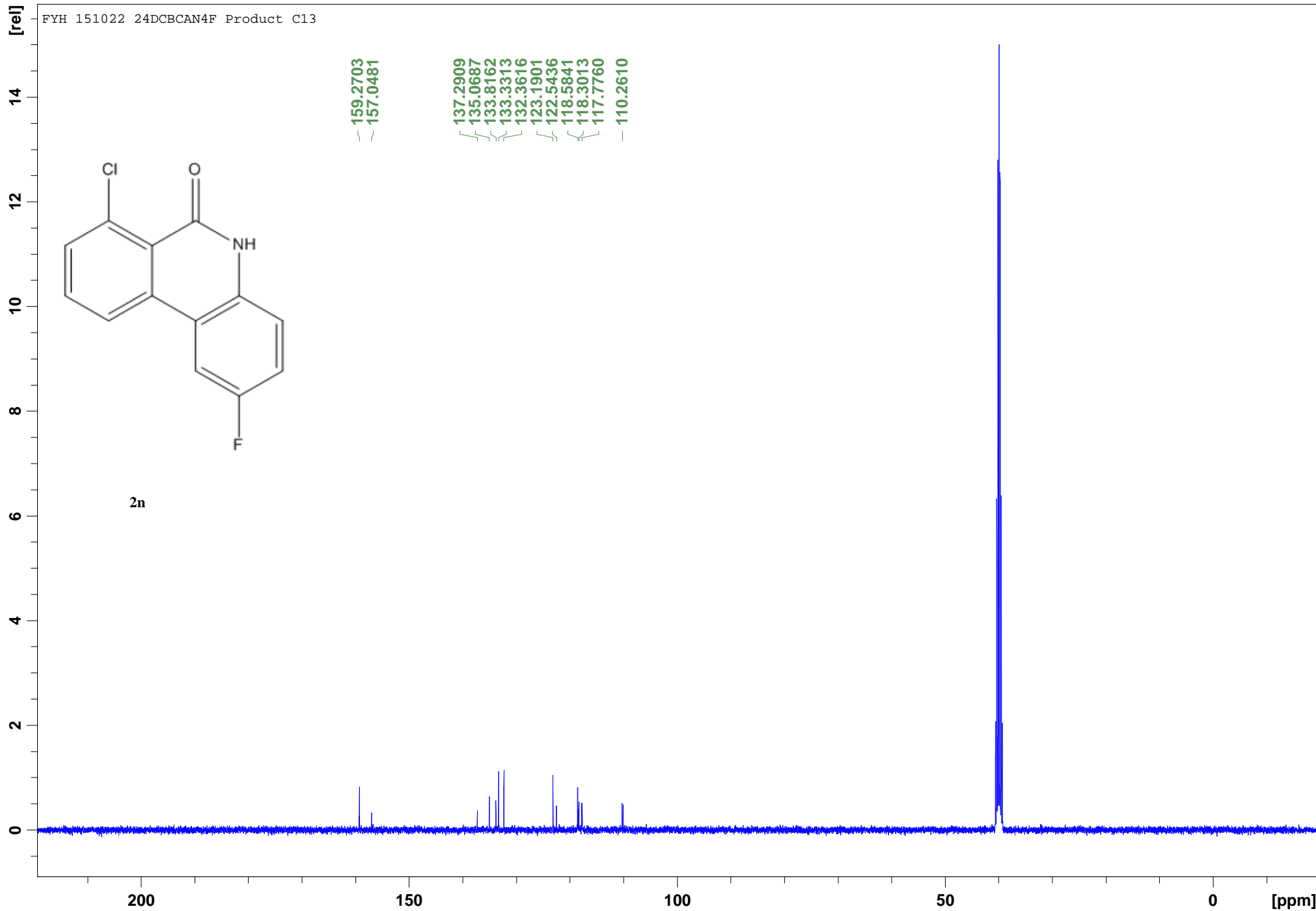
FYH 151022 26DCBCAN4Cl Product C13



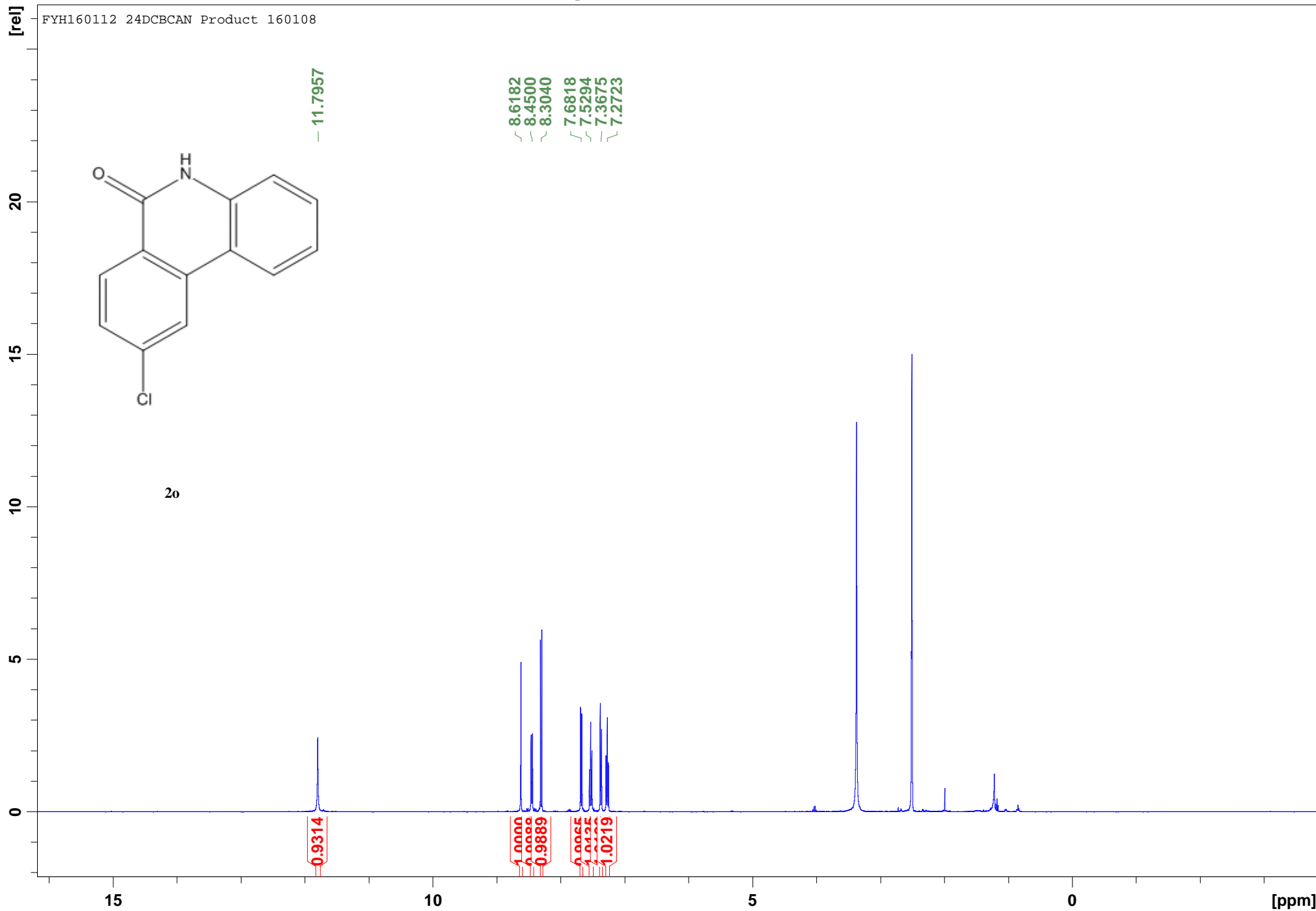
FYH 151022 24DCBCAN4F Product



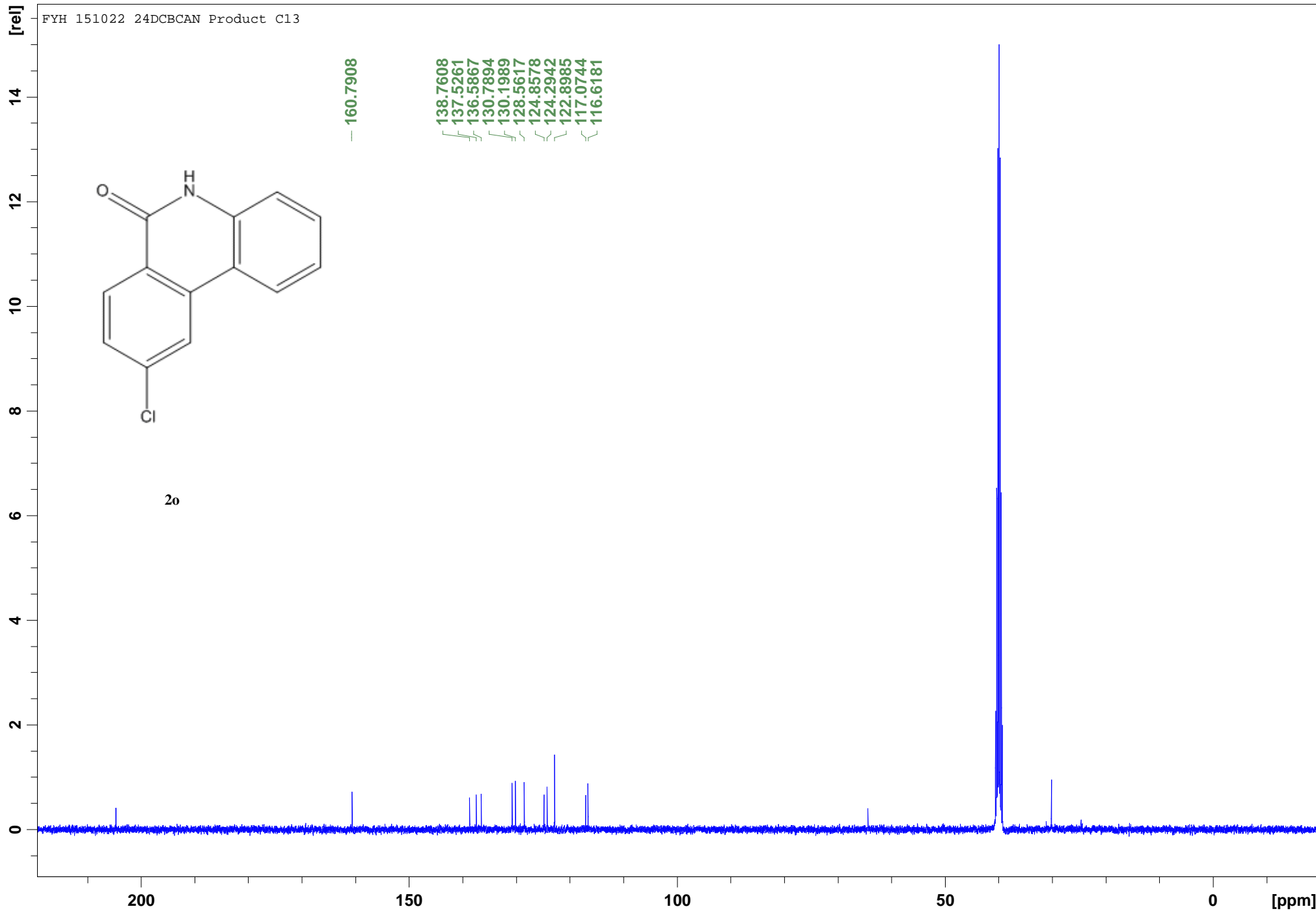
FYH 151022 24DCBCAN4F Product C13



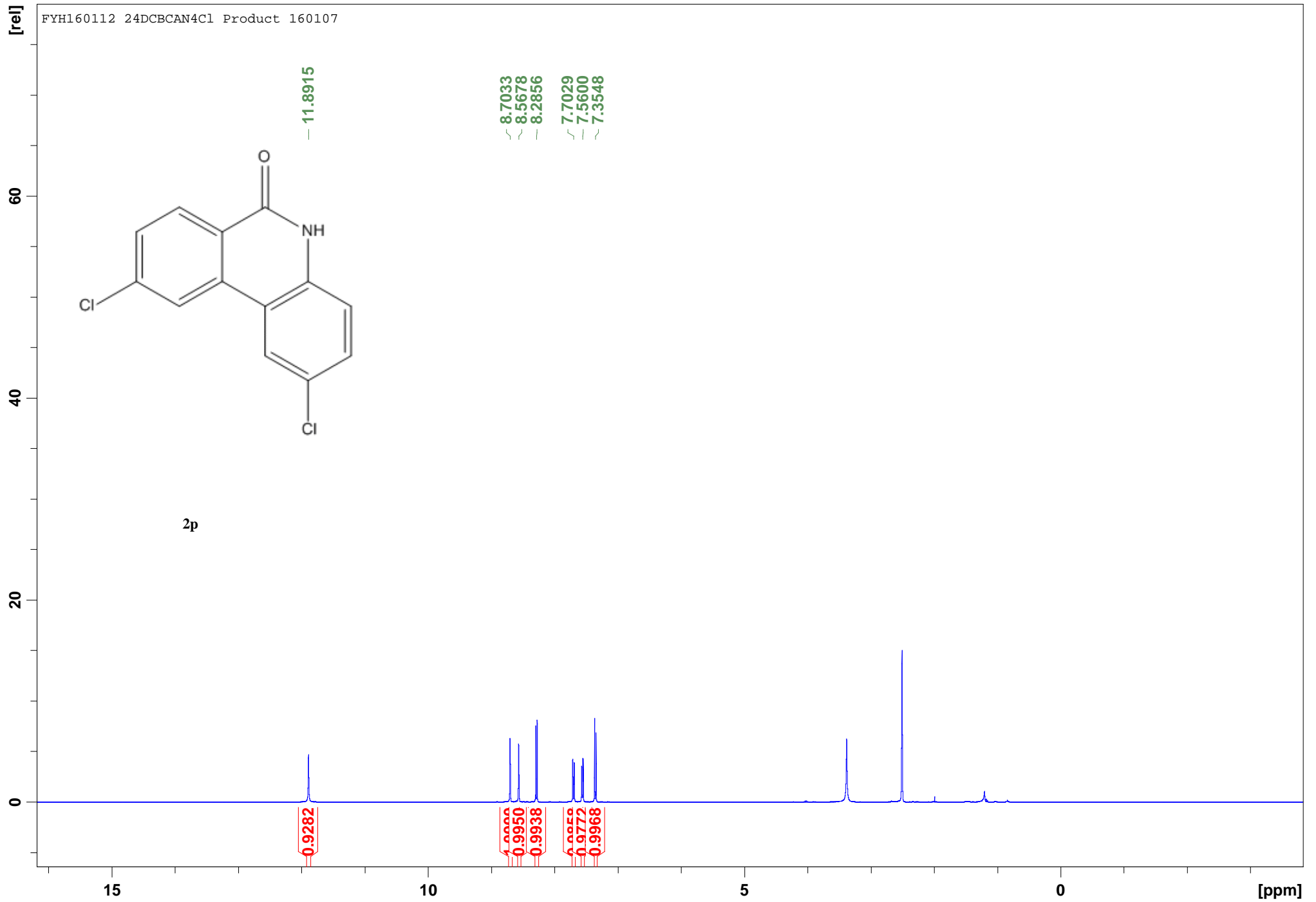
FYH160112 24DCBCAN Product 160108

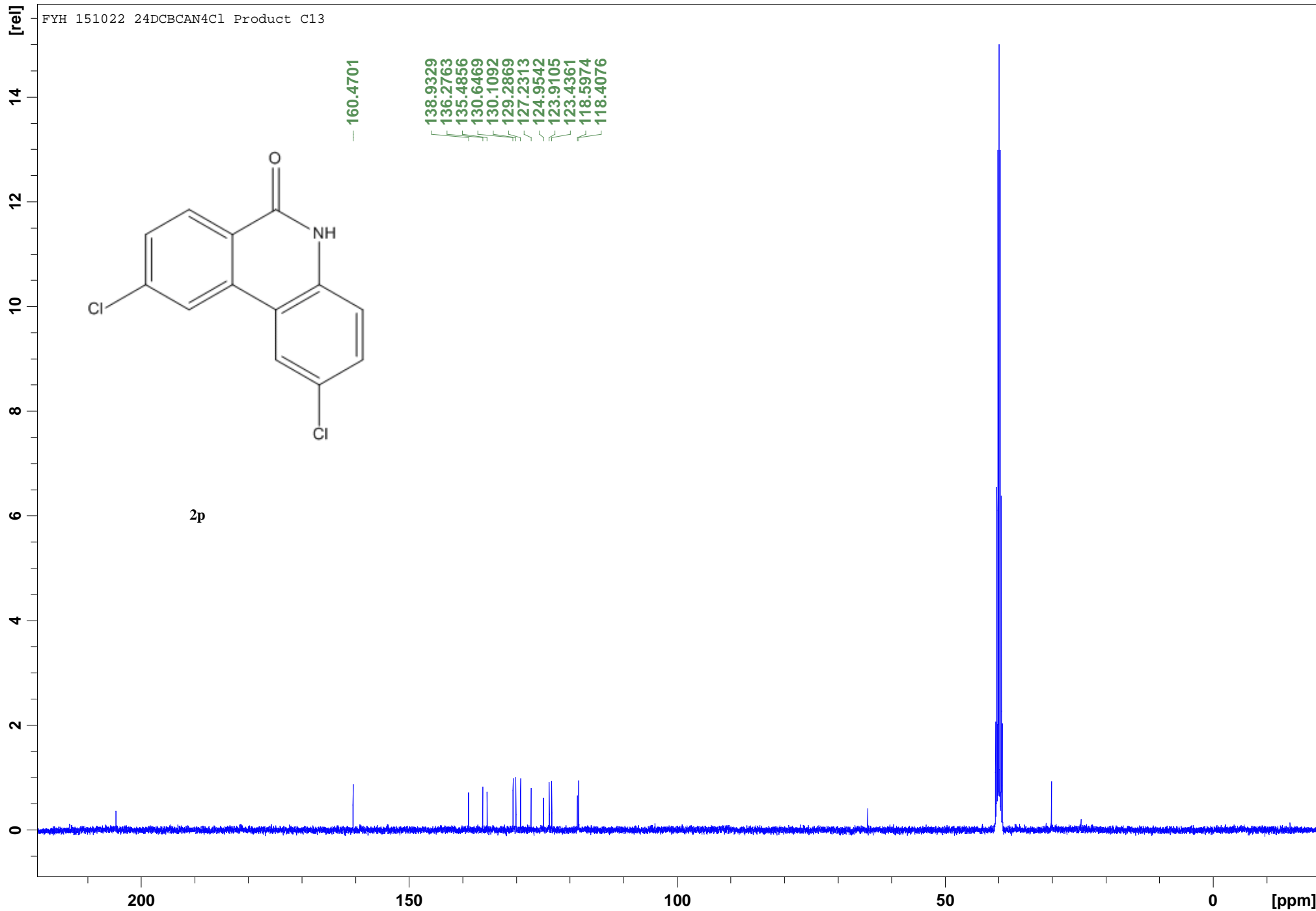


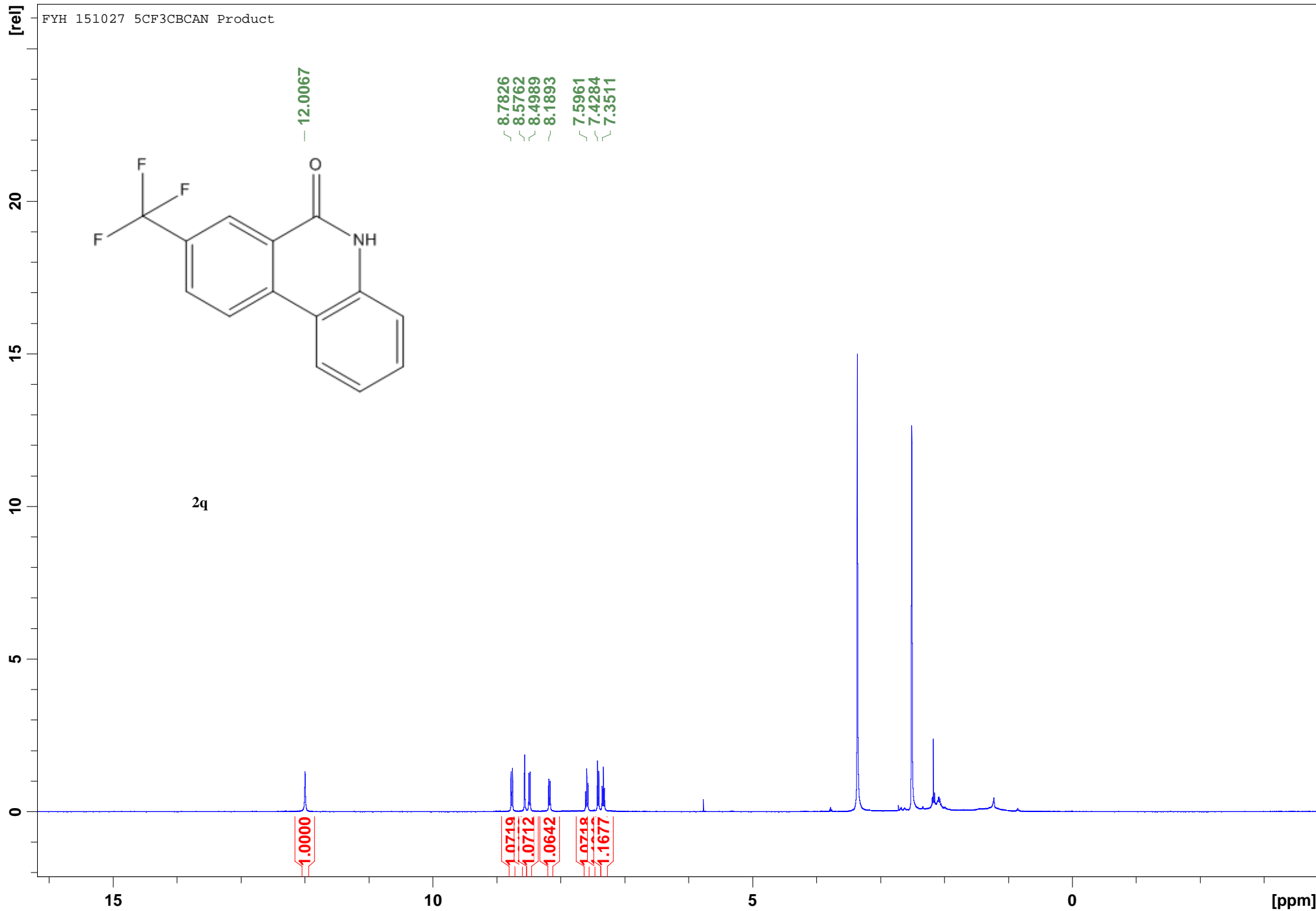
FYH 151022 24DCBCAN Product C13

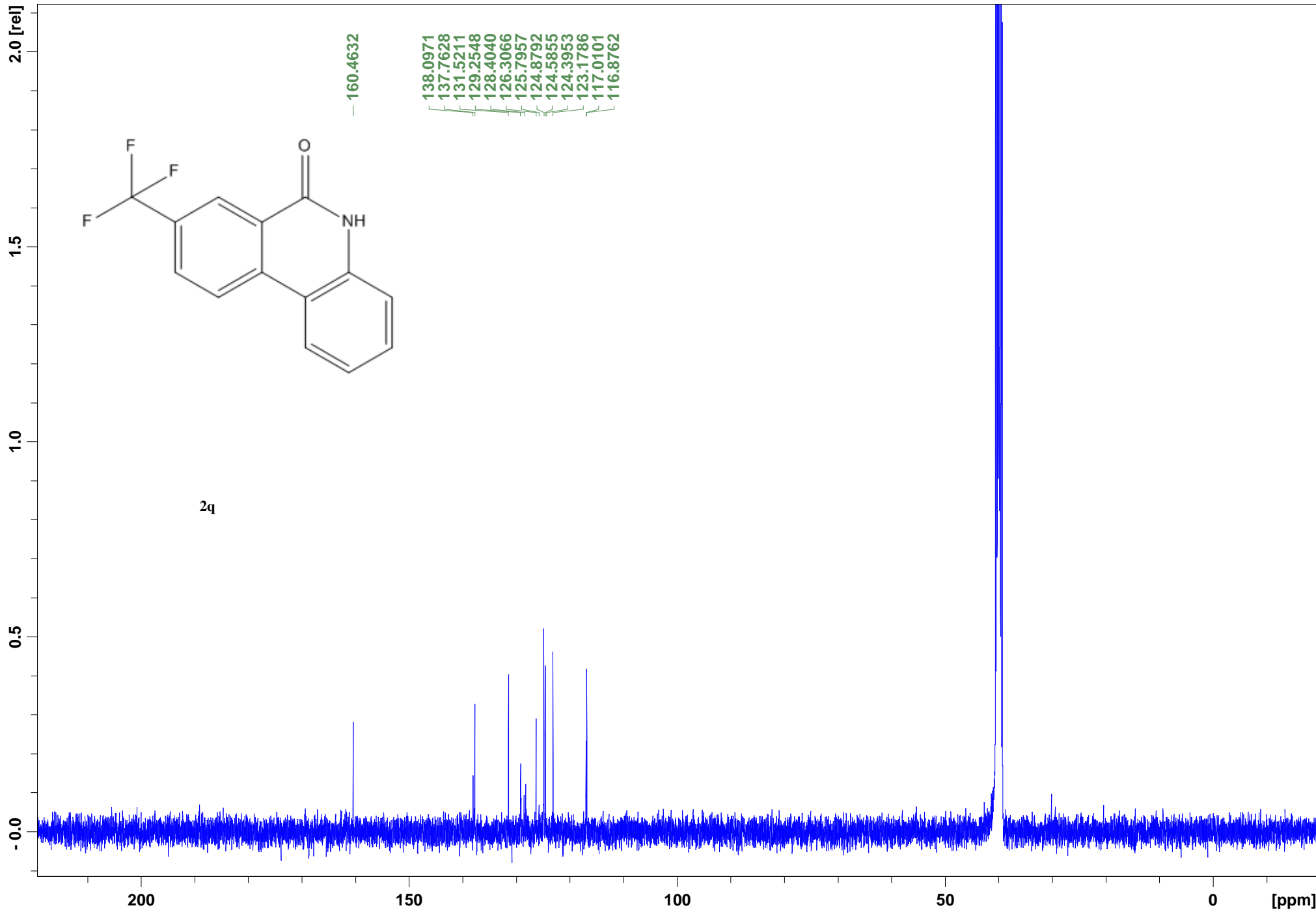


FYH160112 24DCBCAN4Cl Product 160107

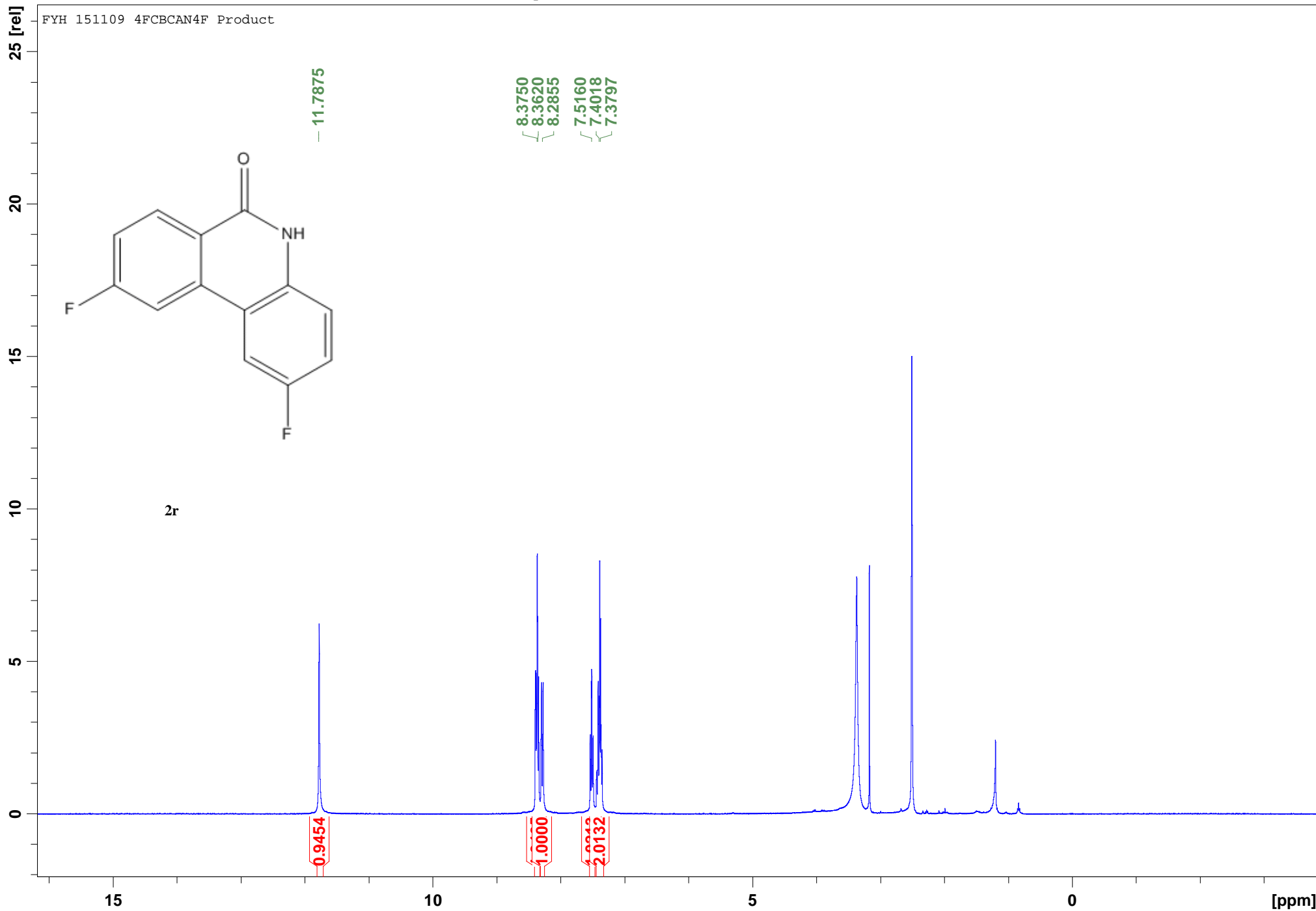








FYH 151109 4FCBCAN4F Product



FYH 151109 4FCBCAN4F Product C13

